SAPIENZA
UNIVERSITÀ DI ROMA

Ph.D in Chemical Sciences

XXV Cycle

Curriculum: Synthesis and Reactivity

Salophen-uranyl complexes and (thio)ureas moieties as versatile building blocks in Supramolecular Chemistry.

Supervisor **Candidate**

Prof. Antonella Dalla Cort **Michele Bruschini**

Table of Contents

General Outline. 4
Bibliography. 6

Chapter 1. ***Dinuclear Salophen-uranyl complexes as potential building blocks for the construction of switchable rotaxanes.***

1. Introduction. 7
1.1. "Top-down" and "bottom-up" approach for the construction of molecular level devices. 7
1.2. The quest for artificial molecular-level machines. 9
1.3. Rotaxane-based molecular switches. 12
1.4. Salophen-uranyl complexes: versatile building blocks for the synthesis of potential axles for rotaxane-based switchable catalyst. 17
1.4.1. Receptorial and catalytic properties of salophen-uranyl complexes. 17
1.5. Synthesis of novel dinuclear salophen-uranyl complexes. 20
2. Results and discussion. 24
3. Conclusions. 28
4. Experimental section. 30
5. Bibliography. 36

Chapter 2. ***Non-symmetrically substituted salophen-uranyl complexes as receptors for ion pairs in solution.***

1. Introduction. 42
1.1. The quest for Ion-Pair recognition: general remarks. 42
1.2. Classification of Ion-Pair receptors. 43
1.3. Use of Salen/Salophen-uranyl moieties for anion complexation in ion pair receptors. 44
1.4. Aim of the work. 48
2. Results and discussion. 49
2.1. Synthesis of receptors **11a-d**. 49
2.2. Binding measurements. 51

2.2.1. UV-Vis study of the binding constants. 51

2.2.2. Optical properties of receptor 11a and study of the association with TBA halides. 53

2.2.3. ^{1}H NMR investigation of the substituent influence upon p-cation interactions between TMACl and receptors **11a-d**. 57

3. Conclusions. 60

4. Experimental section. 62

5. Bibliography. 66

Chapter 3. ***Novel fluorescent benzimidazole-based receptors for sensing of carboxylate anions in a competitive medium.***

1. Introduction. 68

2. Urea and thiourea-based receptors for anions. 72

2.1. Introduction. 72

2.2. Anion sensing with use of fluorescent (thio)urea based receptors. 74

3. Benzimidazole-based (thio)ureas for the fluorescent sensing of carboxylate anions in competitive media. 78

4. Aim of the work. 82

4.1. Synthesis of receptors **19a-b**/**20a-b**. 82

4.2. UV-Vis and fluorescence measurements. 85

5. Conclusions. 89

6. Experimental section. 90

7. Bibliography. 95

GENERAL OUTLINE

Supramolecular Chemistry, defined as "the chemistry beyond the molecule"[1], focuses its attention on multi-molecular systems held together by weak intermolecular forces, such as hydrogen bonding, Lewis acid-base interactions, electrostatic or hydrophobic effects.[2]

Nature offers amazing examples of how non-covalent bonding interactions are involved in the successful execution of vital processes. It is enough to think, for example, to the crucial role of the hydrogen bonding between adjacent complementary residuals in the association of the two polynucleotidic strands of DNA, the molecule responsible for the storage and the transmission of genetic information (Figure 1).[3] Weak bonding interactions also play an important role in the metabolic transformations within the living cells, which are performed by catalytic proteins called enzymes.[4]

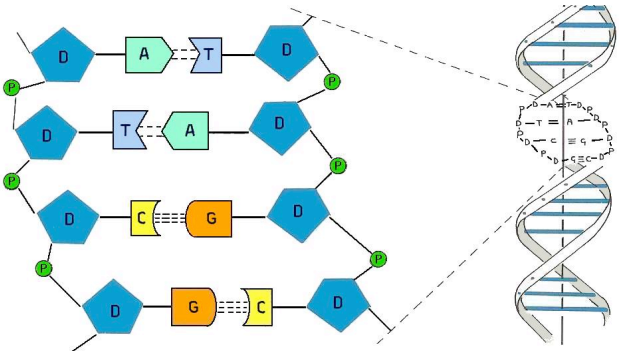

Figure 1 Illustration of the role exerted by hydrogen bonding in the assembly of the double helix of DNA (abbreviations: A = adenine, T = tymine, C = cytosine, G = guanine).

A thorough study of these systems and the comprehension of their working mechanism led to define the fundamental principles of modern Supramolecular Chemistry. The most renowned among them is undoubtedly the "lock and key" principle proposed by Emil Fischer in 1894 to explain enzymatic catalysis.[5] Its extension from biological to artificial systems has allowed the birth and development of Host-Guest chemistry. It deals with systems in which a molecule endowed with a suitable recognition site (called "*host*") is able to form a complex with a substrate (called "*guest*") having sterical and geometrical requirements complementary to those of the *host*. (Figure 2)

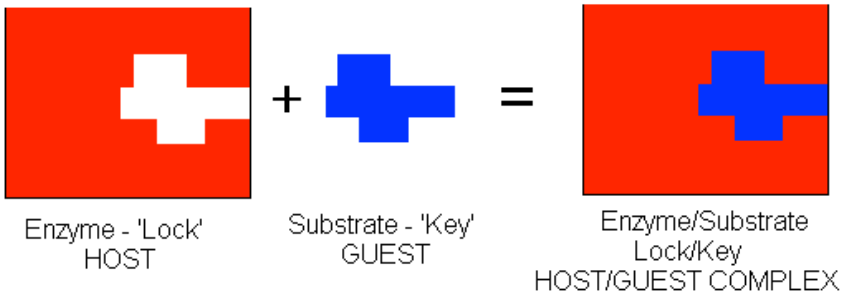

Figure 2 Illustration of the lock-key principle and its extension to artificial host-guest systems

Compared to the single starting molecules, the supramolecular structures arising from the complexation process may have new and improved functions.

Moving from the pioneering work of Cram, Pedersen and Lehn during the 1960's, which allowed them to win the Nobel Prize for Chemistry in 1987,[6] many others results have been achieved so far, especially in the fields of molecular recognition[7], transport[8] and catalysis[9].

In more recent times, thanks to the development of new synthetic methodologies and to the availability of sophisticated instrumental techniques, Nanotechnology is becoming the frontier of the research in Supramolecular Chemistry. Many efforts have been done toward the construction of molecular machinery[10] and highly self-assembled supramolecular architectures[11].

Moving within the Supramolecular area, the work done during this PhD program has followed three main themes, which are developed in the following chapters. Versatility of the salophen-metal scaffold for the construction of supramolecular devices will be discussed in Chapter 1. Particularly, the use of bimetallic salophen-uranyl complexes as building blocks for the construction of functional supramolecular systems will be illustrated. In the second chapter, the results obtained using non-symmetrically substituted salophen-uranyl complexes as receptors for ion pairs in solution will be shown and discussed. Finally, the results obtained using novel fluorescent benzoimidazole-based receptors for the qualitative and quantitative sensing of carboxylate anions in competitive media will be the object of discussion in the third chapter.

Bibliography

[1] Desiraju, G.R., *Nature*, **2001**, 412, 397-400; For textbooks, see: Lehn, J.M., *Supramolecular Chemistry: Concepts and Perspectives*, VCH, Weinheim, **1995**; Vogtle, F. *Supramolekulare Chemie*, Teubner, Stuttgart, **1995**; Schneider, H.J.; Yatsimirsky, A. *Principles and Methods in Supramolecular Chemistry*, Wiley, New York **2000**; Steed, J.W.; Atwood, J.L. *Supramolecular Chemistry*, Wiley, New York, **2000**; Diederich, F.; Stang, P. J. Tykwinski, R. R. *Modern Supramolecular Chemistry* Ed. Wiley-VCH, Weinheim, **2008.**

[2] Schalley, C.A. *Analytical methods in Supramolecular Chemistry*, Chapter 1; Wiley-VCH, New York, **2007**;

[3] Kornberg, A.; Baker, T. A. *DNA Replication, 2nd ed.*; W. H. Freeman and Company, New York, **1992**.

[4] Fersht, A. *Structure and Mechanism in Proteine Science: A guide to enzyme catalysis and protein folding*; W.H. Freeman, New York, **1998**.

[5] Fischer, E. *Ber. Dt. Chem. Ges*. **1894**, *27*, 2985–2993.

[6] Pedersen, C.J., *J. Am .Chem. Soc*, **1967**, 89, 7017-7036; Cram, D.J.; Maverick, E.F.; Knobler, C.B.; Yoon, J. *Chem.Comm.* **1997**, 1303-1304 and references cited therein; Lehn, J.M., *Acc. Chem. Res*., **1978**, *11*, 49.

[7] For a series of reviews on this topic, see *Chem. Rev.*, **1997**, *97*, issue 5.

[8] Lehn, J.M., *Supramolecular Chemistry: Concepts and Perspectives*, Chapter 6 and references cited therein; VCH, Weinheim, **1995.**

[9] Selected references: (a) Fiedler, D.; Leung, D.H.; Bergman, R.G.; Raymond, K.N. *Acc. Chem. Res.*, **2005**, *38*, 349-358; (b) Vriezema, D.M.; Comellas Aragonés, M.; Elemans, J.A.A.W.; Cornelissen, J.J.L.M.; Rowan, A.E.; Nolte, R.J.M. *Chem. Rev*. **2005**, *105*, 1445-1489. For textbooks, see: Van Leeuwen, P.W. N.M *Supramolecular Catalysis*, Wiley-VCH, Weinheim, **2008.**

[10] Browne, W.R.; Feringa, B.L. *Nature Nanotechnology*, **2006**, *1*, 25-35 and references cited therein.

[11] Elemans, J.A.A.W.; Rowan, A.E.; Nolte, R.J.M. *J.Mater.Chem.* **2003**, *13*, 2661-2670.

CHAPTER 1

Dinuclear Salophen-uranyl complexes as potential building blocks for the construction of switchable rotaxanes.

The construction of molecular assemblies able to perform a specific function as a result of an external stimulus is a very challenging research field, at the frontier of modern Supramolecular Chemistry.

This chapter is not meant to be a comprehensive digest on the question of molecular machines, but rather aims to give to the reader a general overview on the approaches followed to promote motion in these systems and the potential applications of these systems.

The emergence of a "bottom-up" approach towards fabrication of nanometric-sized devices, also possible thanks to the advances in instrumentation for visualization and manipulation of the single molecules, is discussed in the first part of the chapter. The second part focuses on the use of simple pre-programmed components for the construction of supramolecular machines, particularly switchable rotaxanes, with some examples from the recent literature. In conclusion of the chapter, the potentialities offered by the salophen-metal moiety as building block for the construction of molecular machines are discussed and the synthesis of new dinuclear salophen-uranyl complexes, potentially useful as axles in the construction of switchable rotaxanes, is reported.

1. Introduction.

1.1 Top-down" and "bottom-up" approaches for the construction of molecular-level devices.

The use of different devices has become an integral part of our everyday life. Broadly speaking, they are assemblies of different components designed to achieve a specific function. Each of the constituents performs a single act, while the device is able to perform a more complex and useful function. These principles, valid for the macroscopic objects, can be extended to the microscopic scale to define a *molecular-level device.* It is defined as the assembly of pre-programmed nanometric building blocks into more complex and useful supramolecular structures.[1]

Over the past decades, a variety of nanometric-sized devices have been constructed for the collection, storage and processing of information using the so-called "top-down" approach.[2] Photolithography and the related techniques have enabled engineers and physicists to manipulate progressively smaller pieces of matter for the construction of the miniaturized components of the modern electronic devices. Moreover, the potentialities offered by laser techniques in the top-down approach to miniaturization have also been exploited for the construction of microelectromechanical systems (MEMS), which consist of a central unit designed for data processing and several components that interact with the outside acting as microsensors.[3] These systems are commonly used in accelerometer sensors contained within automotive airbags and are key components in inkjet printers and disposable blood pressure-meters.[4]

The top-down approach, however, is rapidly approaching to the limits of its physical capabilities also due to the intrinsic limitations of the lithographic techniques, which do not allow handling pieces of matter smaller than 100 nanometers. This issue has prompted many researchers to think about a new strategy towards the realization of miniaturized systems using atoms or molecules as "bricks" for their construction.

R.P. Feynman firstly proposed this new approach, commonly known as "bottom-up", in 1959 during his famous talk to the American Physical Society "There is plenty of room at the bottom".[5] The key point of Feynman's talk is that "the principles of physics do not speak against the possibility of maneuvering things atom by atom". The "atom-by-atom" approach was reproposed by K.E. Drexler[6] in the 80's, when he postulated the possibility of constructing a building nanodevice, called *assembler*, able to build every object starting from the single atoms. This possibility would open the way to revolutionary discoveries in every field of science, with particular regard to the manufacturing of new extremely strong materials useful to transportation and also in biomedical applications. Although these ideas are at a first glance astonishing, the "atom-by-atom" approach proposed by Drexler appears quite unrealistic from the practical point of view. Indeed, chemists know very well that atoms cannot be manipulated as isolated species due to their high reactivity and their tendency to interact with other atoms through different chemical bonds to form molecules. These species, in which atoms can be combined in a properly designed fashion through a plethora of chemical transformations, are definitely more convenient than atoms for the construction of nanometric devices. Compared to atoms, molecules are stable species and already possess distinct shape and properties that can be manipulated using appropriate inputs (chemical, photochemical or electrochemical). Last but not least, molecules can self-assemble or be connected to give larger structures.

The idea of using molecular components for the "bottom-up" construction of miniaturized devices began to arise toward the end of the 70's and gained a foothold during the 1980's, in the frame of the research on Supramolecular Chemistry.[7-8] The great number of building blocks supplied by organic synthesis, and the use of photochemical and electrochemical investigation tools, allowed the flourishing of a number of interesting examples of molecular devices and machines.[9] More recently, the supramolecular "bottom-up" approach towards the construction of nanodevices and nanomachines has been further developed thanks to the use of single-molecule fluorescence spectroscopy[10] and of different probe microscopies (AFM, STM, TEM).[11] These extremely powerful techniques have enabled the visualization and the manipulation of objects on the molecular scale: it has been possible for example to make ordered arrays of molecules on surfaces[12] and even to investigate bimolecular reactions at single molecule level.[13]

1.2 The quest for artificial molecular-level machines.

Molecular-level machines can be defined as devices in which the molecular constituents can change their relative position after the application of an external stimulus, with the subsequent production of mechanical work.[14-15] Similarly to the macroscopic machines used in the everyday life, they need an energy source to work and their functioning should be verified by monitoring an appropriate signal.

The simplest way to supply energy to a chemical system is through the exothermic reaction of a chemical fuel. This is what happens normally in the countless molecular machines that operate inside the human body, where the chemical energy produced by the hydrolysis of adenosine triphosphate (ATP) is responsible for their functioning.[16]

In addition to being the "molecular unit of currency" of cells from most organisms, ATP also plays a crucial role in signal transduction pathways performed by kinases, enzymes able to phosphorylate proteins and lipids. Moreover, it is used by the enzyme adenylate cyclases as substrate for the production of cyclic adenosine monophosphate (cAMP), an important second messenger involved in intracellular activation processes.[17]

ATP is produced by the ATP synthase in the final step of the respiratory metabolism, called phosphorylative oxidation. The energetic supply for ATP production is provided by the proton gradient between the two sides of the mitochondrial membrane, arising from the oxidative methabolism processes (Glycolysis and Krebs cycle). ATP synthase, which represents an astonishing example of nanometric sized molecular motor (**Fig. 1.1**) is essentially made of two rotating motors (conventionally indicated as $\mathbf{F_0}$ and $\mathbf{F_1}$), connected

through a stator. The first one F_0 is situated within the mitochondrial membrane and acts as a proton pump, allowing H^+ ions to flow from the outer to the inner part of the mitochondrial membrane. The proton flow causes a rotation of the F_0 subunit that, in its turn, promotes the rotation of the F_1 subunit, which catalyzes ATP synthesis starting from adenosine diphosphate (ADP) and inorganic phosphate.

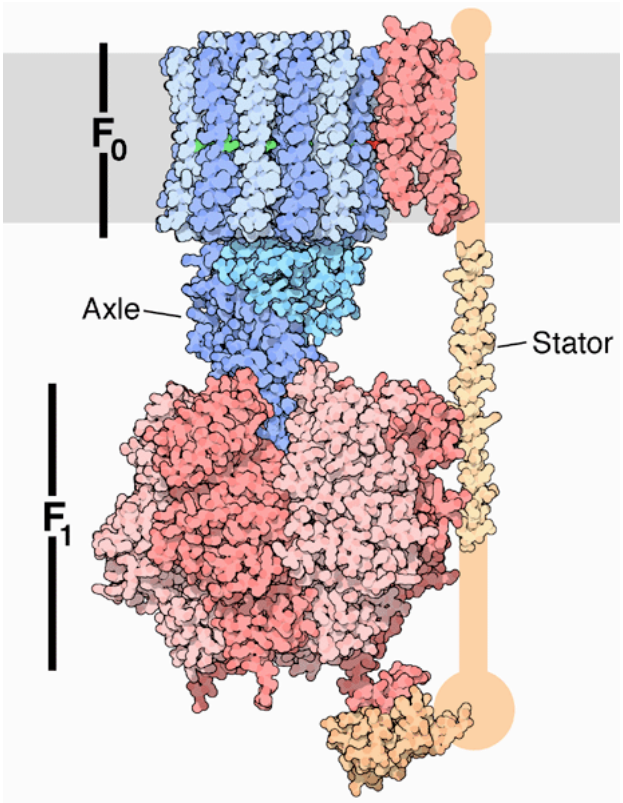

Figure 1.1 Illustration of the two subunities F_0 and F_1 of the ATP synthase, connected through a stator devoted to the transmission of rotational movement from F_0 to F_1.

Taking inspiration from ATP synthase and many other naturally occurring molecular machines, many research teams have directed their efforts towards the assembly of prototypal molecular architectures able to perform very simple movements, such as rotation or shuttling, using different energetic inputs (chemical, photochemical or electrochemical).[18] The use of carefully designed molecular components able to self-assemble and self-organize into a definite topology led, during the last decade, to the emergence of a new research field in the framework of Supramolecular Chemistry, that of mechanically-interlocked architectures.

A "mechanically-interlocked architecture" can be defined as an assembling of different molecules, in which the components are held together not through classical bonds, but in virtue of their topology. In recent times, J.F. Stoddard proposed a new type of chemical bond, named *mechanical bond*, to indicate the non-covalent interaction between interlocked

molecules.[19] The superstructures arising from a mechanical bond between two or more molecular components can be properly considered true molecules and not supramolecules, since they are mechanically linked one to another.

Browsing the literature concerning mechanically interlocked molecular architectures, several main topological motifs can be distinguished and classified into four categories (**Fig. 1.2**, from left to right): [20]

- rotaxanes
- catenanes
- knots (also named "knotanes")[21]
- molecular Borromean rings

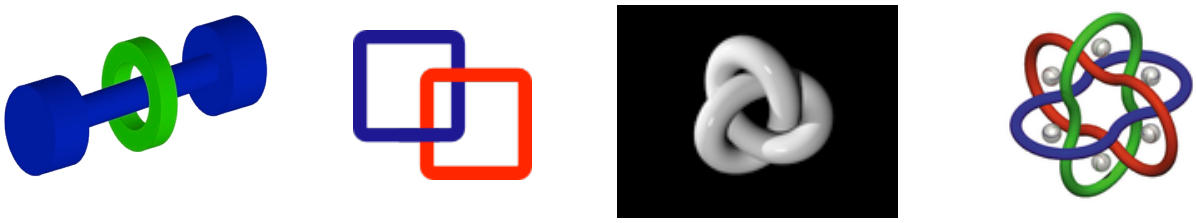

Figure 1.2 From left to right: a [2]rotaxane, a [2]catenane, a trefoil knot and a Borromean ring

As shown in **Fig. 1.2**, a [2]rotaxane is made of two components, a dumbbell-shaped molecule (the axle) and a macrocyclic wheel: the end-capping of the axle with bulky groups (stoppers) prevents the unthreading of the wheel from the axle. When the mechanically interlocked molecules are both macrocycles, the system is a [2]catenane.

On the other hand, a knot[22] (here depicted as a trefoil knot) arises from looping of one molecule in foils, while Borromean rings consist of three topological circles linked in such a way that removing of any circle results in two unlinked circles.[23]

Among these structures, the most investigated have been those of rotaxanes and catenanes. A careful design of the molecular components in combination with a suitable fuel capable of promoting a mechanical movement in these assemblies (using light, electrons or a chemical fuel) opened the way to the utilization of these architectures in the construction of molecular devices and machines, potentially useful for nanotechnological applications. In the next section our attention will be mainly focused on switchable [2]rotaxanes, in which the structure can be switched between two different topologies using an appropriate physical or chemical input, with regard to some significant examples from recent literature.

1.3 Rotaxane-based molecular switches.

Before going forward on the question of switchable 2[rotaxanes], it is worthy on the story of these molecular aggregates and on the strategies used for their synthesis.

[2]rotaxanes were synthesised for the first time in 1967 by Schill and Zollenkopf using a multistep synthesis[24] and by Harrison and Harrison with a statistical synthesis.[25] For a long time, these species were considered only laboratory curiosities, also due to their low synthetic accessibility. It was only during the 80's that rotaxanes became obtainable in preparative yields and really raised interest in the chemical community, thanks to the application of template-directed synthetic protocols developed by the research groups of Sauvage[26] and Stoddart.[27] These protocols rely on the use of molecular components containing well-defined structural motifs, able to master the self-assembling process leading to the [2]rotaxane.

The most successful approaches for the templated synthesis of rotaxanes are the capping and the clipping methods (**Fig. 1.3**).

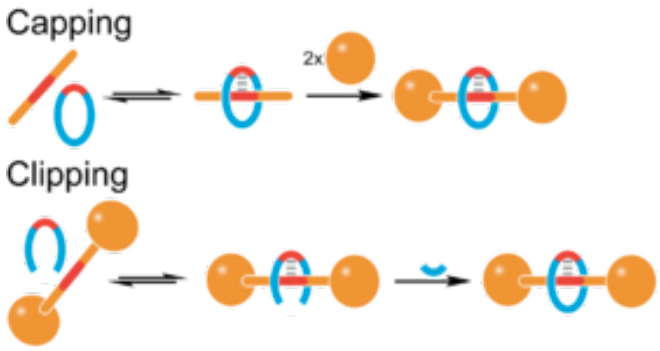

Figure 1.3 **"**Capping" and "clipping" strategies for the template-directed synthesis of rotaxanes.

In the first method, the dynamic complex between the axle and the wheel (called *pseudorotaxane*) is converted into the rotaxane by the end capping of the axle with two bulky substituents (stoppers) to prevent dissociation of the complex. Many reactions have been used for the stoppering step, including the copper-catalysed azide-alkyne cycloaddition (CuAAC) click reaction[28] and the reductive amination.[29] The second method is similar to the first, except that the dumbbell shaped component is already formed and acts as a template for the ring closure reaction, usually olefin metatheses[30] and imine bond formation.[31] In more recent times, Leigh et al. introduced another template-based strategy for the synthesis of rotaxanes, which makes use of a metal ion for promoting the final step of formation of the mechanical bond between the axle and the wheel (**Fig. 1.4**). In this strategy, called "active template", the

metal ion can play a dual role, acting either as a template for entwining the molecular precursors or as a catalyst for the formation of the covalent bond between the two halves of the axle to give the rotaxane.[32]

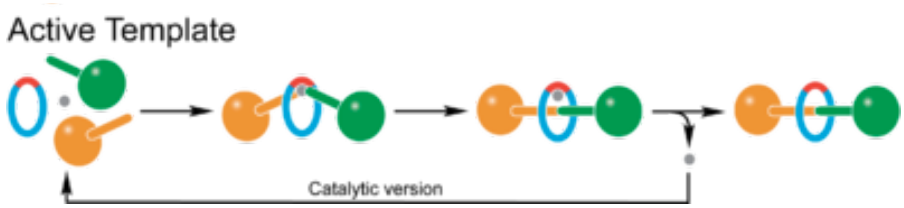

Figure 1.4 "Active-template" approach for the synthesis of rotaxanes. The metal ion can act either as a template or as catalyst in the formation of the mechanical bond of the rotaxane.

With a proper design, two different recognition sites can be inserted within the dumbbell component. In this case, the wheel can shuttle between the two sites as a consequence of an external stimulus, and the rotaxane can be used as a switching molecular machine. The different topological states of the rotaxane are characterized by different chemical and physical properties and can be detected using electrochemical or spectroscopic techniques.[33]

Switchable devices equipped with proper input-output architectures that allow their interrogation and the communications with the external world offer great potentialities for the construction of molecular logic gates[34] and molecular memories.[35] Significant contributions in this regard sprout out from Stoddart and coworkers, which investigated the use of switchable devices for molecular electronics since 1999.[36]

This research group reported in 2007 the assembly of a 160-Kb molecular memory using the [2]rotaxane showed in **Fig. 1.5**. This device has the same characteristics of a dynamic random access memory (DRAM) circuit, but unlike the latter has a lower pitch (33 vs. 140 nm) and a smaller memory cell size (0.0011 vs. 0.0408 μm^2). The binary behavior observed for this system relies on the switching of the tetracationic macrocycle between the tetrathiafulvalene (TTF) moiety and the dioxynaphthalene station upon repetitive oxidation/reduction steps of the TTF unit.[37]

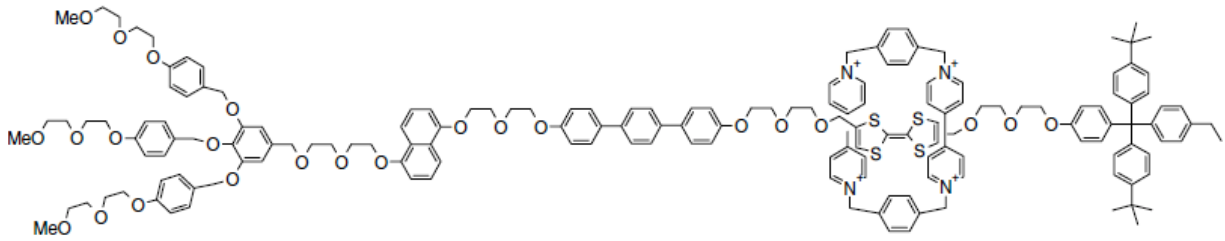

Figure 1.5 An electrochemically driven molecular switch used as a 160-Kb molecular memory.

Moving towards the use of switchable machines in medicine, interesting results were published in 2008 by Coutrot and Busseron concerning the use of glycosides as stoppers for the synthesis of glicorotaxanes.[38] Due to important role played by glycosides in a wide range of biological recognition processes, their incorporation into [2]rotaxanes could open the way to new devices useful for biomedical applications. In the mannosyl [2]rotaxane reported in **Fig. 1.6**, the macrocyclic wheel (a crown ether) can shuttle between two different stations, an anilinium ion and a triazolium ion, using protonation-deprotonation inputs. On the basis of ^{1}H NMR measurements, the authors suggest that, in the initial state, the macrocycle sit over the anilinium station, which interacts with the polyethereal cavity of the macrocycle through strong hydrogen bonds. Addition of diisopropylethylamine (DIEA) causes the deprotonation of the anilinium ion and induces the displacement of the wheel from the anilinium to the triazolium station. On the other hand, when hydrochloric acid is added to the system, the anilinium site is again protonated and the wheel goes back on it.

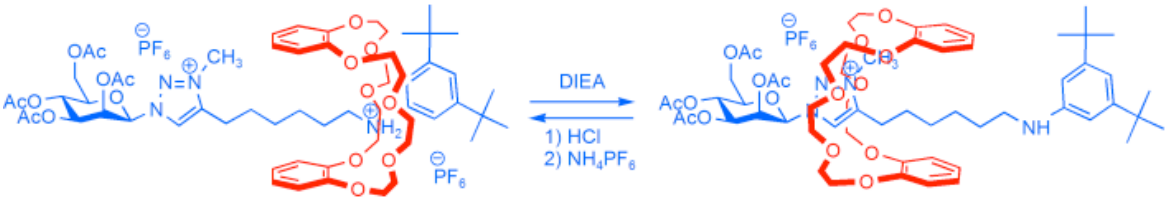

Figure 1.6 An Acid-base switchable glycorotaxane.

Aside from protonation-deprotonation reactions, rotaxanes can be also switched using ionic species such as cations[39] and anions.[40] A remarkable example in this regard has been published in 2012 by You, Tzeng and coworkers and is reported in **Fig. 1.7**. This rotaxane, which contains three different stations in its axle (respectively a guanidinium ion, a 2,2'-bipyridyl unit and a carbamate unit), can operate in two switching modes depending on the charge of the ion employed.[41]

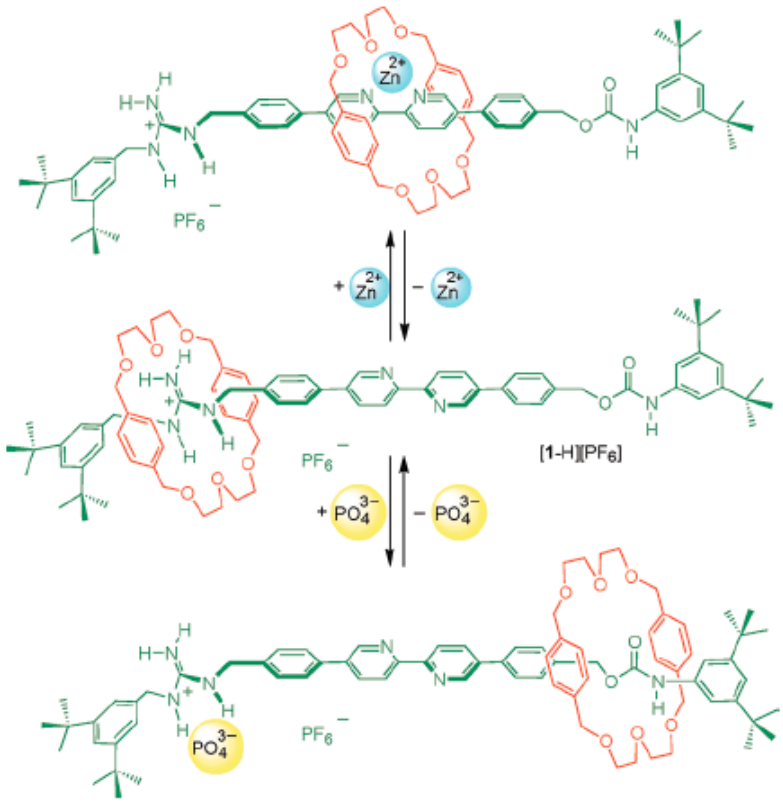

Figure 1.7 Structure of a double-switchable [2]rotaxane.

^{1}H NMR data collected for this rotaxane in CD_3CN allowed the authors to point out that the macrocycle can migrate not only between the guanidinium and the 2,2'-bipyridyl stations using positively charged ions (H^+ or Zn^{2+}), but also between the guanidinium and the carbamate motifs in the presence of an anion (PO_4^{3-}). This dual mode switching is particularly appealing for the construction of molecular actuators and sensors for ion pairs.

So far, the importance of switching the physical properties of molecules (optical, photochemical or electrochemical) by an appropriate external stimulus has been highlighted relatively to molecular electronic and sensing applications. On the other hand, the role of switching in controlling the chemical reactivity, and specifically catalysis, has only recently gained attention.[42]

Moving in the research line on switchable rotaxanes, Leigh and al. have recently published an example of rotaxane-based switchable organocatalyst, shown in **Fig. 1.8**.[43]

The spectral changes observed in the ^{1}H NMR spectrum of the rotaxane **1-H•3PF$_6$** after treatment either with a aqueous solution of NaOH or with 2-*tert*-butylimino-2-dietylamino-1,3-dimethylperhydro-1,3,2-diazaphosphorine (BEMP) phosphazene resin, led the authors to suggest that the rotaxane is switched on from the catalytically inactive form **1-H•3PF$_6$**, in which the wheel is on the ammonium station, to the catalytically active form **1•2PF$_6$**, where the wheel dwells on the triazolium station and the N-H group is available for iminium

organocatalysis. The switching is completely reversible and the addition of trifluoroacetic acid switches the rotaxane off in the **1-H•3PF$_6$** form.

A preliminary kinetic study performed on the Michael Addition of an aliphatic thiol to *trans*-cynnamaldehyde (reaction conditions: 5% mol catalyst, CH_2Cl_2, RT, 5 days) demonstrated that no conversion of the starting materials is observed using rotaxane **1-H•3PF$_6$**, while both rotaxane **1•2PF$_6$** and the axle **2-H•3PF$_6$** catalyze the reaction equally effectively. Furthermore, switching of the rotaxane **1-H•3PF$_6$** *in situ* made possible to control the progress of the Michael reaction. A brief washing of the rotaxane **1-H•3PF$_6$** solution in dichloromethane with 1M aqueous NaOH resulted in a virtually complete conversion of the starting materials to the product within 1 hour.

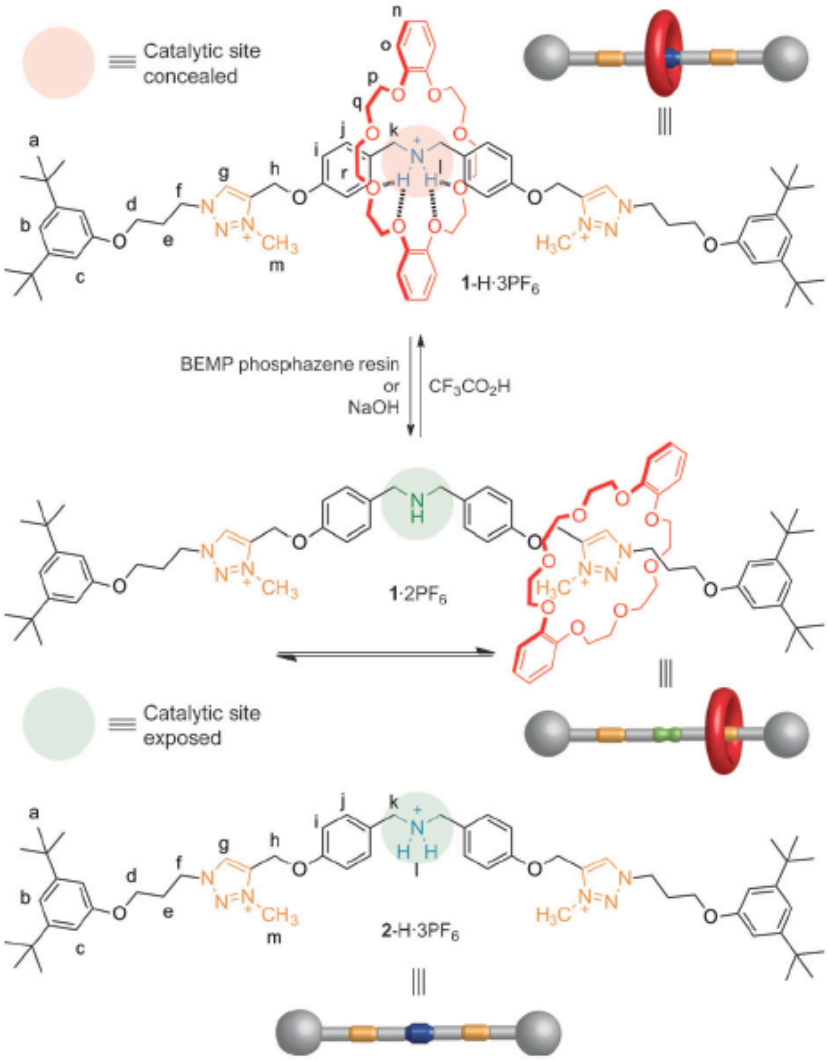

Figure 1.8 A switchable rotaxane-based organocatalyst.

As shown in the previous example, the on-off switching of the activity in a synthetic catalyst is advantageous both for influencing the rate and the outcome of a chemical transformation in

analogy with the regulatory activity of many enzymes, performed naturally through cofactors and allosteric effect.[44] But compared to the system reported in **Fig. 1.8**, enzymes are able to switch autonomously between states with different catalytic activity when triggered by a suitable chemical stimulus. Therefore, the construction of a catalytic switch able to work autonomously and with turnover in the presence of a chemical fuel would be a very challenging task.

The next section of this chapter is devoted to the first steps performed towards the realization of such a system, in particular to the synthesis of dinuclear salophen-uranyl complexes as potential two-stationed axles for the construction of a catalytically driven molecular switch.

1.4 Salophen-uranyl complexes: versatile building blocks for the synthesis of potential axles for rotaxane-based switchable catalysts

1.4.1 Receptorial and catalytic properties of Salophen-uranyl complexes.

Salen and the closely related salophen belong to the important class of Schiff base ligands, which have been conveniently used in Coordination Chemistry for the synthesis of a plethora of metal complexes.[45] The popularity of these compounds arises essentially from their high synthetic accessibility, in association with their ability to accommodate and stabilize different metal ions in various oxidation states.

Salophen-uranyl complexes are obtained with good yields by the condensation reaction between two equivalents of salycilaldehyde and an equivalent of 1,2-phenylenediamine in the presence of uranyl acetate, which acts as a template for the imine formation (**Scheme 1.1**).

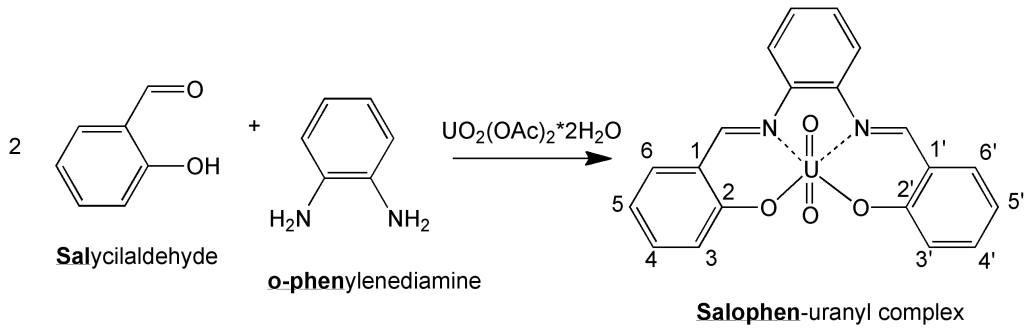

Scheme 1.1 Synthesis of the salophen-uranyl complex. IUPAC name of salophen N,N'-*o*-phenylenebis(salicyldimine).

With the exception of few cases of hexagonal bypiramidal coordination geometries reported for the uranyl dication[46], its salophen derivatives display a well-defined preference for a pentagonal bipyramidal coordination geometry. In this arrangement, the donor atoms of the ligand occupy four of the five equatorial coordination sites of the uranium, while the two oxygen atoms of the uranyl ion occupy the apical positions. The fifth equatorial coordination site generally accommodates a solvent molecule, such as water or methanol, in the absence of other guests.[47] From the structural point of view, salophen-uranyl complex possess a characteristic "bird-like" shape (**Fig. 1.9**). This particular conformation arises from the large ionic radius (r = 1.38 Å) of the uranyl dication which, to fit the cavity of the ligand, causes the distortion of its planar backbone.[48]

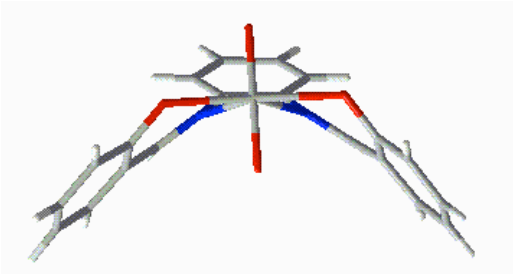

Figure 1.9 Calculate model of the basic salophen-uranyl complex, with its peculiar "bird-like" shape.

Salophen-uranyl complexes can be regarded as Lewis acid immobilized into an organic framework, able to interact with species endowed with donor atoms or, generally speaking, with hard Lewis bases. Many research groups took advantage of this peculiar feature to incorporate salophen-uranyl moieties into receptors[49] and catalysts.[50] As shown previously in Scheme 1.1, the 3-3' positions on the salophen-uranyl skeleton are the closest to the metal centre, and a proper decoration of these positions with designed pendant arms allows to modulate the affinity and the selectivity of the complex.

The macrocyclic salophen-uranyl complex **1** reported in **Fig. 1.10** has been synthesised by Reinhoudt and coworkers and used as supramolecular receptor for the urea molecule.[51] The receptor shows an incredible affinity for its substrate (K_{ass} estimated to be > 10^8 M^{-1}), mimicking the binding site of the enzyme urease. As confirmed by X-ray analysis, the recognition process combines the Lewis acid base interaction between the carbonyl and the uranyl center and additional hydrogen bonds between the amido groups and the oxygen atoms of the polyethereal chain.

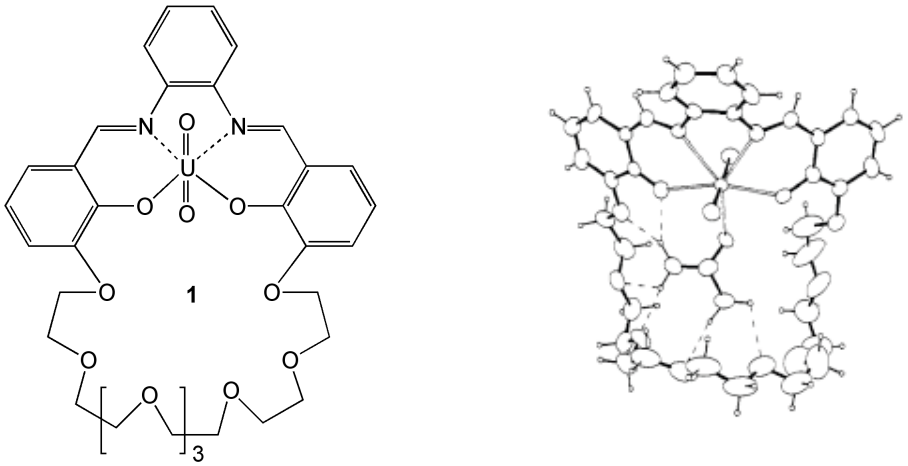

Figure 1.10 Salophen-uranyl complex **1** (left) and X-ray structure of the complex with urea (right).

As far as supramolecular catalysis is concerned, the coordination to uranyl-salophen derivatives proved to activate the carbonyl group towards nucleophilic attack and stabilize the transition state of addition reactions. Examples of such an electrophilic catalysis are the Diels-Alder cycloaddition between benzoquinone and 1,3-cyclohexadiene, performed by derivative **2**[50e] (**Fig. 1.12**, top), and the Michael-type conjugate addition of thiophenol to 2-cyclopenten-1-one performed by compound **3**.[50b](**Fig. 1.12**, bottom)

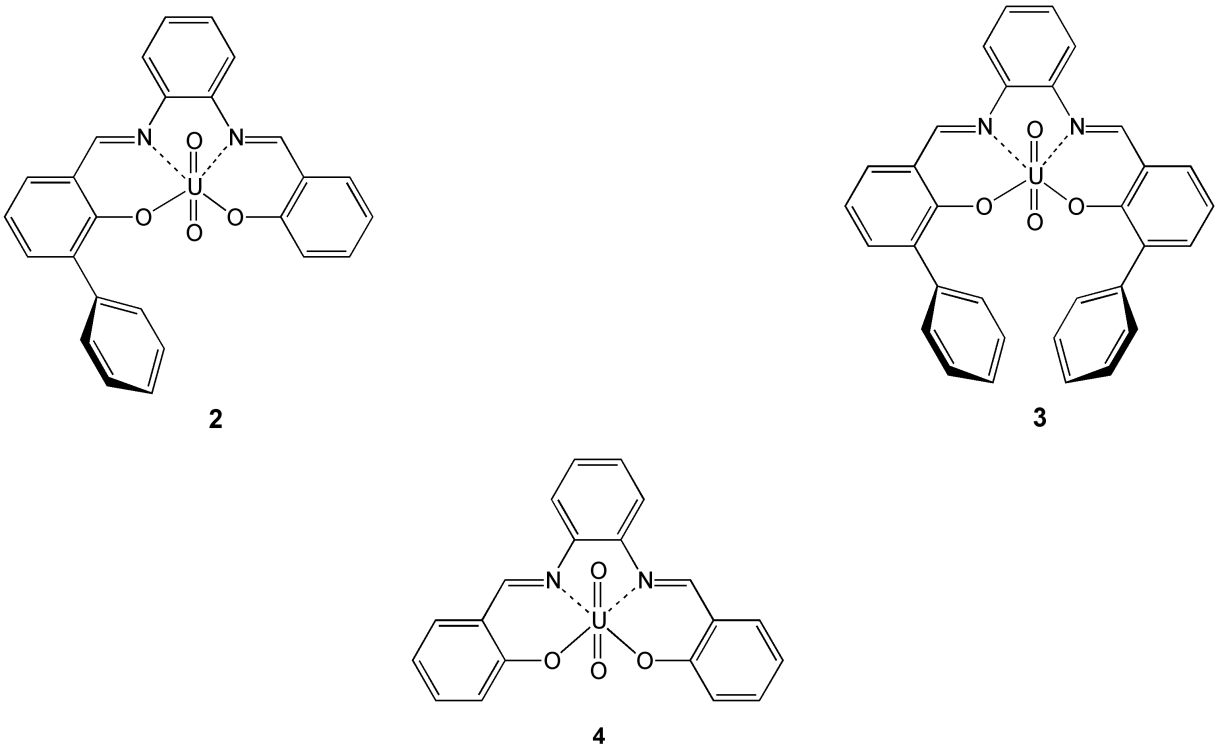

Figure 1.11 Structures of salophen-uranyl complexes **2**, **3** and **4**.

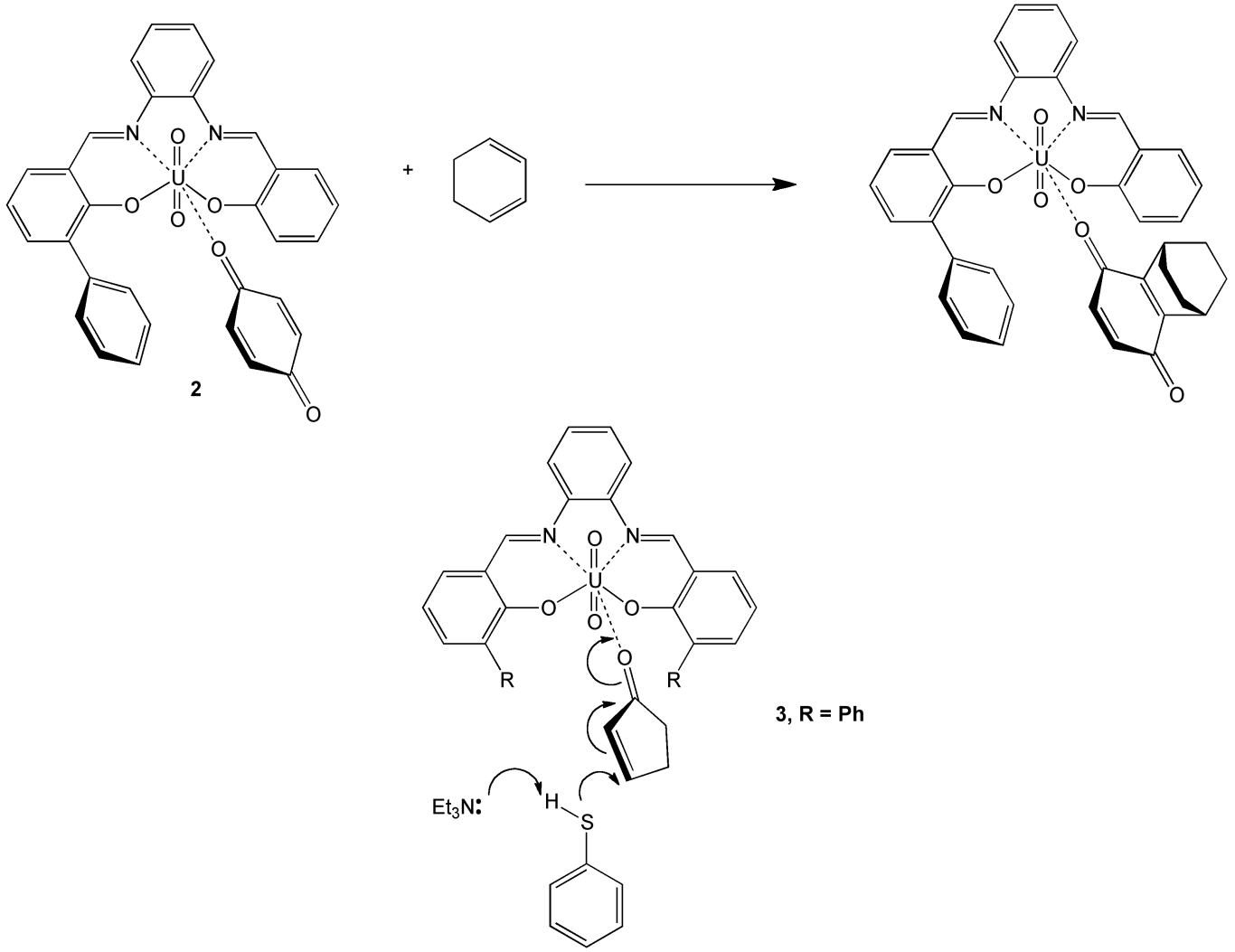

Figure 1.12 Diels-Alder reaction cycloaddition between 1,4-benzoquinone and cyclohexadiene catalyzed by receptor **2** (top) and illustration of the transition state for the Michael-type addition of thiophenol to 2-cyclopenten-1-one catalyzed by complex **3** (bottom).

The good coordinating properties of salophen-uranyl complexes, together with their ability to act as electrofilic catalysts make these molecules ideal candidates to be incorporated into dimetallic complexes potentially useful as axles of rotaxane-based switchable catalysts. In the next paragraph the features of such an ideal system and the motivations that prompted us towards the synthesis of dinuclear salophen-uranyl complexes will be adequately discussed.

1.5 Synthesis of novel dinuclear salophen-uranyl complexes.

The design and the realization of an autonomously switchable catalyst triggered by a chemical stimulus is a very intriguing task, which requires a proper selection of the components and a careful evaluation of the interactions involved in the device's switching from the inactive to the active catalytic form.

From the previous considerations on the receptorial and catalytic properties of salophen-uranyl complexes, emerges that these compounds possess good requirements for their insertion into a rotaxane-based switchable catalyst powered by a chemical fuel, whose scheme is depicted in **Fig. 1.13**.

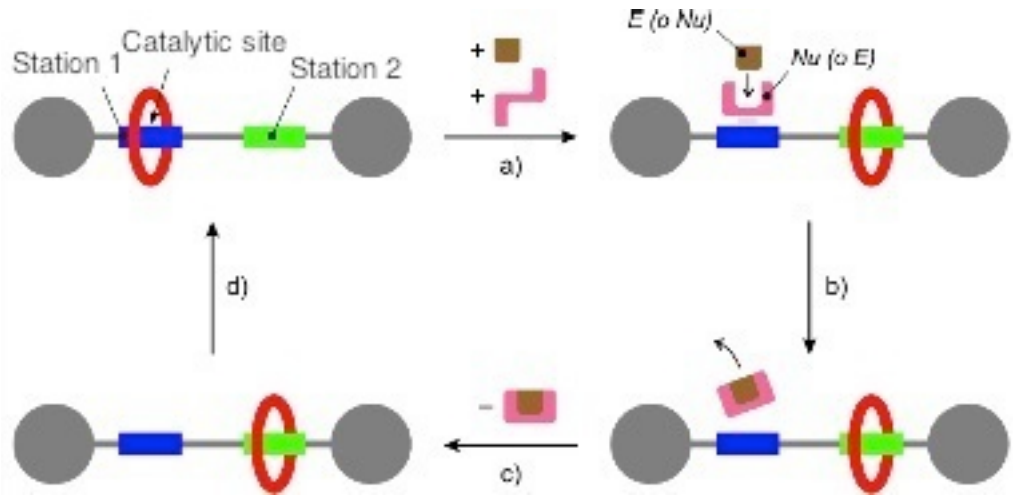

Figure 1.13 Pictorial representation of an ideal molecular shuttle powered by catalysed reaction of a chemical fuel.

In this ideal system, the macrocyclic wheel resides initially on the Station 1 (blue rectangle in **Fig. 1.13**), which can act as catalyst for a certain reaction. In the presence of a chemical species that coordinates reversibly to this site, the wheel should move on the second station (the green rectangle in **Fig. 1.13**) and remain here until the reaction of the chemical fuel is complete. Once the product is formed, it must leave the catalytic site, thus allowing the wheel to return in its initial position.

Salophen-uranyl complex **2**, decorated with a phenyl pendant, could be used as the catalytic site of a two-stationed axle. Indeed, in addition to the reversible binding of enones, ketones and aldehydes with different affinities[49c], is also able to catalyse the Diels-Alder reaction between 1,4-benzoquinone and 1,3-cyclohexadiene through electrophilic catalysis.[50e]

On the other hand, basic salophen-uranyl complex **4** could be used as the second station for the rotaxane switching. This complex binds reversibly the carbonyl compounds previously mentioned, but with a lower affinity respect to **2**. In Table 1 are reported as example the binding constant values obtained for the association between receptors **2** and **4** with a ketone (cyclopentanone) and an enone (2-cyclopenten-1-one). The higher affinity of receptor **2** for the guests considered is ascribable in both cases to hydrophobic interactions between the guest and the aromatic pendant, which summed up to the prominent Lewis acid base

interaction between the carbonyl and the uranyl centre are responsible for the strongest binding ability towards carbonyl-containing guests (Table 1).[49c] Furthermore, the enonic guest binds more strongly to receptor **2** than the corresponding unsaturated compound. This is due to the higher negative density charge on the carbonylic oxygen promoted by the direct conjugation between the double bond and the carbonyl group in the enone, which is not possible in the saturated analogue.

Table 1.1 Binding constants (K, M^{-1}) obtained for the association of receptors **2** and **4** with cyclopentanone and 2-cyclopenten-1-one (Determined by UV-Vis spectroscopy in $CHCl_3$ at 25°C)

Guest	2	4
cyclopentanone	258	< 3
2-cyclopenten-1-one	870	14

As a rule, considering a rotaxane having a macrocyclic ketone as wheel, the shuttling movement should be triggered by feeding the system with a reagent that coordinates better to the catalytic site than the wheel, ideally an enone. Once the rotaxane has been switched on, the catalytic process can take place leading to product formation. Diels-Alder reaction could be used as model reaction to test the functioning of this system, since complex **2** catalyse this reaction with high efficiency and low product inhibition. Once the product has formed, it should leave the system so that the rotaxane can switch back in its catalytically inactive form.

As a preliminary part of the work, dedicated to the synthesis of potential two-stationed axles, we decided to incorporate the two complexes **2** and **4** into the dinuclear species **14** and **17** (**Figure 1.14**).

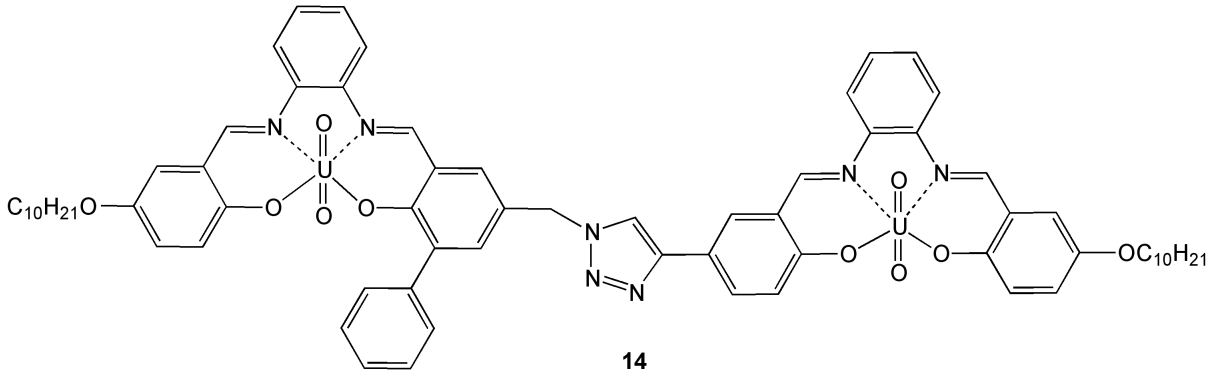

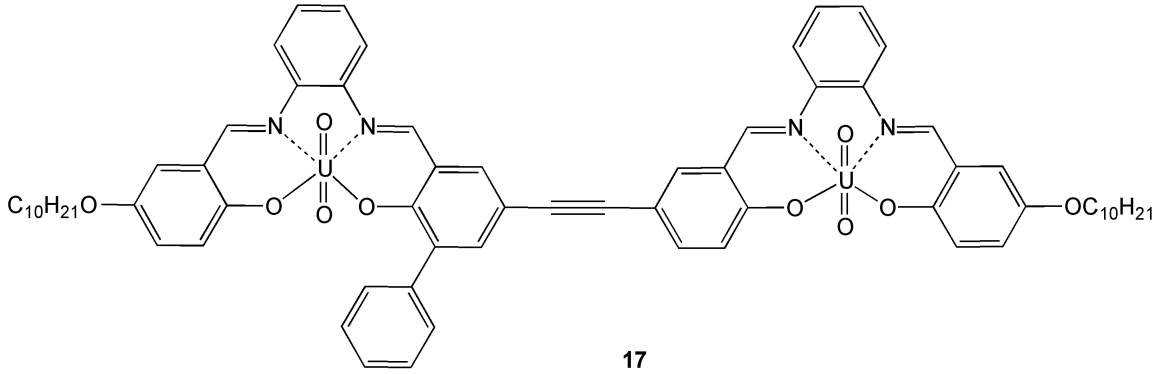

Figure 1.14 Non-symmetrically substituted complexes **14** and **17.**

2. Results and discussion

The synthetic strategies that have been adopted for the synthesis of complexes **14** and **17** involved in both cases the use of a non-symmetrical dialdehyde (**11** or **16**) and of the monoimine **9**, functionalized with a long alkyl chain.

The non-symmetrically substituted dialdehydes **11** and **16** have been prepared using coupling reactions between easily available starting materials, as described further on in this paragraph.

In **Scheme 1.2a** the synthesis of salicylaldehydes **7** and **10** is described. They were both prepared according to literature procedures starting from already available compounds **5** and **8**.[51]

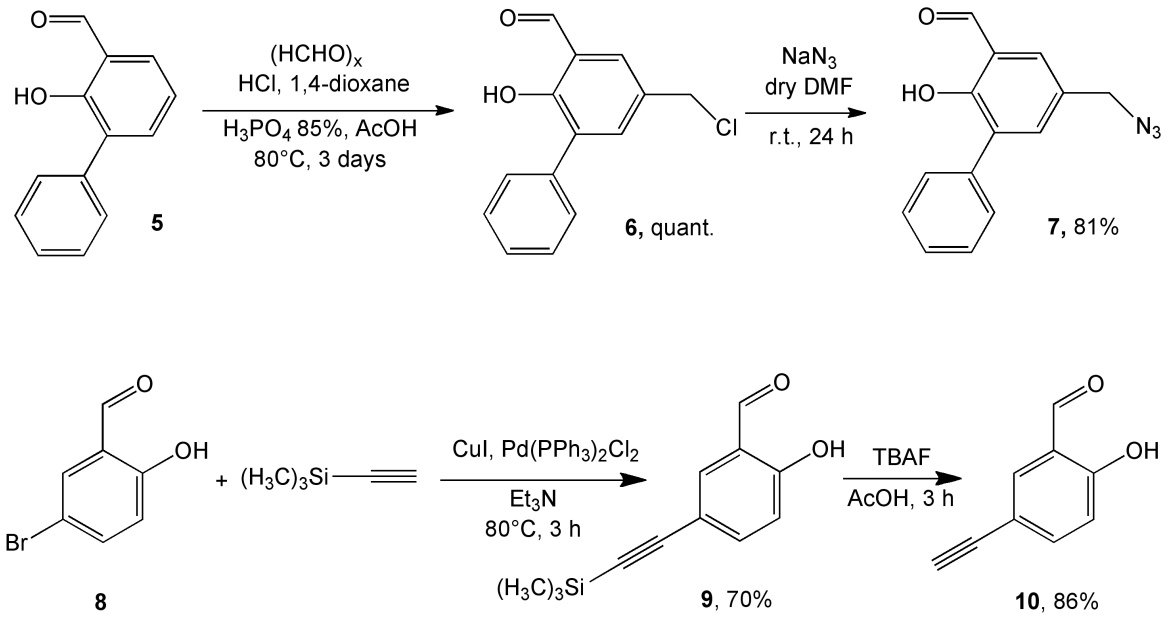

Scheme 1.2a Synthesis of compounds **7** and **10.**

These molecules were subsequently employed as starting materials for the synthesis of dialdehyde **11** using the popular copper-catalysed Huisgen 1,3-dipolar cycloaddition (CuAAC) between azide **7** and alkyne **10**.[52] For its wide applicability, the CuAAC (copper azide-alkyne cycloaddition) has been used in many different fields ranging from the biomolecule tagging[53] to the covalent coverage of surfaces[54] and it was defined as the "cream of the crop"[55] of the click-chemistry. An interesting characteristic of the CuAAC is that, unlike the non-catalyzed reaction, it is 100% regioselective and affords the anti isomer as the only product (**Fig. 1.15**).[56]

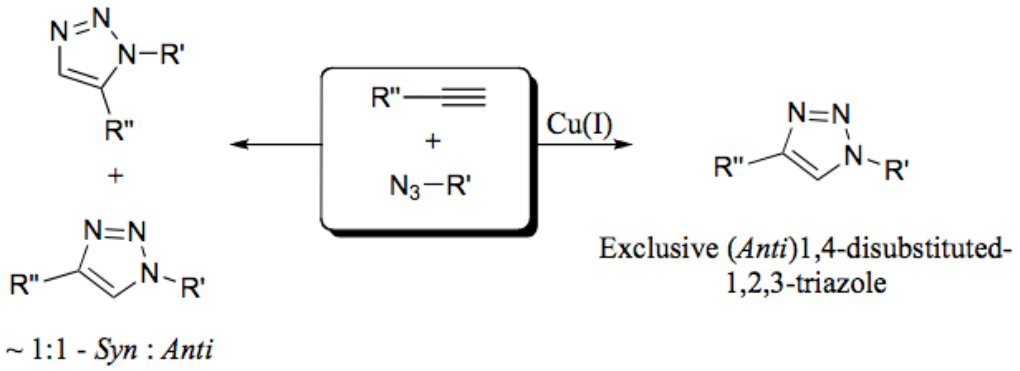

Figure 1.15 Product distribution pattern for the Cu(I) catalyzed (right) and the spontaneous (left) Huisgen-1,3-dipolar cycloaddition of an azide to an alkyne.

The synthesis of dialdehyde **11** was carried out in the classic conditions reported for the Huisgen CuAAC, using ascorbic acid as reducing agent to generate Cu(I) *in situ* (**Scheme 1.2b**).

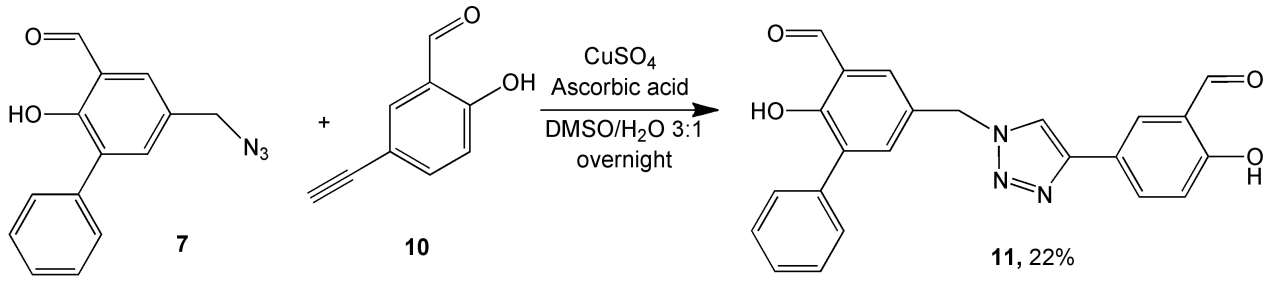

Scheme 1.2b Synthesis of compound **7.**

Monoimine **13**, the second building block required for the synthesis of complex **14**, was prepared through a simple condensation reaction between commercial 1,2-phenylenediamine and salicylaldehyde **12**, available from a previous synthesis (**Scheme 1.3**).[57] The final mixing of two equivalents of **13** with dialdehyde **11** in the presence of a stoichiometric amount of uranyl acetate dehydrate afforded complex **14** in an excellent yield (**Scheme 1.4**)

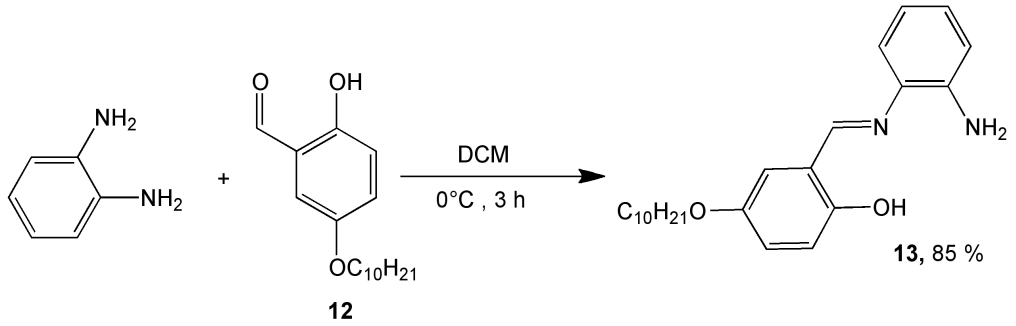

Scheme 1.3 Synthesis of the monoimine **13.**

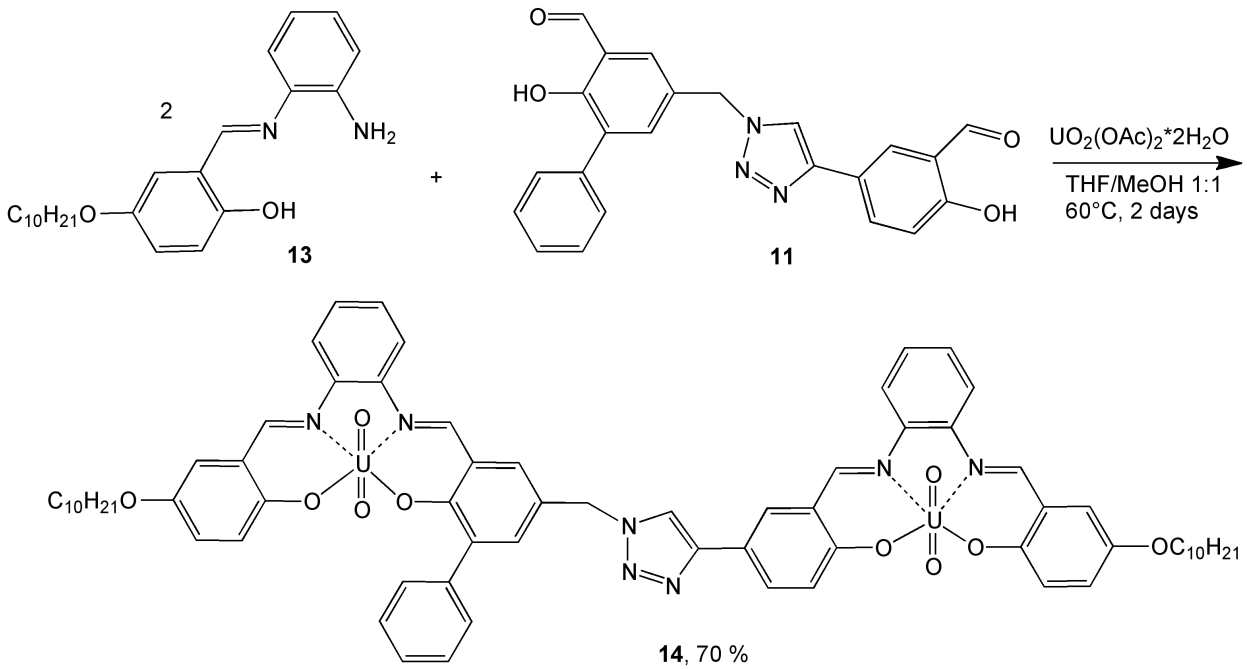

Scheme 1.4 Synthesis of complex **14.**

A modular approach similar to that used for the synthesis of dialdehyde **11** was used also for the preparation of dialdehyde **16**, precursor of complex **17**, using the Sonogashira cross-coupling reaction.

This reaction, whose general scheme is illustrated in **Scheme 1.5**, makes use of a Pd(0) catalyst (usually $Pd(PPh_3)_2Cl_2$) to promote the formation of a carbon-carbon bond between a terminal alkyne and an aryl or vinyl halide.[58] According to the postulated mechanism for this reaction, a source of Cu^+ (often provided as CuI) is also necessary as co-catalyst and for promoting the activation of the alkyne to a copper (I) acetylide.[59]

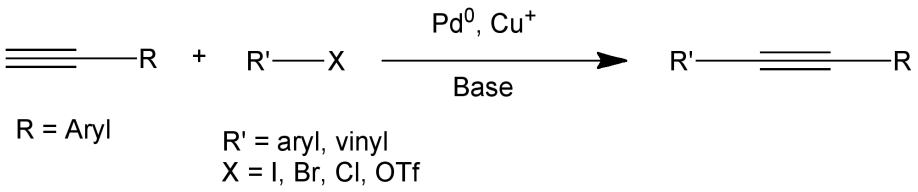

Scheme 1.5 General procedure for the Sonogashira cross-coupling reaction.

For the simplicity of its experimental conditions, this reaction has been extensively used for the synthesis of many compounds, including pharmaceuticals[60] and nanomaterials.[61]

Dialdehyde **16** was prepared according the procedure shown in **Scheme 1.6a**, starting from 5-ethynylsalicylaldehyde **10** and 5-bromo-3-phenylsalicylaldehyde **15**.[62] In its turn, compound **15** was prepared by bromination of 3-phenylsalicylaldehyde **5** with N-bromosuccinimide (NBS).[51a]

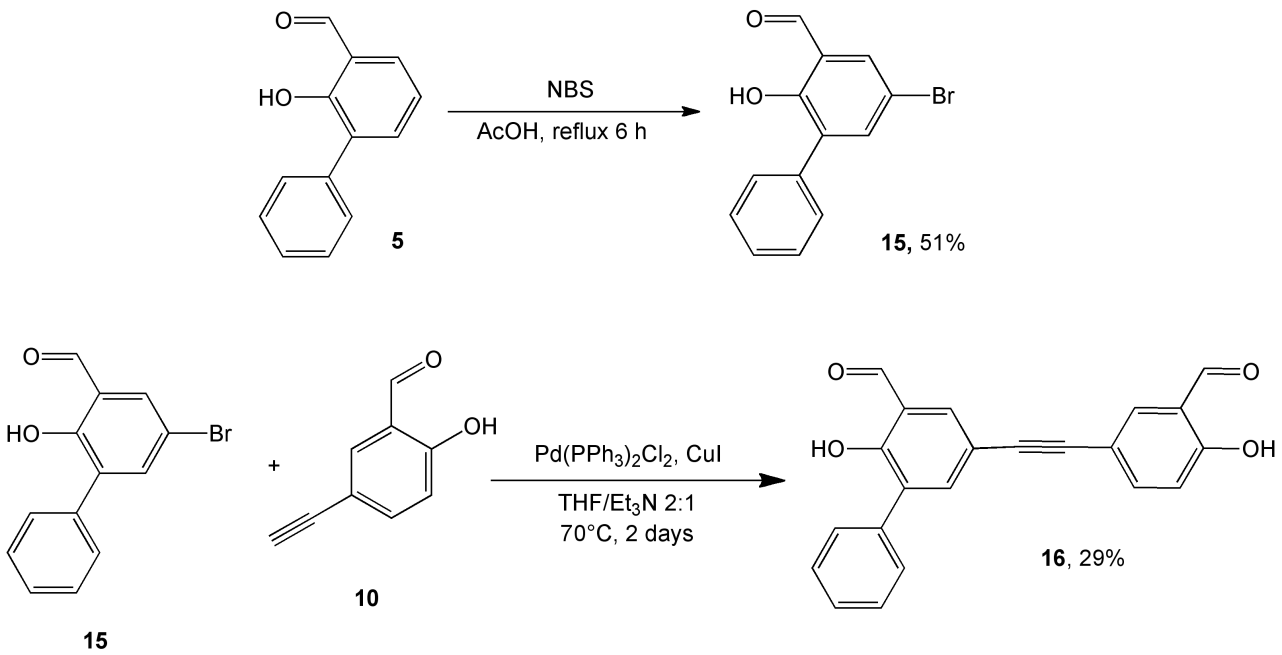

Scheme 1.6a Synthesis of compounds **15** and **16.**

The reaction of dialdehyde **16** with two equivalents of monoamine **13**, in the presence of a stoichiometric amount of uranyl acetate dehydrate, afforded complex **17** with an excellent yield (**Scheme 1.6b**).

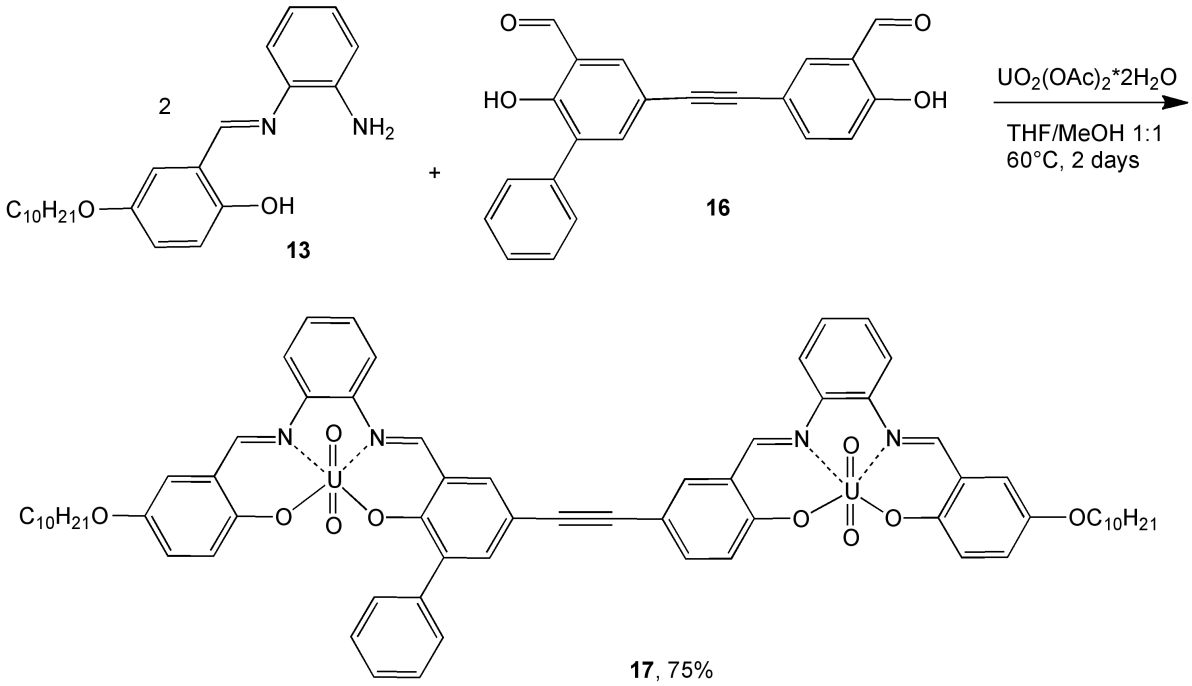

Scheme 1.6b Synthesis of complex **17.**

3. Conclusions

In conclusion, the salophen-uranyl moiety revealed to be, from a synthetic viewpoint, a good candidate for the synthesis of novel dinuclear salophen-uranyl complexes **14** and **17** (**Fig. 1.16**). These bimetallic complexes have been synthesised with high yields using a modular approach starting from properly designed dialdehydes and monoimine, and contain two different binding sites potentially able to coordinate carbonyl compounds. The presence of an aromatic sidearm appended to one of the receptorial sites is meant to influence not only its affinity towards carbonyl compounds with different electron density on the oxygen atom, but also its behaviour as electrophilic supramolecular catalyst. Nevertheless, the low solubility of these complexes in non-competitive solvents, such as chloroform or dichloromethane, did not allow us to proceed further on the investigation of their binding properties towards carbonyl compounds. The use of a non-competitive solvent, indeed, is an essential requirement for an accurate evaluation of the interactions involved in the catalytic switching processes. Future developments towards the use of these complexes for the construction of a rotaxane-based catalytic switch are the design of a suitably sized wheel and the setting up of adequate experimental conditions to monitor the shuttling/switching mechanisms in the presence of a carbonyl-containing guest.

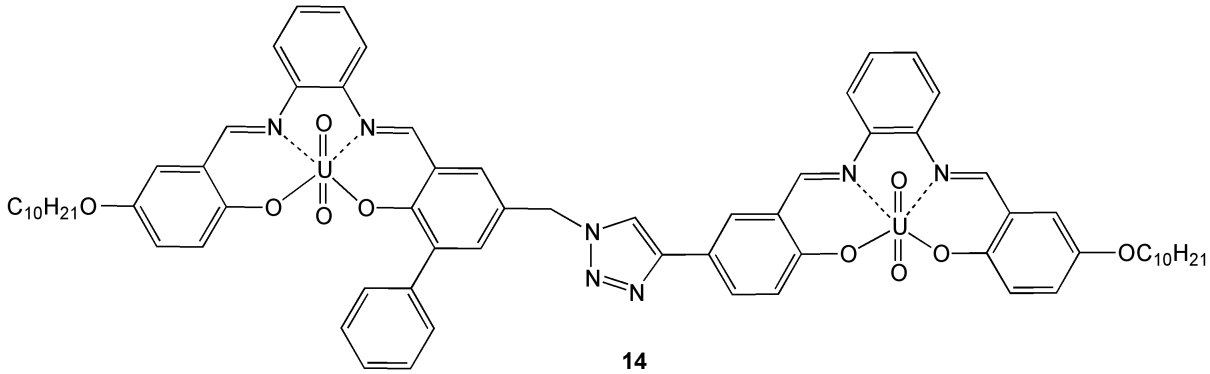

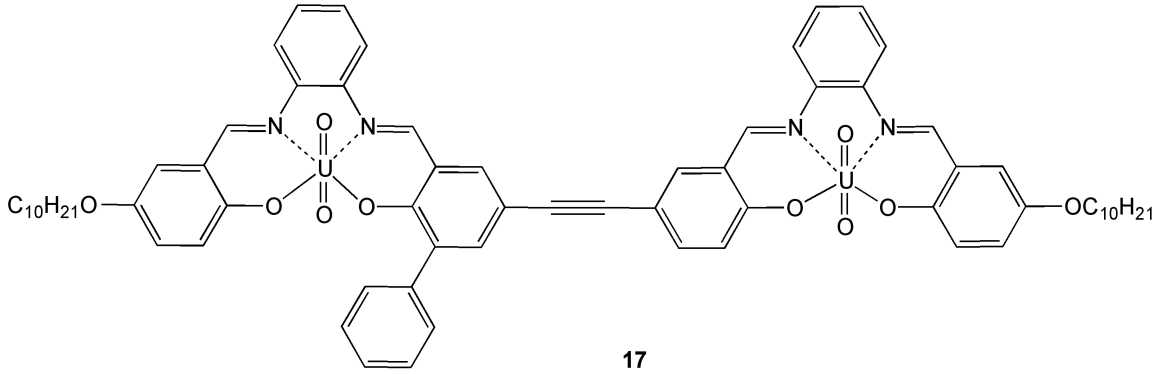

Figure 1.16 Non-symmetrically substituted complexes **14** and **17.**

4. Experimental section

Materials 2-hydroxy-[1,1'-biphenyl]-3-carbaldehyde (**5**)[51a] and 5-(decyloxy)-2-hydroxybenzaldehyde (**12**)[63] were available from previous syntheses and prepared following literature procedures. All the other chemicals were purchased from Sigma Aldrich and used as received. All the manipulations were carried out in flame-dried glassware working under inert atmosphere, unless otherwise stated. The solvents were distilled and degassed prior to their use (CH_3CN was distilled over CaH_2, DCM over KOH, THF over Na/K alloy, Et_3N over metal sodium).

Instruments and methods ^1H and ^{13}C NMR spectra were recorded either on a Bruker AC200 or AC300 instruments. ESI-MS and HRMS were obtained using a Micromass Q-TOF instrument. Elemental analyses were obtained using a EAGER 200 software for elaboration of the experimental data.

5-cloromethyl-3-phenyl-2-hydroxybenzaldehyde (6)[51b]

2-hydroxy-[1,1'-biphenyl]-3-carbaldehyde **5** (0.321 g, 1.3 mmol) was dissolved in a mixture of 1,4-dioxane (3 mL), H_3PO_4 85% (0.62 mL), glacial acetic acid (0.62 mL) and HCl 37% (29 mL). Then paraformaldehyde (0.913 g, 30.4 mmol) was added and the mixture was heated for 2 days at 80°C.

The reaction mixture was allowed to cool, and the crude product was extracted using DCM. The organic phase was separated, washed with water and dried over sodium sulphate. After evaporation of the solvent, 0.313 g of product (1.27 mmol) were obtained as pale yellow oil. Assumed yield = 100%.

^{1}H-NMR (300 MHz, $CDCl_3$) δ (ppm): 11.55 (s, 1H); 9.96 (s, 1H); 4.61 (s, 2H).

5-azidomethyl-3-phenyl-2-hydroxybenzaldehyde (7)[51c]

In a dried two-necked round-bottomed flask, compound **6** (0.313 g, 1.27 mmol) and sodium azide (0.097 g, 1.49 mmol) were charged under an argon atmosphere and dissolved in 1.2 mL of dry DMF. The reaction mixture was allowed to stir at room temperature for 24 hours.

The raw material was extracted twice with ethyl acetate (20 mL), the organic phase was washed with water (3 x 20 mL) and dried over sodium sulphate. 0.260 g of product (1.03 mmol) were obtained as a yellow oil, Y = 81%.

^{1}H-NMR (300 MHz, $CDCl_3$) δ (ppm): 11.53 (s, 1H); 10.48 (s, 1H); 7.36-7.58 (m, 7 H); 4.38 (s, 2H) **^{13}C-NMR (75 MHz, $CDCl_3$)** δ (ppm): 196.48; 158.75; 137.52; 137.38; 132.38; 129.63; 129.20; 129.16; 128.31; 128.22; 128.11; 127.91; 53.73.

5-trimethylsilylethynyl-2-hydroxybenzaldehyde (9)[51d]

In a two-necked round-bottomed flask, 5-bromo-2-hydroxybenzaldehyde **8** (1.167 g, 5.8 mmol), $Pd(PPh_3)Cl_2$ (0.161 g, 0.23 mmol) and CuI (0.071 g, 0.37 mmol) were dissolved in 19 mL of triethylamine. Then trimethylsilylacethylene (1.3 mL, 9.2 mmol) was syringed into the flask and the mixture was stirred at 80°C for 3 hours.

After cooling, the solution was filtered over a Buchner funnel and the solvent was taken off. The crude product was purified through column chromatography (SiO_2, eluent diethyl ether/n-hexane 3:2). 0.891 g of product were obtained as a yellow solid, Y = 70%.

^{1}H-NMR (300 MHz, $CDCl_3$) δ (ppm): 11.07 (s, 1H); 9.83 (s, 1H); 7.68-7.67 (d, 1H, ^{4}J = 1.8 Hz); 7.59-7.56 (dd, 1H, ^{3}J = 6.3 Hz, ^{4}J = 1.8 Hz); 6.92-6.9 (d, 1H, ^{3}J = 6.3 Hz); 0.23 (s, 9H)

5-ethynyl-2-hydroxybenzaldehyde (10)[51d]

Compound **9** (0.891 g, 4.08 mmol) was mixed with 0.25 mL of TBAF (solution 1M in THF) and glacial acetic acid (0.13 mL). The mixture was stirred for 3 hours at room temperature, then the crude product was extracted with DCM. The organic phase was then washed with water, dried over sodium sulphate and filtrated. After evaporation of the solvent, 0.513 g of product (3.51 mmol) were obtained as a pale brown solid, Y = 86%.

^{1}H-NMR (300 MHz, $CDCl_3$) δ (ppm): 11.53 (s, 1H); 10.48 (s, 1H); 7.36-7.58 (m, 7 H); 4.38 (s, 2H).

5-((4-(3-formyl-4-hydroxyphenyl)-1*H*-1,2,3-triazol-1-yl)methyl)-2-hydroxy-[1,1'-biphenyl]-3-carbaldehyde (11)

5-ethynyl-2-hydroxybenzaldehyde (**10**) (0.063 g, 0.43 mmol) and 5-azidomethyl-3-phenyl-2-hydroxybenzaldehyde (**7**) (0.149 g, 0.59 mmol) were dissolved in 12 mL of DMSO. Then $CuSO_4$ (0.027 g, 0.11 mmol in 2 mL of water) and ascorbic acid (0.034 g, 0.19 mmol in 2 mL of water) were added. After stirring for 24 hours at room temperature, the reaction mixture was poured into a separating funnel and diluited with ethyl acetate (20 mL). The organic phase was separated, washed with water and finally dried over sodium sulphate. Purification of the crude product by column chromatography (SiO_2, eluent diethyl ether) afforded 0.038 g of product as a pale yellow solid, Y = 22%.

^{1}H NMR (300 MHz, $CDCl_3$) δ (ppm): 11.57 (s, 1H); 11.02 (s, 1H); 9.93 (d, 2H, J = 2.4 Hz); 8.08 (d, 1H, J = 2.4 Hz); 7.88-7.85 (dd, 1H, J = 8.4 Hz, J = 2.4 Hz); 7.68 (s, 1H); 7.59-7.52 (m, 4H); 7.46-7.24 (m, 3H); 7.02 (d, 1H, J = 8.4 Hz); 5.59 (s, 2H) **^{13}C NMR (75 MHz, $CDCl_3$)** δ (ppm): 196.45; 196.26; 161.5; 159.24; 137.12; 134.14; 132.36; 130.69; 129.09; 128.37; 128.12; 126.07; 120.76; 118.64; 118.19; 53.23 **ESI-MS**: 422.14 ($M+Na^+$) **HRMS** (ESI-TOF): calculated for $C_{23}H_{17}N_3O_4Na^+$ 422.1117, found 422.1122

(*E*)-2-(((2-aminophenyl)imino)methyl)-4-(decyloxy)phenol (13)[57]

In a round-bottomed flask, 1,2-phenylenediamine (0.662 g, 6.12 mmol) was dissolved in 12 mL of DCM. After cooling the solution in a ice bath for 10 minutes, a solution of aldehyde **12** (1.702 g, 6.11 mmol) was added dropwise over a period of two hours, keeping the temperature below 5°C.

After the end of the addition, the reaction was left stirring at 0°C for one hour. The solvent was finally taken off, and the solid residue was triturated with cold methanol, filtered and dried under vacuum. 1.912 g of yellow monoimine (5.19 mmol) were obtained, Y = 85%.

^{1}H NMR (200 MHz, $CDCl_3$) δ (ppm): 12.54 (s, 1H); 8.57 (s, 1H); 7.16-6.76 (m, 7H); 4.02 (s, 2H); 3.95 (t, 2H, J = 6.5 Hz); 1.86-1.72 (m, 2H); 1.45 (m, 16 H); 0.92-0.86 (t, 3H, J = 6.7 Hz) **^{13}C NMR (75 MHz, $CDCl_3$)** δ (ppm): 163.32; 161.69; 155.50; 154.82; 151.83; 140.85; 135.22; 128.08; 121.41; 120.93; 119.57; 119.11; 118.76; 118.68; 118.23; 117.73; 116.22; 115.73; 68.87; 31.86; 29.56; 29.53; 29.38; 29.32; 29.29; 26.01; 22.65; 14.09 **ESI-MS**: 391.24

($M+Na^+$) **HRMS**: calculated for $C_{23}H_{32}N_2O_2Na^+$ 391.2361, found 391.2346 **Elemental analysis**: calculated for $C_{23}H_{32}N_2O_2$ C 74.96; H 8.75; N 7.6 found: C 75.08; H 9.24; N 7.51

Dinuclear complex 14

Uranyl acetate dihydrate (84.97 mg, 0.2 mmol) and compound **11** (36.60 mg, 0.092 mmol) were dissolved in a 1:1 mixture THF/methanol. The solution was heated at 60°C, then a solution of monoimine **13** (69.63 mg, 0.19 mmol in 5 mL of THF) was added dropwise over a period of one hour. The reaction mixture was left stirring at 60°C for two days.

After cooling, the reaction mixture was poured into a separating funnel with 10 mL of chloroform and 10 mL of water. The organic layer was separated and washed twice with water (10 mL). The solvent was evaporated under vacuum, and the residue was washed three times with absolute ethanol (5 mL), triturated with an excess of diethyl ether, filtered and finally washed with n-hexane (5 mL) and methanol (5 mL). After drying under high vacuum, 105.11 mg (0.064 mmol) of a dark purple solid were obtained, Y = 70%.

^{1}H NMR (300 MHz, DMSO-d_6) δ (ppm): 9.64-9.51 (m, 4H); 8.53-6.84 (m, 25H); 5.73-5.62 (m, 2H), 3.89-3.87 (m, 4H); 1.65-1.63 (m, 4H); 1.62-1.35 (m, 28H); 0.79 (m, 6H) **^{13}C NMR (75 MHz, DMSO-d_6)** δ (ppm): 170.08; 167.57; 166.91; 166.69; 166.6; 165.15; 164.99; 150.11; 149.97; 147.12; 147.00; 146.8; 139.01; 136.77; 133.61; 132.75; 130.47; 130.15; 129.17; 129.06; 128.54; 128.39; 128.05; 125.58; 125.07; 124.51; 124.39; 123.54; 121.63; 120.55; 120.14; 119.94; 118.23; 68.59; 31.65; 29.4; 29.33; 29.17; 29.06; 25.94; 22.45; 14.32 **Elemental analysis**: calculated for $C_{69}H_{73}N_7O_{10}U_2 + 2H_2O$: C 49.55, H 4.64, N 5.86. Found: C 49.24, H 4.88, N 6.56

5-bromo-2-hydroxy-[1,1'-biphenyl]-3-carbaldehyde (15)[51a]

1.023 g (5.16 mmol) of aldehyde **5** and 1.123 g (6.31 mmol) of N-bromosuccinimide (NBS) were dissolved in 15 mL of glacial acetic acid. After refluxing the mixture for three hours, it was allowed to cool and the solvent was evaporated under vacuum. The oily residual was dissolved in diethyl ether and the insoluble material filtered off. The filtrate was taken to dryness and purified via column chromatography (SiO_2, eluent toluene), to afford 0.745 g (2.69 mmol) of product, Y = 52%.

^{1}H NMR (300 MHz, $CDCl_3$) δ (ppm): 11.42 (s, 1H); 9.87 (s, 1H); 7.69-7.37 (m, 7H) **^{13}C NMR (75 MHz, $CDCl_3$)** δ (ppm): 195.73; 158.14; 139.98; 134.89; 134.78; 133.31-132.67; 131.42; 129.95; 129.19; 129.06; 128.68; 128.4; 128.21; 121.5

5-((3-formyl-4-hydroxyphenyl)ethynyl)-2-hydroxy-[1,1'-biphenyl]-3-carbaldehyde (16)[62]

Under inert atmosphere, compound **15** (0.505 g, 1.82 mmol), compound **10** (0.138 g, 0.94 mmol), PPh_3 (6 mg, 2.4% mol), $Pd(PPh_3)_2Cl_2$ (15 mg, 2.3% mol) and CuI (6 mg, 3.3% mol) were dissolved in a mixture of Et_3N (7 mL) and THF (14 mL). The reaction mixture was heated at 70°C for two days, then was poured into a separating funnel with DCM (10 mL) and HCl 1M (10 mL). The organic layer was separated, washed with HCl 1M (5 x 10 mL) and dried over sodium sulphate. Purification of the crude product by column chromatography (SiO_2, eluent toluene), afforded 0.092 g (0.27 mmol) of product as a yellow solid, Y = 29%.

^{1}H NMR (300 MHz, $CDCl_3$) δ (ppm): 11.63 (s, 1H); 11.12 (s, 1H); 9.93 (s, 1H); 9.88 (s, 1H); 7.74-7.73 (m, 3H), 7.66-7.56 (m, 3H); 7.47-7.37 (m, 3H); 6.97 (d, 1H). **^{13}C NMR (75 MHz, $CDCl_3$)** δ (ppm): 196.25; 195.97; 161.44; 158.81; 140.23; 139.62; 136.75; 135.91; 135.28; 131.13; 129.15; 128.31; 127.99; 120.71; 120.45; 118.19; 118.1; 114.85; 114.76; 87.09 **ESI-MS**: 365.09 [$M+Na^+$] **HRMS** (ESI-TOF): calculated for 365.0790, found 365.0800

Dinuclear complex 17

Dialdehyde **16** (36.21 mg, 0.11 mmol), monoamine **13** (79.02 mg, 0.22 mmol) and uranyl acetate dihydrate (101.99 mg, 0.24 mmol) were mixed using the same procedure followed for the synthesis of complex **11**. 128.95 mg of product (0.082 mmol) were obtained as a dark purple solid, Y = 75%.

^{1}H NMR (300 MHz, DMSO-d_6) δ (ppm): 9.66-9.51 (m, 4H); 8.01-6.85 (m, 24H); 3.92-3.88 (m, 4H); 1.68-1.63 (m, 4H); 1.36-1.2 (m, 28H); 0.8 (m, 6H). **^{13}C NMR (75 MHz, DMSO-d_6)** δ (ppm): 170.33; 167.81; 167.01; 166.82; 166.59; 165.15; 164.92; 164.82; 150.21; 149.97; 147.16; 147.12; 147.08; 146.96; 139.33; 138.84; 138.72; 138.55; 132.89; 130.2; 129.25; 129.06; 128.45; 127.34; 125.63; 125.54; 124.79; 123.58; 123.51; 121.9; 121.62; 120.66; 118.25; 111.09; 110.78; 87.92; 87.64; 68.59; 31.66; 29.4; 29.34; 29.17; 29.06; 25.94; 22.46;

14.32. **ESI-MS**: 1601.89 [M+Na^+] **HRMS** (ESI-TOF): calculated for 1601.6005, found 1601.6050 **Elemental analysis**: calculated for $C_{68}H_{70}N_4O_{10}U_2$ + $2CH_3OH$: C 51.16, H 4.78, N 3.41; found C 51.03, H 4.73, N 3.48

5. Bibliography

[1] Balzani, V.; Credi, A.; Venturi, M. *Chem.Eur.J.* **2002**, *24*, 5525-5532. For textbooks, see: Balzani, V.; Credi, A.; Venturi, M. *Supramolecular Science: where it is and where it is going*, Kluwer, Dordrecht, **1999**, p. 1; Balzani, V.; Credi, A.; Venturi, M. *Stimulating concepts in Chemistry* Wiley-VCH, Weinheim, **2000**, p.255.

[2] Prasad, S. *The Top-Down approach to Nanotechnology*, available on line at web.pdx.edu.

[3] Waldner, J.B. *Nanocomputers and Swarm Intelligence,* John Wiley & Sons, London, 2008, p. 205; Judy, J.W. *Smart Mater. Struct.* **2001**, *10*, 1115; Barrow, D.; Cefai, J. and Taylor, S. *Chem. Ind.* **1999**, *2*, 591; Amato, J. *Science* **1998**, *282*, 402.

[4] (a) Nanotechnology Now: MEMS and Nanotech in Inkjet Printing, http://www.nanotech-now.com/columns/?article=034. (b) Miyake, R.; Okabe, S.; Sakamoto, K.; Murakami, Y. and Ishikawa, T. *"Paper MEMS chip for ink-jet printer-like clinical auto analyser",* 14th International Conference on Miniaturized Systems for Chemistry and Life Sciences, 3-7 October 2010, Groningen, The Netherlands. (c) Khoshnoud, F.; de Silva, C.W. *Instrumentation & Measurement Magazine*, **2012**, *15*, 8-14.

[5] Feynman, R.P. *Eng.Sci.* **1960**, *23*, 22 and *Saturday Rev.* **1960**, *43*, 45. See also www.its.caltech.edu/feynman.

[6] Drexler, K.E. *Engines of Creation, The Coming Era of Nanotechnology*, Anchor Press, New York, **1986**.

[7] Pedersen, C.J. *Angew. Chem.* **1988**, *100*, 1053 and *Angew. Chem. Int. Ed. Engl.* **1988**, *27*, 1021; Cram, D.J. *Angew. Chem.* **1988**, *100*, 1041 and *Angew. Chem. Int. Ed. Engl.* **1988**, *27*, 1009; Lehn, J.M. *Angew. Chem.* **1988**, *100*, 91 and *Angew. Chem. Int. Ed. Engl.* **1988**, *27*, 89.

[8] (a) Aviram, A.; Ratner, M.A. *Chem. Phys. Lett.* **1974**, *29*, 277. (b) *Molecular Electronic Devices*, Dekker, New York, **1982**. (c) *Molecular Electronic Devices II*, Dekker, New York, **1987**. (d) *Molecular Electronic Devices*, Elsevier, Amsterdam, **1988**. (e) *Molecular Electronics–Science and Technology*, Engeneering Foundation, New York, **1989**. (f) Miller, J.S. *Adv. Mater.* **1990**, *2*, 378. (g) Miller, J.S. *Adv. Mater.* **1990**, *2*, 495. (h) Miller, J.S. *Adv. Mater.* **1990**, *2*, 603. (i) Metzger, R.M.; Panetta, C.A. *New J. Chem.* **1991**, *15*, 209. (j) Mirkin, C.A.; Ratner, M.A. *Annu. Rev. Phys. Chem.* **1992**, *43*, 719.

[9] (a) Shinkai, S.; Nakaji, T.; Ogawa, T.; Shigematsu, K.; Manabe, O. *J. Am. Chem. Soc.* **1981**, *103*, 111. (b) Seta, P.; Bienvenue, E.; Moore, A.L.; Mathis, P.; Bensasson, R.V.; Liddell, P.; Pessiky, P.J.; Joy, A.; Moore, T.A.; Gust, D. *Nature* **1985**, *316*, 653. (c) Alpha, B.; Balzani, V.; Lehn, J.M.; Perathoner, S.; Sabbatini, N. *Angew. Chem.* **1987**, *99*, 1310; *Angew. Chem. Int. Ed. Engl.* **1987**, *26*, 1266.

[10] (a) *Single Molecule Spectroscopy* (Eds.: R. Rigler, M. Orrit, I. Talence, T. Basché), Springer, Berlin, **2001**. (b) Moerner, W.E. *J. Phys. Chem. B* **2002**, *106*, 910. (c) *Single Molecule Detection in Solution* (Eds.: Ch. Zander, J. Enderlein, R. A. Keller), Wiley-VCH, Weinheim, **2002**.

[11] Hla, S.W.; Meyer, G.; Rieder, K.H. *ChemPhysChem* **2001**, *2*, 361.

[12] Schulz, W. *Chem. Eng. News* **2000**, *78*, 41.

[13] See, for example: Christ, T.; Kulzer, F.; Bordat, P.; Basché, T. *Angew. Chem.* **2001**, *113*, 4323; *Angew. Chem. Int. Ed.* **2001**, *40,* 4192.

[14] Ballardini, R.; Balzani, V.; Credi, A.; Gandolfi, M.T., Venturi, M. *Acc. Chem. Res.* **2001**, *34*, 445-455 and references cited therein.

[15] Browne, W.R.; Feringa, B.L. *Nature Nanotechnology* **2006**, *1*, 25-35.

[16] Roux, B. *Molecular Machines* World Scientific, Hackensack, **2011**.

[17] Knowles, J.R. *Annu. Rev. Biochem.* **1980**, *49*, 877-919; Boyer, P.D. *Annu. Rev. Biochem.* **1997**, *66*, 717-749; Stock, D. Leslie, A.G.W.; Walker, J.E. *Science* **1999**, *286*, 1700-1705; Junge, W.; Lill, H.; Engelbrecht, S. *Trend in Biochemical Sciences,* **1997**, *22*, 420-423.

[18] (a) Kelly, T. R.; De Silva, H.; Silva, R. A. *Nature*, **1999**, *401*, 150–152. (b) Fletcher, S. P.; Dumur, F.; Pollard, M. M.; Feringa, B. L. *Science*, **2005**, *310*, 80–82. (c) Leigh, D. A.; Wong, J. K. Y.; Dehez, F.; Zerbetto, F. *Nature* **2003**, *424*, 174–179.

[19] Stoddart, J.F. *Chem .Soc .Rev.* **2009**, *38*, 1802-1820.

[20] Molecular Catenanes, Rotaxanes and Knots: A Journey Through the World of Molecular Topology, ed. J. P. Sauvage and C. Dietrich-Buchecker, Wiley-VCH, Weinheim, **1999**. Breault, G.A.; Hunter, C.A. and Mayers, P.C. *Tetrahedron,* **1999**, *55*, 5265-5293.

[21] Safarowsky, O.; Nieger, M.; Fröhlich, R. and Vögtle, F. *Angew. Chem. Int. Ed.* **2000**, *39,* 1616-1618.

[22] Vögtle, F. and Lukin, O. *Angew. Chem. Int. Ed.* **2005**, *44*, 1456-1477.

[23] Ayme, J.F.; Beves, J. E.; Leigh, D.A.; McBurney, R.T.; Rissanen, K. and Schultz, D. *Nature Chem.* **2012**, *4*, 15-20. Chichak, K.S.; Cantrill, S.J.; Pease, A.R.; Chin, S.-H.; Cave, G.W.V.; Atwood, J.L and Stoddart, J.F. *Science* **2004,** *304*, 1308-1312.

[24] Schill, G.; Zollenkopf, H. *Nachr. Chem. Tech.* **1967**, *15*, 149-151.

[25] Harrison, T; Harrison, S. *J. Am. Chem. Soc.* **1967**, *89*, 5723-5724.

[26] Dietrich-Buchecker, C.O.; Sauvage, J.P.; Kintzinger, J.P. *Tetrahedron Lett.* **1983**, *24*, 5095-5098. Dietrich-Buchecker, C.O.; Sauvage, J.P *Chem. Rev.* **1987**, *87*, 795-810.

[27] Amabilino, D. and Stoddart, J.F. *Chem. Rev.* **1995**, *95*, 2725-2828.

[28] Spruell, J.M.; Dichtel, W.R.; Health, J.R.; Stoddart, J.F. *Chem. Eur. J.* **2008**, *14*, 4168. Coutrot, F.; Busseron, E. *Chem. Eur. J.* **2009**, *15*, 5186. Dichtel, W.R.; Miljanić, O.Š.; Spruell, J.M.; Heath, J.R and Stoddart, J.F. *J. Am. Chem. Soc.* **2006**, *128*, 10388. Mullen, K.M.; Gunter, M.J. *J. Org. Chem.* **2008**, *73,* 3336.

[29] Williams, A.R.; Northrop, B.H.; Chang, T.; Stoddart, J.F.; White, A.J.P.; Williams, D.J. *Angew. Chem.* **2006,** *118*, 6817 and *Angew. Chem. Int. Ed.* **2006**, *45*, 6665.

[30] Mullen, K.M.; Mercurio, J.; Serpell, C.J.; Beer, P.D. *Angew. Chem.* **2009,** *121***,** 4875.

[31] Leigh, D.A.; Morales, M.A.F.; Perez, E.M.; Wong, J.K.Y. et al. *Angew. Chem*. **2005**, *117*, 3122 and *Angew. Chem*. *Int. Ed.* **2005**, *44*, 3062.

[32] Aucagne, V; Berna, J.; Crowley, J.D.; Goldup, S.M.; Hänni, K.D.; Leigh, D.A.;Lusby, P.J.; Ronaldson, V.E.; Slawin, A.M.Z.; Viterisi, A and Walkers, D.B. *J. Am. Chem. Soc.* **2007**, *129*, 11950-11963.

[33] *Molecular Switches, Vol. 1 and 2*, eds B.L. Feringa and W.R. Browne, Wiley-VCH, Weinheim, **2011**.

[34] Prasanna de Silva, A. "Molecular logic gates" in *Supramolecular Chemistry: From Molecules to Nanomaterials* eds. P.A. Gale and J.W. Steed, Wiley, **2012**.

[35] Shipway, A.N.; Katz, E. and Willner, I. *Molecular Memory and Processing Devices in Solution and on Surfaces* in " Molecular Machines and Devices" *Structure & Bonding*, **1999**, 237-281.

[36] Collier, C. P.; Wong, E. W.; Belohradsky, M. et al. *Science* **1999**, *285*, 391–394. Collier, C. P.; Mattersteig, G.; Wong, E. W. et al. *Science* **2000**, *289*, 1172–1175.

[37] Green, J. E.; Choi, J. W.; Boukai, A. et al. *Nature* **2007,** *445*, 414–417.

[38] Coutrot, F.; Busseron, E. *Chem. Eur. J.* **2008**, *14*, 4784-4787. Coutrot, F.; Busseron, E. and Montero, J.L. *Org. Lett.* **2008**, *10*, 753-756. Archut, A.; Müller, W.M.; Baumann, S.; Habel, M and Vögtle, F. *Liebigs Ann./Recl.* **1997**, 495-499. Ashton, P.R.; Everitt, S.R.L.; Gomez-Lopez, M.; Jayaraman, N. and Stoddart, J.F. *Tetrahedron Lett.* **1997**, *38*, 5691-5694

[39] (a) Davidson, G. J. E.; Sharma, S.; Loeb, S. J. *Angew. Chem., Int. Ed.* **2010**, *49***,** 4938–4942. (b) Yen, M.-L.; Chen, N.-C.; Lai, C.-C.; Liu, Y.-H.; Peng, S.-M.; Chiu, S.-H. *Dalton Trans.* **2011**, *40***,** 2163–2166. (c) Ishiwari, F.; Nakazono, K.; Koyama, Y.;

Takata, T. *Chem. Comm.* **2011**, *47***,** 11739–11741. (d) Tokunaga, Y.; Kawabata, M.; Matsubara, N. *Org. Biomol. Chem.* **2011**, *9*, 4948–4953. (e) Iijima, T.; Vignon, S.A.; Tseng, H.-R.; Jarrosson, J.K.; Sanders, M.; Marchioni, F.; Venturi, M.; Apostoli, E., Balzani, V. and Stoddart, J.F. *Chem. Eur. J.* **2004,** *10*, 6375.

[40] (a) Keaveney, C. M.; Leigh, D. A. *Angew. Chem., Int. Ed*. **2004**, *43*, 1222–1224. (b) Laursen, B.W.; Nygaard, S.; Jeppesen, J. O.; Stoddart, J. F. *Org. Lett.* **2004**, *6***,** 4167–4170. (c) Lin, C.-F.; Lai, C.-C.; Liu, Y.-H.; Peng, S.-M.; Chiu, S.-H. *Chem. Eur. J.* **2007**, *13***,** 4350–4355. (d) Huang, Y.-L.; Hung, W.-C.; Lai, C.-C.; Liu, Y.-H.; Peng,S.-M.; Chiu, S.-H. *Angew. Chem., Int. Ed.* **2007**, *46***,** 6629–6633. (e) Barrell, M. J.; Leigh, D. A.; Lusby, P. J.; Slawin, A. M. Z. *Angew. Chem. Int. Ed.* **2008**, *47***,** 8036–8039. (f) Ng, K.-Y.; Felix, V.; Santos, S. M.; Reesa, N. H.; Beer, P. D. *Chem. Comm***.** **2008**, 1281–1283. (g) Lin, T.-C.; Lai, C.-C.; Chiu, S.-H. *Org. Lett.* **2009**, *11***,** 613–616

[41] You, Y.-C.; Tzeng, M.-C.; Lai, C.-C.; Chiu, S.H.; *Org. Lett.* **2012**, *14*, 1046-1049.

[42] Lüning, U. *Angew. Chem. Int. Ed.* **2012**, *51*, 8163-8165 and references cited therein.

[43] Blanco, V.; Carlone, A.; Hänni, K.D.; Leigh, D.A.; Lewandowski, B. *Angew. Chem. Int. Ed.* **2012**, *124*, 5256-5259 and *Angew. Chem. Int. Ed.* **2012**, *51*, 5166-5169.

[44] Traut. T. *Allosteric Regulatory Enzymes*, Springer, New York, **2008**.

[45] Vigato, P.A.; Tamburini, S. *Coord. Chem. Rev,* **2004**, *248*, 1717.

[46] Sessler, J.L.; Melfi, P.J.; Dan Patos, G. *Coord. Chem. Rev.* **2006**, *250*, 816-843.

[47] Bandoli, G.; Clemente, D.A.; Croatto, U.; Vidali, M. and Vigato, P.A. *J. Chem. Soc. D*, **1971**, 1330-1331.

[48] Dalla Cort, A.; Mandolini, L.; Pasquini C. and Schiaffino, L. *New. J. Chem.* **2004**, *28*, 1198-1199.

[49] (a) Van Doorn, A.R.; Verboom, W.; Reinhoudt, D.N. "Molecular recognition of neutral molecules by synthetic receptors" in *Advances in Supramolecular Chemistry*, **1993**, *3*, 159-206 (JAI Press, Greenwich). (b) Antonisse, M.M.G.; Reinhoudt, D.N. *Chem. Comm.* **1998**, 443–448. (c) van Axel Castelli, V.; Dalla Cort, A.; Mandolini, L.; Pinto, V.; Reinhoudt, Snellink-Ruel, B.H.M. *Supramol. Chem.* **2002**, *14*, 211–219. (d) Dalla Cort, A.; Pasquini, C.; Miranda Murua, J.I.; Pons, M.; Schiaffino, L. *Chem. Eur. J.* **2004**, *10*, 3301–3307. (e) Cametti, M.; Nissinen, M.; Dalla Cort, A.; Mandolini, L.; Rissanen, K. *J. Am. Chem. Soc.* **2007**, *129*, 3641–3648.

[50] (a) van Axel Castelli, V.; Cacciapaglia, R.; Chiosis, G.; van Veggel, F.C.J.M.; Mandolini, L.; Reinhoudt, D.N. *Inorg. Chim. Acta* **1996,** *246*, 181. (b) van Axel Castelli, V.; Dalla Cort, A.; Mandolini, L.; Reinhoudt, D.N. *J. Am. Chem. Soc.* **1998**, *120*, 12688–12689. (c) van Axel Castelli, V.; Dalla Cort, A.; Mandolini, L.;

Reinhoudt, D.N.; Schiaffino, L. *Chem. Eur. J.* **2000**, *6*, 1193–1198. (d) van Axel Castelli, V.; Dalla Cort, A.; Mandolini, L.; Reinhoudt, D.N.; Schiaffino, L. *Eur. J. Org. Chem.* **2003**, *62*, 7–633. (e) Dalla Cort, A.; Mandolini, L.; Schiaffino, L. *Chem. Comm.* **2005**, 3867–3869. (f) van Axel Castelli, V.; Dalla Cort, A.; Mandolini, L.; Pinto, V.; Schiaffino, L. *J. Org. Chem.* **2007**, *72*, 5383–5386; (g) Dalla Cort, A.; Mandolini, L.; Schiaffino, L. *J. Org. Chem.*, **2008**, 73, 9439-9442.

[51] (a) Verner, E.; Katz, B. A.; Spencer, J. R.; Allen, D.; Hataye, J.; Hruzewicz, W.; Hui, H. C.; Kolesnikov, A.; Li, Y.; Luong, C.; Martelli, A. et al. *J. Med. Chem.* **2001**, *44*, 2753-2771. (b) Ciogli, A.; Dalla Cort, A; Gasparrini, F.; Lunazzi, L.; Mandolini, L.; Mazzanti, A.; Pasquini, C.; Pierini, M.; Schiaffino, L.; Yafteh Mihan, F. *J. Org. Chem.* **2008**, *73*, 6108–6118. (c) Ayala, V.; Corma, A.; Iglesias, M.; Rincon, J. A.; Sanchez, F. *Journal of Catalysis* **2004**, *224*, 170-177. (d) Beyer, C.; Wagenknecht, H.A. *J. Org. Chem.* **2010**, *75*, 2752 – 2755.

[52] Amblard, F.; Cho, J.H.; Schinazi, R.F. *Chem. Rev.*, **2009**, *109*, 4207-4220.

[53] Ami, T; Fujimoto, K. *ChemBioChem*, **2008**, *9*, 2071-2074.

[54] (a) Rozkiewicz, D.I.; Jańczewski, D.; Verboom, W.; Ravoo, D.J.; Reinhoudt, D.N. *Angew. Chem. Int. Ed.* **2006**, *45*, 5292-5296. (b) Balachander, N.; Sukenik, C.N. *Langmuir* **1990**, *6*, 1621-1627.

[55] (a) Kolb, H.C.; Finn, M.G.; Sharpless, K.B. *Angew. Chem. Int. Ed.* **2001**, *40*, 2004-2021. (b) Moses, J.E.; Moorhouse, A.D. *Chem. Soc. Rev.* **2007**, *36*, 1249-1262.

[56] (a) Sharpless, K.B.; Manetsch, R. *Expert Opin. Drug Disc.*, **2006**, *1*, 525-538. (b) Tornøe, C.W.; Christensen, C.; Meldal, M. *J. Org. Chem.* **2002**, *67*, 3057-3064. (c) Rostovtsev, V.V.; Green, L.G.; Fokin, V.V.; Sharpless, K.B. *Angew. Chem. Int. Ed.* **2002**, *41*, 2596-2599.

[57] Li, J.Z.; Wang, Y.; Zeng, W.; Quin, S.Y. *Supramol. Chem.* **2008**, *20*, 249-254.

[58] (a) Sonogashira, K.; Tohda, Y.; Hagihara, N. *Tetrahedron Lett.*, **1975**, *16*, 4467-4470. (b) Sonogashira, K. *J. Organometallic Chem.*, **2002**, *653*, 46-49.

[59] (a) Chinchilla, R.; Najera, C. *Chem. Rev.* **2007**, *107*, 874-922. (b) Chinchilla, R.; Najera, C. *Chem. Soc. Rev.* **2011**, *40*, 5084-5121.

[60] (a) Bleicher, L.S.; Cosford, N.D.P.; Herbaut, A.; McCallum, J.S.; McDonald, I.A. *J. Org. Chem.* **1998**, *63*, 1109-1118. (b) King, A.O.; Yasuda, N. *Top. Organomet. Chem.* **2004**, *6*, 205-245.

[61] (a) Xue, C.; Arumugam, G.; Palaniappan, K.; Hackney, S.A.; Liu, H.; Liu, J. *Chem. Comm.* **2005**, *8*, 1055-1057. (b) Lin, J.C.; Kim, J.H.; Kellar, J.A.; Hersam, M.C.; Nguyen, S.T.; Bedzyk, M.J. *Langmuir*, **2010**, *26*, 3771-3773.

[62] Kuo, K; Huang, C.; Lin, Y. *Dalton Trans.* **2008**, 3889-3898.

[63] Ilaria Giannicchi, Ph.D thesis, **2011.**

CHAPTER 2

Non-symmetrically substituted salophen-uranyl complexes as receptors for ion pairs in solution.

During the last decades, a number of receptors able to bind charged species have been synthesised, allowing the recognition of anions and cations to become a well-established research field in Supramolecular Chemistry. In order to point out the counterion's role in modulating the strength and the selectivity of the recognition process, many research teams have been focusing their efforts towards the design of receptors able to bind simultaneously both the anion and the cation of an ion pair.

In the first part of the chapter, the quest for ion pair recognition and the approaches followed so far to achieve this purpose is introduced, with particular emphasis on the use of tailored salen/salophen-uranyl complexes as valid ion-pair receptors both in solution and in the solid state. In the second part, the synthesis of new salophen-uranyl receptors is reported and after a brief overview on the spectrometric methods used for the quantitative assessment of the binding constants, the results obtained using these compounds for ion pair recognition are illustrated.

1. Introduction.

1.1 The question for Ion-pair recognition: general remarks.

The supramolecular recognition of anionic and cationic species has attracted an increasing attention from many researchers, due to the important roles played by charged species both in biological and in environmental processes. In the human body, indeed, many cofactors[1] and enzymes substrates are anionic molecules, and DNA itself is a polyanion. Many neurotransmitters, as the acetylcholine, are instead ammonium ions, while cations such as sodium and calcium are involved in fundamental processes like the nerve signals transmission.[2]

Despite the number of synthetic anion[3] or cation[4] receptors published so far, only in recent times the role of counterion in modulating the strength and the selectivity of the recognition process has been taken into account. In fact we have to consider that the two partners of an ion pair hardly exist as separated ions, unless using a strongly solvating medium.

Broadly speaking, we can distinguish three different types of ion pairs in solution, as depicted in **Fig. 2.1**. In polar solvents the solvation energy is high enough to overcome the electrostatic mutual attraction of ion pairs, and consequently the predominant species are solvent-separated ion pairs. In less polar media, instead, ions are poorly solvated and form either contact ion pairs, where the two partners are bound through electrostatic interactions, or aggregated contact ion pairs in which a number of ions form a small cluster, solvated by the surrounding medium.[5]

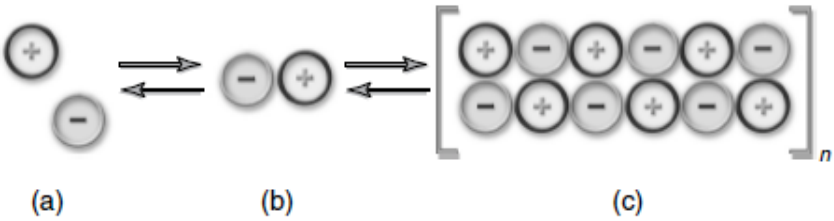

Figure 2.1 Possible states of ions in solution: (a) solvent-separated ion pair; (b) contact ion pair; (c) aggregated contact ion pairs.

Working with synthetic receptors in organic solvents, where the competition between the receptor and the counterion for the charged guest is not negligible, the best way to circumvent this problem implies the insertion of two different binding sites into the receptor, one for the anion and one for the cation.[6] Most of the ion pair receptors make use of hydrogen bond donors or Lewis acidic sites for the recognition of the anion[1, 3], whereas crown ethers[7] and calixarenes[8] are the most frequently used moieties for the recognition of the cation.

The use of ditopic receptors able to accommodate an ion pair could be advantageous in terms of strength and selectivity of binding. Indeed, these species might show an allosteric behaviour in the binding process, so that the affinity of the receptor toward an ion could be induced by the other through conformational effects and electrostatic interactions.[6]

1.2 Classification of ion pair receptors.

As pointed out by Sessler[6c] in his recent review on this topic, ion pair receptors can bind ion pairs in a sequential or in a concurrent fashion. In the sequential binding mode a first ion binds to the receptor, becoming itself the binding sites for its counterion. Once bound, the first ion enhances the affinity of the receptor for its counterion through an allosteric effect. By contrast, in the concurrent binding the receptors bind simultaneously the two ions, which can be separated by one or more solvent molecule or by the receptor skeleton. Another

classification can be made on the basis of how the ion pair is accommodated within the receptor molecule. The three limit situations are schematically depicted in **Fig. 2.2**.

In the first example, defined a *cascade receptor* (**Fig. 2.2**, a), the distance between the two binding functionalities is so short as to allow the sequential binding of a contact ion-pair. As the distance between the two binding sites increases, the receptor can either accommodate a solvent-bridged ion pair (**Fig. 2.2**, b) or separate completely the two ions in different compartments (host-separated ion pair, **Fig. 2.2**, c).[6b]

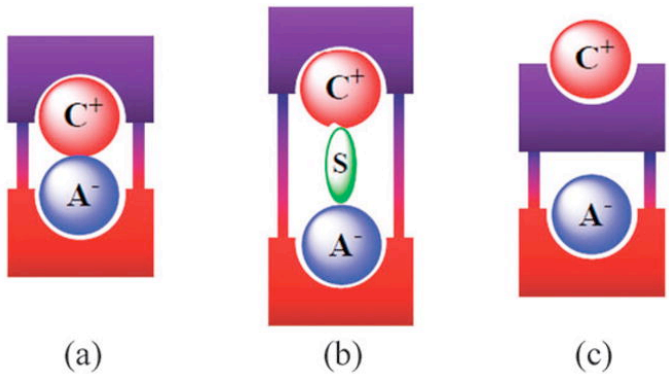

Figure 2.2 Schematic representations of the three limit binding modes for ion pairs. (a) Contact ion-pair; (b) Solvent-bridged ion pair; (c) host-separated ion pair.

1.3 Use of salen/salophen-uranyl moieties for anion complexation in ion pair receptors.

Amongst the great number of structural motifs used to achieve complexation of both components of an ion pair, in this paragraph our attention will be focused on some selected examples of ion pair receptors that make use of salen/salophen-uranyl moieties for anion recognition, in combination with different motifs for cation complexation.

Salen- and the related salophen-uranyl complexes have been used by a number of research teams for the construction of ion pair receptors.[9] The reasons for this choice are essentially the well-known ability of uranyl dication to bind anions, together with the countless synthetic routes to functionalize the salen/salophen backbone with groups able to bind cations.

Reinhoudt and coworkers were the first to perceive the potentialities offered by the salen-uranyl unit in the design of ion pair receptors **1** and **2**, shown in **Fig. 2.3**.

Cyclic voltammetry and FAB-mass spectrometry revealed that receptor **1**, in which the salen-uranyl unit is covalently linked to two benzo[15]crown-5 rings, binds K^+ and $H_2PO_4^-$

concurrently. The K^+ is sandwich-complexed by the two crown ether rings, while the phosphate anion interacts with the Lewis-acidic uranyl group.[10]

Receptor **2**, which makes use of a calix[4]arene tetraethylester subunit as a cation recognition site, was found to bind simultaneously Na^+ and $H_2PO_4^-$ to give a complex (**2** : NaH_2PO_4) with a 1:1 stoichiometry: the high affinity of Na^+ for its recognition site has been carefully exploited for the correct design of the receptor.[11]

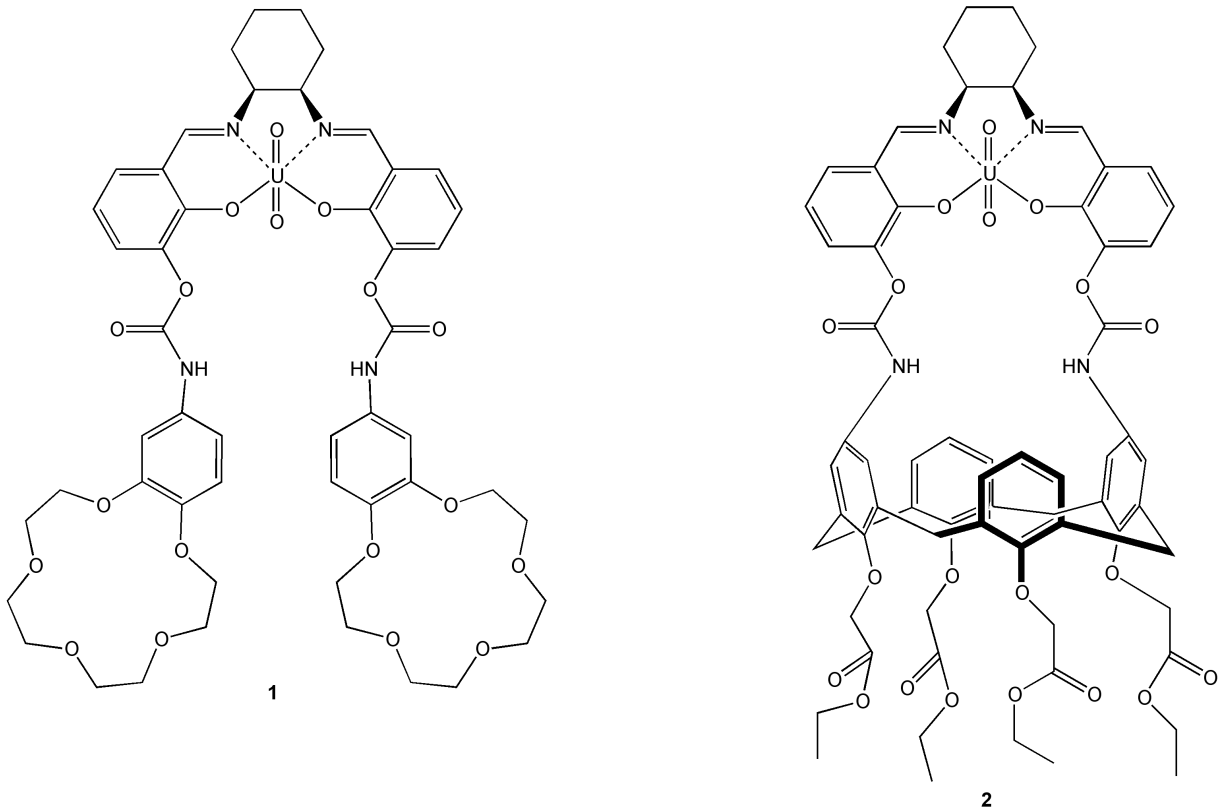

Figure 2.3 Structures of receptors **1** (left) and **2** (right).

Moving ahead on this research field, our research group reported in 2003 the synthesis of salophen-uranyl complexes **3a-e** and **4** (**Fig. 2.4**, top), decorated with aromatic pendant groups, and their use as ion pair receptors for a number of quaternary ammonium and iminium halide salts.[12-14]

^{1}H NMR studies gave the evidence that receptors **3a** and **4**, compared to the control receptor **6** (Fig. 2.4, bottom), are able to bind tetrabutylammonium (TBA) and tetramethylammonium (TMA) chloride with improved efficiency in chloroform. This is due in both cases to the stabilizing π−cation interactions between the cation and the aromatic pendants, in addition to the Lewis acid-base interaction between chloride and the uranyl centre which remains the major driving force for the binding process.[12] Moreover, the affinity of receptor **4** towards tetramethylammonium, acetylcholine (Ach), N-methylpyridine (NMP) and N-

methylisoquinoline (NMiQ) salts is greater than that of receptor **3a**. This is likely due to the larger surface and the higher quadrupolar moment of the naphthalene rings in receptor **4** compared to the benzenic ones in **3a**.[14]

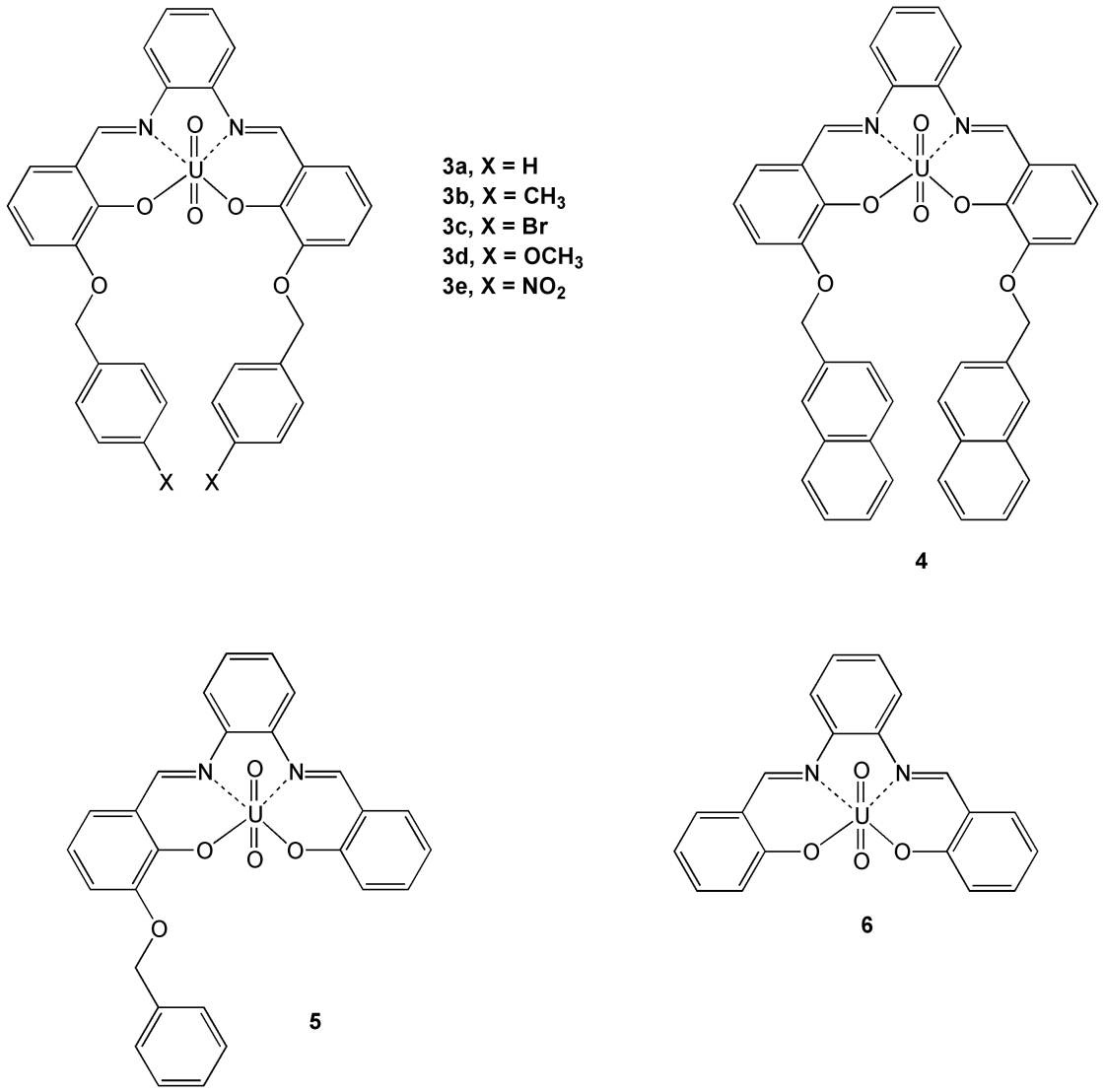

Figure 2.4 Structures of receptors **3a-e**, **4**, **5** and **6**.

More recently, the effect of substituents on the cation-π interaction has been evaluated using a series of salophen-uranyl receptors decorated with X-substituted aromatic pendants **3a-e** (X = H, NO_2, OCH_3, Br, CH_3), and measuring their affinity for TMA chloride. This study pointed out that the resonance effects on cation-π interactions play an important role in determining the strength of binding.[15]

X-ray diffraction studies confirmed the previous observations and offered further insights on the receptors' behaviour in the solid state. Receptor **3a** and **4** were found to form 4:4 capsule-like assemblies with TMACl, in which four chloride-bound receptors surround a core

made of four TMA cations disposed in a tetrahedral arrangement. As an example, the 4:4 complex between receptor **3a** and TMACl is shown in **Fig. 2.5**.[14]

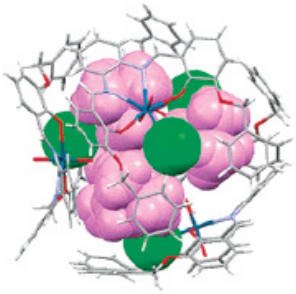

Figure 2.5 4:4 assembly of receptor **3a** with TMACl. Four chloride-bound receptors fully enclose a cluster of four cations disposed in a tetrahedral fashion. Acetonitrile molecules, cations, and anions outside the capsular assembly are excluded for clarity.

Receptor **3a** was also successfully used as receptor for alkaline metal halide contact ion pairs. Analysis of the X-ray diffraction data obtained for the complexes with KCl, RbCl, CsF, and CsCl revealed the formation of capsule-like dimeric (2 : 2) assemblies (**Fig. 2.6**), in which the halide anions are bound to the uranyl centre and interact directly with the alkaline cations that in turn are bound to the oxygen atoms and interact with the π-electron surfaces of the benzylic groups.[13]

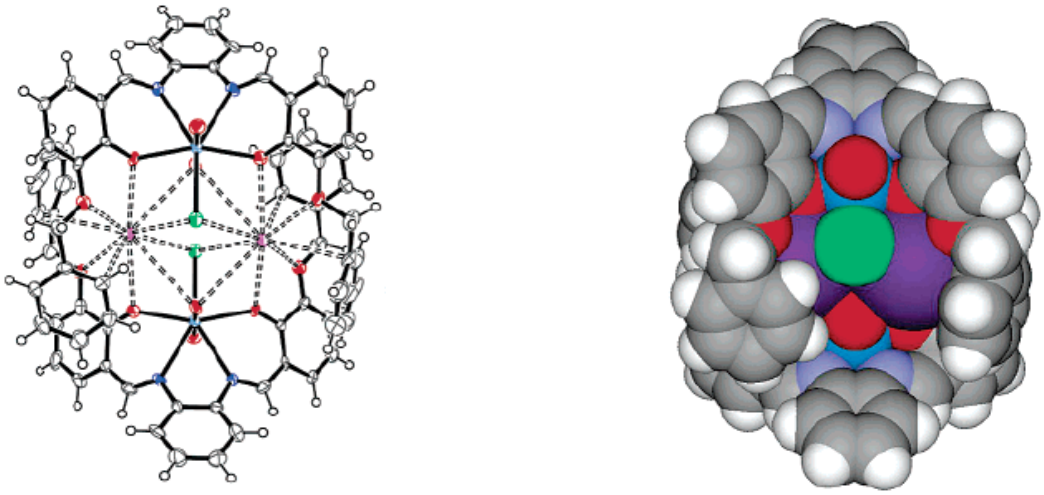

Figure 2.6 2:2 assembly of receptor **3a** with CsCl, drawn as Ortep plot (50% probability level) and as VDW presentation. Chloride is green, Cesium is purple.

Also receptor **5**, provided with a single benzilic arm, forms a complex with CsCl in the solid state, but with a different binding stoichiometry compared to receptor **3a**. In this case, the

formation of a 4:2 receptor-salt adduct was observed, with four receptors molecules disposed to form a capsule-like assembly wrapped around a $(CsCl)_2$ ion quartet. (**Fig. 2.7**).[13]

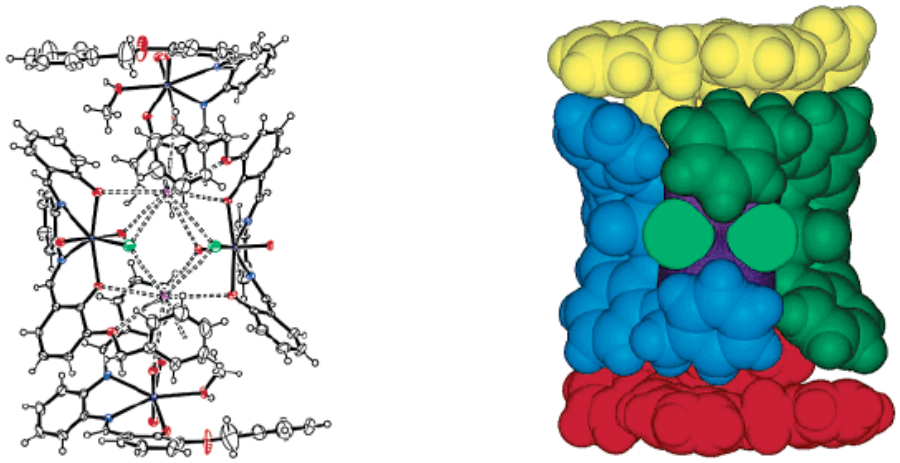

Figure 2.7 Ortep (50% probability level) and VDW presentations of the crystal structure of the CsCl complex of **5**.

1.4 Aim of the work.

Encouraged by the results obtained with receptors **3-5**, we became interested on finding out how a structural modification of the receptor's skeleton would influence the binding of ion pairs. In particular, we wanted to focus our attention on the role of pre-organization in determining the strength of the binding event moving from receptors **3-5** to receptors **11a-d** and **12** (**Fig. 2.8**).

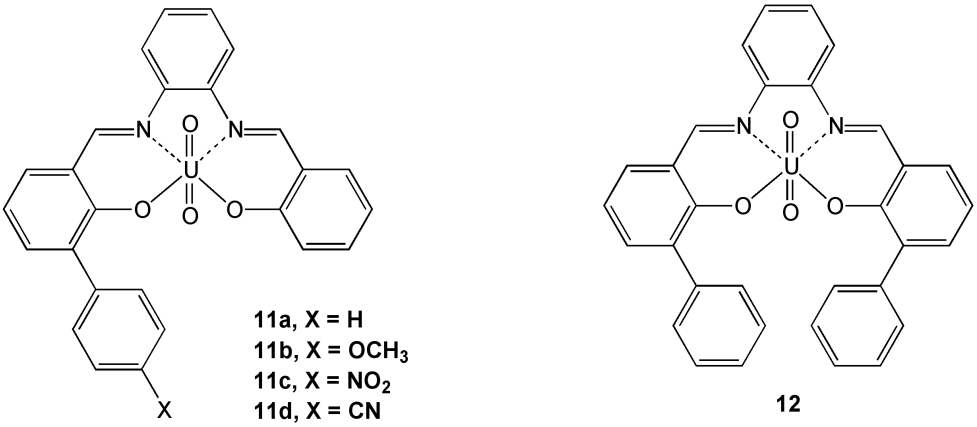

Figure 2.8 Structures of salophen-uranyl complexes **11a-d** and **12.**

Some of these complexes, endowed with one or two aromatic pendants directly linked to the salophen skeleton, have been previously prepared and respectively used as catalysts for the Diels Alder reaction between 1,4-benzoquinone and 1,3-cyclohexadiene[16] and for the Michael

addition of thiophenol to enones,[17] as reported in Chapter 1. Nevertheless the potentialities of derivatives **11** as ion pair receptors have never been evaluated before now.

Compared to receptors **3-5**, in which the flexibility of the aromatic side arms is important to ensure an optimal binding interaction with the cation, receptors **11a-d** and **12** possess a higher degree of structural pre-organization. In our opinion, this feature should result in a greater affinity of these receptors for ion pairs compared to more flexible receptors **3-5**, due to the lower entropic penalty that should be paid in the binding event in case of a more rigid receptor.

To prove the reasonability of the previously stated hypothesis, we decided at first to investigate the ion pair binding ability of receptor **11a** towards TBA halides using UV-Vis spectroscopy. This receptor was chosen for the initial binding studies because a single aromatic sidewall should guarantee not only a lower steric hindrance around the uranyl centre, but at the same time also a recognition site for the cation.

As previously stated in the case of receptors **3b-e**, resonance effects arising from substitution of the aromatic sidewalls are not negligible in determining the strength of the π-cation interactions, that together with the Lewis acid-base interaction between the anion and the uranyl centre are responsible for the ion pair recognition phenomenon.[15] Due to the proximity between the two binding sites in receptors **11a-d** and **12**, these resonance effects of the on π-cation interactions should be even more remarkable. With the aim to highlight these subtle effects, non-symmetrical receptors **11b-d** have been also synthesised and preliminary ^{1}H NMR binding studies between X-substituted receptors **11a-d** (X = H, OCH_3, NO_2, CN) and TMACl have been carried out.

2. Results and discussion.

2.1 Synthesis of receptors 11a-d.

Suzuki cross-coupling reaction has been used for the synthesis of X-substituted 2-hydroxy-[1,1'-biphenyl]-3-carbaldehydes (X = NO_2, OCH_3, CN), precursors of receptors **11b-d**.

As shown in **Scheme 2.1**, Suzuki cross-coupling involves the reaction between an aryl- or vinyl-boronic acid (R_1BY_2, R_1 = aryl, vinyl; Y = OH) and an aryl- or vinyl-halide (R_2X, R_2 = aryl, vinyl; X = Br, Cl, I), in the presence of catalytic amount of Pd(0) and of a base, to afford the cross-coupled product usually with good yields.[18-20]

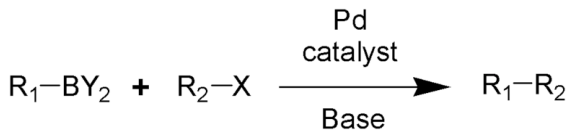

Scheme 2.1 General scheme of Suzuki cross-coupling reaction.

Due to its operative simplicity and to the huge availability of variously functionalized starting materials, we decided to use this methodology for the synthesis of salicylaldehydes **11b-d**, having a phenyl pendant functionalized in position 4' with different substituents (MeO, CN and NO_2). The synthetic route followed is reported in **Scheme 2.2**.

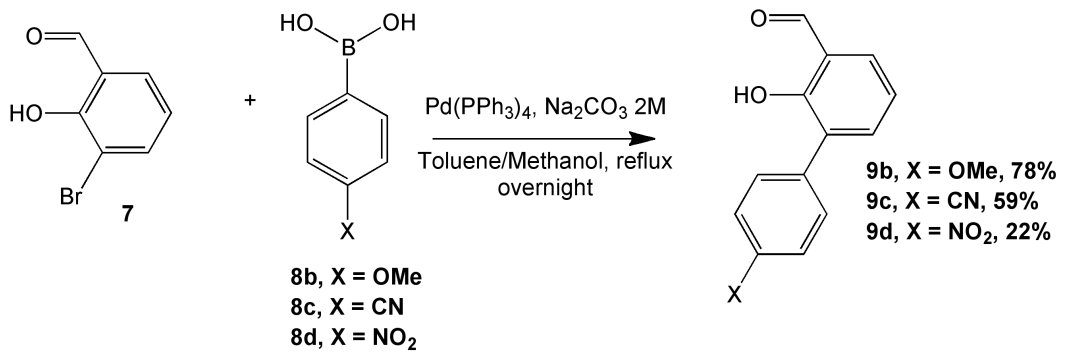

Scheme 2.2 General scheme for the synthesis of aldehydes **9b-d**.

By using commercially available starting materials (3-bromo-2-hydroxybenzaldehyde **7** and the appropriate X-substituted phenylboronic acid **8b-d**), we obtained compounds **9b-d** in good yields. The 2-hydroxy-[1,1'-biphenyl]-3-carbaldehyde, prepared through orto-formylation of commercial 2-hydroxybiphenyl **9a,** was already available from a previous work and.[21]

These aldehydes have been used as precursors in the synthesis of non-symmetrical salophen-uranyl complexes **11a-d**, reported in **Scheme 2.3**.

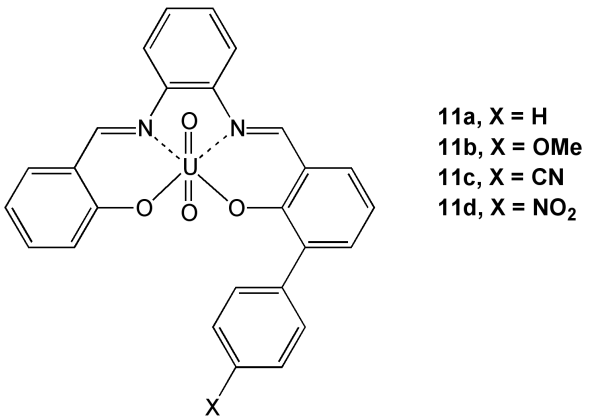

Scheme 2.3 Structures of complexes **11a-d**.

The reaction between monoamine **10**, prepared following a literature procedure[22], and aldehydes **9a-d** in the presence of uranyl acetate gave pure complexes **11a-d** after chromatographic treatment of the raw material (**Scheme 2.4**).

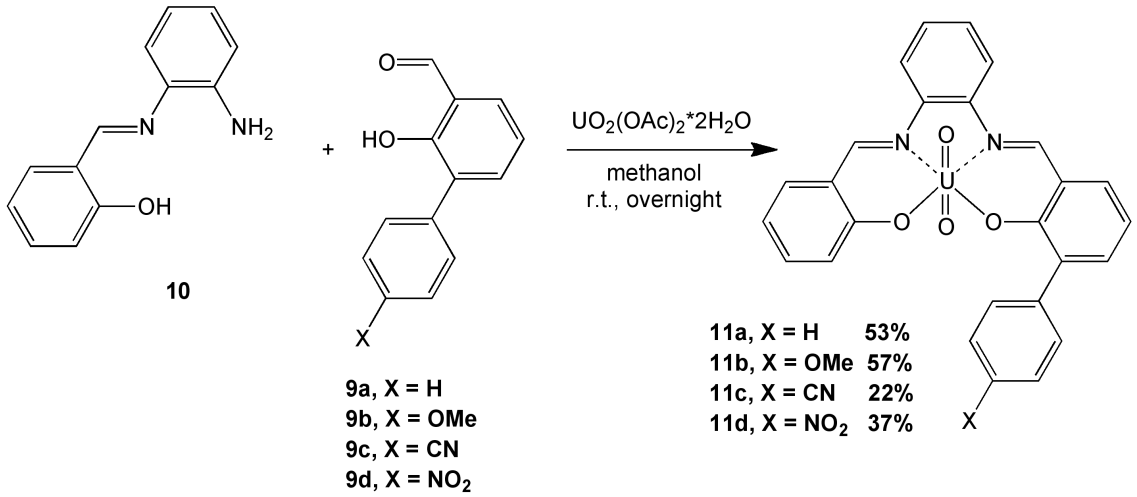

Scheme 2.4 Synthesis of complexes **11a-d**

2.2 Binding measurements

2.2.1 UV-Vis study of the binding constants.

For a preliminary investigation of the receptors' ability with regard to ion pair recognition, we decided to use UV-Vis spectroscopy.

Along with NMR, UV-Vis spectroscopy is the most commonly used technique for the quantitative assessment of the binding phenomena in solution.[23] Its use is particularly advantageous when the *host* molecule possesses a chromophore that adsorbs light in the UV-Vis region. The appropriate choice of the chromophore, indeed, allows lower concentrations of the host to be used in the binding measurement and hence high values of the binding constant can be measured.

In a UV-Vis titration experiment, the changes in the host absorption spectrum are directly related to the addition of increasing amounts of the guest species, working in a region where its absorption is negligible. Considering a 1:1 host-guest binding stoichiometry, the spectral changes observed during the titration course at a fixed wavelength are related, at a given temperature, to the binding constant of the association process, **K**, according to the *binding isotherm equation* (1).

$$\Delta A_0 = \frac{\Delta A_\infty K[G]}{1 + K[G]} \quad (1)$$

In the above reported equation, ΔA_0 is the difference between the total absorbance A measured at a certain concentration of the guest, and the absorbance of the host in absence of the guest, A_0. On the other hand, ΔA_∞ represents the difference between the total absorbance at an infinite guest concentration (A_∞) and the absorbance of the host in absence of the guest A_0.

From the mathematical point of view, this equation states that at every point of the titration, the observed spectral variation ΔA_0 is a fraction of the maximum value ΔA_∞ (obtained theoretically in saturation conditions, when $[G] \rightarrow \infty$), and depends on the K value and on the equilibrium concentration of the guest [G].

The binding constant value can be calculated through a non-linear least squares fitting using Equation 1. However, since the value of [G] is unknown, the total (analytical) guest concentration values are used as initial parameters in the Equation 1 and the binding constant value can be calculated through an iterative procedure. Alternatively Equation 2 can be used, in which the total absorbance at a given point of the titration is expressed as a function of the host initial concentration H_0 and the analytical concentration of the guest G_0 at every addition.[24]

$$\Delta A_0 = \frac{\Delta A_\infty [(G_0 + H_0 + K^{-1}) - \sqrt{(G_0 + H_0 + K^{-1})^2 - 4H_0G_0}]}{2H_0} \quad (2)$$

In the common practice for a UV-Vis titration, H_0 concentration value should be set up in order to work in an absorbance range between 0 and 1. This is essentially depending on the spectroscopic properties of the host, in particular on the molar absorptivity at the wavelength chosen to follow the titration. On the other hand, the explored guest concentration range should be chosen after a preliminary estimation of the binding constant, in such a way to collect as many points as possible in the non-linear portion of the binding isotherm, where the probability of binding *p* ranges between 0.2 and 0.8.[25-26] The probability of binding is defined as follows:

$$p = \frac{[HG]}{[G_0]} \qquad [H_0] \geq [G_0]$$

$$p = \frac{[HG]}{[H_0]} \qquad [H_0] < [G_0]$$

Being the shape of the titration curve dependent on H_0 and K value, the correct range for the guest concentration is usually adjusted using a trial-and-error approach, starting from an estimated value of the binding constant.

Further considerations deserve to be made about the reliability of the binding constant values obtained by titration experiments. If the constant is fairly low ($H_0K<0.01$), a reliable value of K is obtained even with a low accuracy on the value of H_0. On the contrary, if the association is very strong and $H_0K>100$, the non-linear portion of the titration curve is restricted in a small region around one equivalent of guest added. In this case, an uncertainty on the H_0 value results in a high error on the association constant, and only a crude estimation of the lower limit for K can be made.[27]

2.2.2 Optical properties of receptor 11a and study of the associations with TBA halides

The UV-Vis spectrum of compound **11a** in chloroform (**Fig. 2.9**) is characterized by a continuous increase of the absorbance between 600 and 280 nm, with a shoulder at 420 nm and a relative maximum at 348 nm.

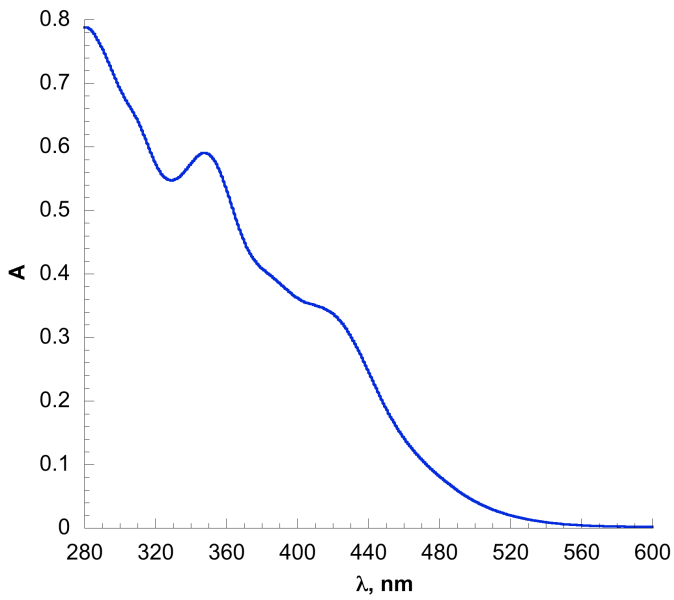

Figure 2.9 UV-Vis spectrum of **11a** (3.73×10^{-5} M) in $CHCl_3$ at 25°C.

A preliminary Lambert-Beer experiment has been also performed in order to rule out any aggregation phenomenon of the host in chloroform solution. As shown in **Fig. 2.10**, a linear relationship between the host concentrations and the experimental absorbances at two

different wavelengths (348 and 420 nm) is observed in the concentration range explored. It follows that an ideal host concentration of ≈ 10^{-5} M is ideal to perform the titration experiment, since the Lambert-Beer Law is fulfilled and it is possible to work in an absorbance range between 0 and 1.

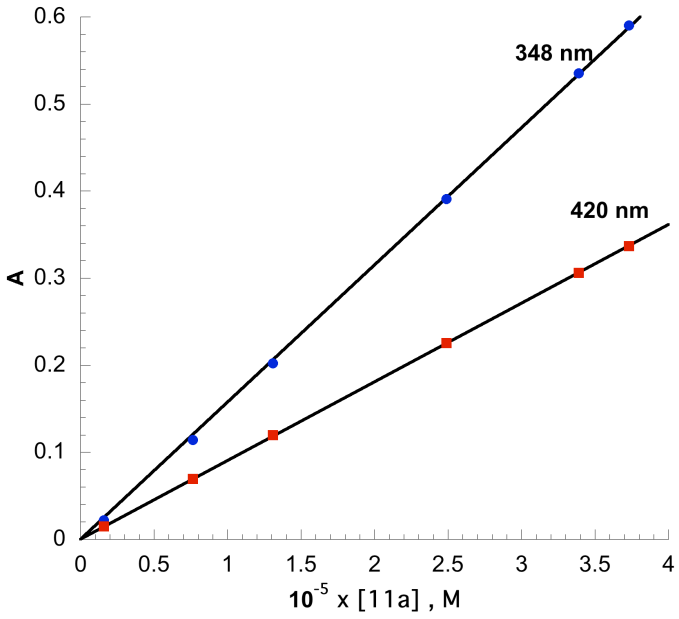

Figure 2.10 Lambert-Beer plots for receptor **11a** at 348 (blue circles) and 420 nm (red squares).

The spectrophotometric titrations of compound **11a** with TBA halides (iodide, bromide, chloride and fluoride) have been carried out in chloroform at 25°C. With the exceptions of TBA iodide and TBA fluoride, reproducible spectral variations were observed in the region between 280-450 nm upon addition of increasing amounts of a stock solution of either TBACl or TBABr.

As an example of a typical titration experiment, in **Fig. 2.11** are reported the UV-Vis spectra obtained upon addition of increasing amounts of a stock solution of TBACl to a solution of salophen-uranyl complex **11a**. The presence of three well-defined isosbestic points at 310, 384 and 494 nm respectively, as well as the close adherence of the experimental data to Equation 2 (see inset in **Fig. 2.11**) are both indicative for a 1:1 host-guest binding stoichiometry.

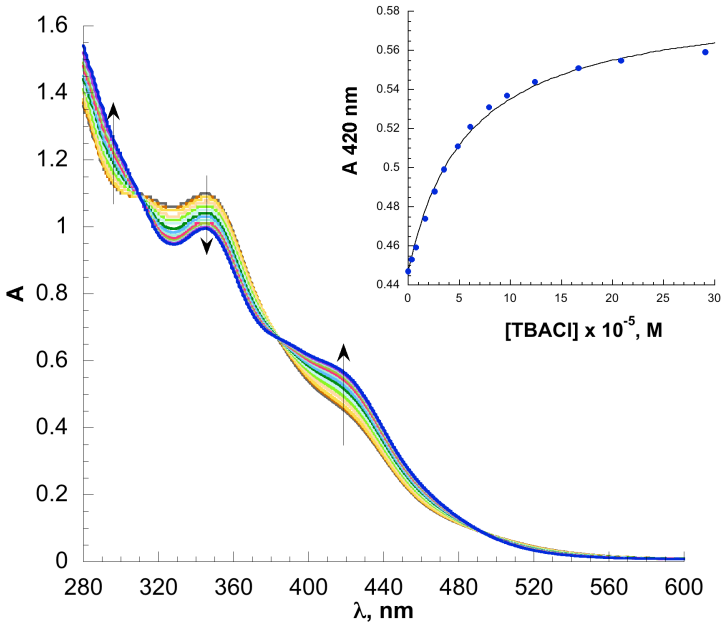

Figure 2.11 UV-Vis absorption spectra obtained of upon addition of increasing amounts of a stock solution of TBACl (4.22 x 10^{-3} M) to a solution of complex **11a** (7.07 x 10^{-5} M), showing the three isosbestic points in the range 280-600 nm. The inset shows the titration plot at 420 nm: the points are experimental, the curve is calculated using Equation 2 (See above).[27]

The association constant values obtained for receptor **11a** with the TBA halides in $CHCl_3$ are summarized in **Table 2.1**. The first thing that catches the eye is the high affinity of receptor **11a** towards TBACl, about 10^2 times greater than that observed for TBABr and 10^5 times than that for TBAI. The observed trend in the binding constants values is in agreement with the hard and soft acid base (HSAB) theory. Indeed, since the major driving force in the binding is the interaction between the Lewis acidic uranyl and the anion of the ion pair, the harder the anion the stronger the association.

Table 2.1 Equilibrium constants K for the association between receptor **11a** and TBA halides in $CHCl_3$ at 25°C.

TBA halide	K, M^{-1} [(a)]
TBA F	n.d. [(b)]
TBA Cl	$(13.7 \pm 0.4) \times 10^4$
TBA Br	$(12.1 \pm 0.4) \times 10^2$
TBA I	<10

[(a)] Errors are calculated as ± 2σ, the K values are the σ-weighed average of those obtained in three different runs.

[(b)] Not determined due to receptor's decomposition upon titration.

Focusing our attention on the recognition of TBACl, other interesting cues of discussion are offered by the comparison of the data obtained for receptors **3a**, **5**, **6** and **11a**, collected in **Table 2.2** (see above for the structures of the five receptors). Moving from receptor **6** (having no aromatic pendants) to receptors **5** and **3a** (having one or two flexible aromatic sidearms), the entity of the association constants for TBACl varies of factor 2 and 4 respectively. Moving to receptor **11a**, in which the aromatic sidewall is directly linked to the salophen skeleton, the increase of the affinity towards TBACl with respect to receptor **6** is quantified by a factor of ≈ 25. Moreover, a comparison between the binding abilities of receptors **11a** and **5** towards TBACl shows that the more pre-organized receptor **11a** binds TBACl more strongly than flexible receptor **5** by a factor of about 11.

Table 2.2 Equilibrium constants K for the association between receptors **3a**, **5**, **6**, **11a** and TBACl in $CHCl_3$ at 25°C.

Receptor	K, M^{-1}
6	5.4×10^3 [(a)]
5	1.2×10^4 [(*)]
3a	2.2×10^4 [(a)]
11a	13.7×10^4 [(b)]

[(a)] Determined by ^1H NMR, see reference 14.

[(b)] Determined in the present work by UV-Vis spectroscopy.

[(*)] M. Cametti, Ph.D. Thesis, unpublished data.

The observed effect is quite small due to the weak character of the π-cation interactions between the TBA cation and the aromatic sidearm. However, UV-Vis studies allowed us to verify the validity of the initial hypotheses, that an higher degree of the receptor preorganization and the closer proximity of the two binding sites (the uranyl centre for the anion recognition and the aromatic pendant for the cation recognition) are responsible for a stronger binding of receptor **11a** towards tetra-alkylammonium ion pairs compared to more flexible receptor **5**.

2.2.3 ^{1}H NMR investigation of the substituent influence upon π-cation interactions between TMACl and receptors 11a-d.

In order to gain further insights into the recognition of TBACl by receptor **11a** and to point out the role exerted by π-cation interactions in this process, we tried several co-crystallization experiments mixing weighed amounts of **11a** with an excess of TBACl in different solvents. All the attempts, however, were unsuccessful due to the precipitation of a powdery material unsuitable for X-ray analysis.

In addition to solid state analysis, which unfortunately did not gave notable results, we decided to use ^{1}H NMR spectroscopy to keep on investigating the ion pair binding ability of receptor **11a** and to establish the substituents' effect on π-cation interactions. For this purpose, we decided to use TMACl as guest for the NMR experiments. This choice was made on the basis of the smaller size of TMA^{+} cation compared to TBA^{+}, which ensures not only a tight association with its counterion but also a more exact localization of the cation in proximity of the π-cloud of the aromatic sidearm. In this way, eventual inductive or resonance effects played by substituents can be pointed out with greater accuracy.

^{1}H NMR titrations are an extremely powerful investigation tool for the study of supramolecular association processes from a structural point of view. The theoretical bases for a ^{1}H NMR titration experiment are the same described above for UV-Vis spectroscopy, with the difference that, in the case of NMR, the chemical shift variation of a definite resonance upon addition of the titrant species is monitored in the course of the titration.

In the classical approach for analysis of NMR titration data, the observed resonance δ is the weighed average between the free host H and the bound host in the complex HG. If the equilibration process between the two species is fast, equations (3) and (4) can be used to calculate the binding constant K by a non-linear least squares fitting program.

$$\Delta\delta_0 = \frac{\Delta\delta_\infty K[H]}{1+K[H]} \tag{3}$$

$$\Delta\delta_0 = \frac{\Delta\delta_\infty[(G_0+H_0+K^{-1})-\sqrt{(G_0+H_0+K^{-1})^2-4H_0G_0}]}{2G_0} \tag{4}$$

In Equation 4, which makes use of the analytical concentrations for both guest and host, $\Delta\delta_0$ is the difference between the guest resonance measured at a certain host concentration δ and the resonance of the guest in absence of the host, δ_0. On the other hand, $\Delta\delta_\infty$ represents the difference between the chemical shift of the guest at an infinite host concentration (δ_∞) and the chemical shift of the guest in absence of the host δ_0.[24]

A preliminary binding study between receptor **11a** and TMACl has been carried out at 25°C using deuterated chloroform as solvent. Upon addition of increasing aliquots of a stock solution of TMACl to a NMR tube containing a weighed amount of receptor **11a** solubilized in a given volume of the same stock solution of the salt, a continuous downfield shift of the TMA^+ signal was observed. The marked curvature of the binding isotherm (**Fig. 2.12**) is indicative for a strong binding: non-linear least squares fitting using Equation 4 gave indeed a binding constant $K>10^5$ M^{-1}, which is commonly assumed by many authors as the limiting value for the execution of an accurate NMR titration experiment.[27]

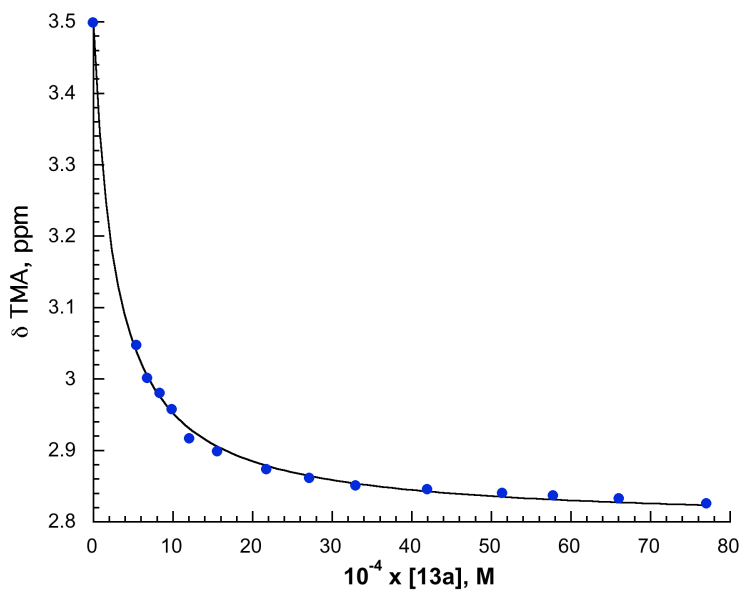

Figure 2.12 ^{1}H NMR titration plot of receptor **11a** with a stock solution of TMACl (75 μM) in $CDCl_3$. The points are experimental and the curve is calculated using Eq. 4.

In order to perform a more accurate evaluation of the substituent effect upon π-cation interactions between the aromatic pendant on receptors **11b-d** and TMACl, we decided at first to perform a competitive titration experiment using a chloroform/1% methanol solvent mixture. The use of a competitor, indeed, results in a lower affinity of the uranyl centre towards anions, and thus in smaller and more reliable values of the binding constants.

In **Fig. 2.13**, is reported as example the titration plot obtained for receptor **13a** upon titration with a stock solution of TMACl in chloroform plus 1% of methanol. In Table 3 are summarized the binding constant values and the limiting upfield shifts ($-\Delta\delta_\infty$) obtained for receptors **13a-e**.

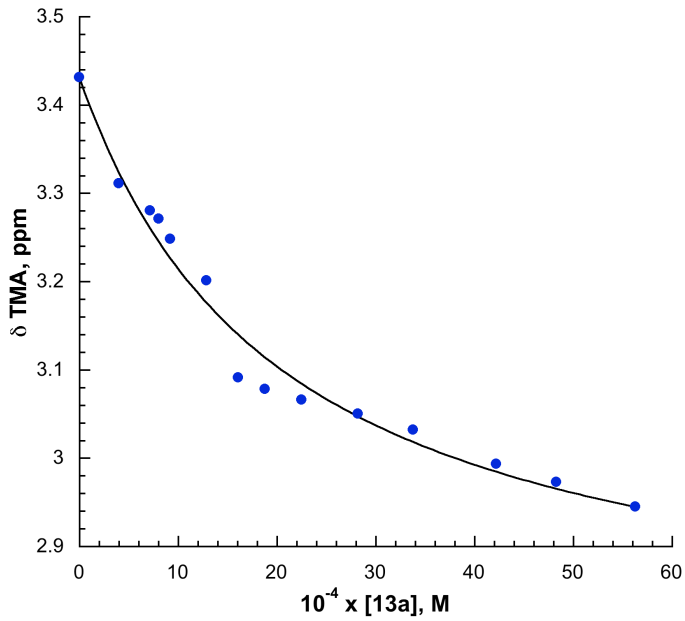

Figure 2.13 ^{1}H NMR titration plot of receptor **11a** with a stock solution of TMACl (1.08 mM) in $CDCl_3/CD_3OD$ 99:1. The points are experimental and the curve calculated using Eq. 4.

Table 2.3 Binding constant values, K_a and limiting upfield shifts ($-\Delta\delta_\infty$) for the association between receptors **11a-e** and TMACl in $CHCl_3/CD_3OD$ 99:1 at 25°C.[a]

Receptor	K_a, M^{-1}	$-\Delta\delta_\infty$, ppm
11a (X = H)	**(9.9 ± 1.9) x 10^2**	**0.58**
11b (X = OCH_3)	**(9.3 ± 2.0) x 10^2**	**0.58**
11c (X = CN)	**(4.46 ± 0.43) x 10^3**	**0.27**
11d (X = NO_2)	**(6.55 ± 0.74) x 10^3**	**0.22**

a. Errors are reported as ± 2σ.

Analysing the data reported in **Table 2.3** we observe that the limiting upfield shift values decrease moving from electron-donating groups (OCH_3) to electron-withdrawing ones (NO_2 and CN) and this could be related to the different degree of interaction between the aromatic sidewall of the receptors and the TMA cation: the higher the electron-withdrawing ability of the substituent on the aromatic sidewall, the lower the interaction with the TMA cation. Nevertheless the preliminary stage of this investigation does not allow us to give even a tentative answer to the question of the relative importance of field/inductive and resonance effects in cation-π interactions. Further studies will be necessary to obtain a more accurate picture of the phenomenon.

3. Conclusions.

In this part of the work, a series of non-symmetrically substituted salophen-uranyl complexes **11a-d** (**Fig. 2.14**) have been synthesised and their binding properties towards ion pairs have been evaluated through UV-Vis and ^{1}H NMR spectroscopies.

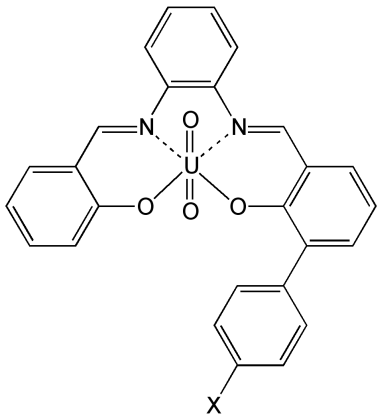

11a, X = H
11b, X = OMe
11c, X = CN
11d, X = NO_2

Figure 2.14 Structures of complexes **11a-d**.

UV-Vis data allowed us to confirm that a higher degree of structural pre-organization of receptor **11a** compared to the previously synthesised **3a** and **5** is responsible for a stronger binding of TBA halides in chloroform, in particular TBACl which benefits of the higher increase of binding affinity moving from receptor **5** to **11a.**

Moreover, ^{1}H NMR spectroscopy was used to investigate the role of substituents present on the pendant aromatic arm of receptors **11a-d** in the binding of TMACl. This salt was used in these studies instead of TBACl, due to its smaller dimension that should ensure a higher degree of interaction with the aromatic moiety. Preliminary measurements of the binding affinity between receptor **11a** and TMACl in deuterated chloroform led to a binding constant

value $>10^5$ M^{-1}. The addition of methanol (1%), which behaves as anion competitor in these conditions, allowed to lower the binding constants and therefore to proceed to a more accurate evaluation of the substituents' effect on the binding between receptors **11a-d** and TMACl. The preliminary results obtained are reported in Table 3 (see above).

4. Experimental section.

Materials 3-bromo-2-hydroxybenzaldehyde **7**, 4-methoxyphenylboronic acid **8b**, 4-cyanophenylboronic acid **8c** and 4-nitrophenylboronic acid **8d** were purchased from Sigma-Aldrich and used as received. 2-hydroxy-[1,1'-biphenyl]-3-carbaldehyde **8a** and monoimine **10** were available from a previous work and synthetized according to literature procedures. Spectrophotometric grade $CHCl_3$ and $CDCl_3$ were passed through a plug of basic Al_2O_3 in order to remove acidic impurities prior to their use.

Instrument and methods UV-Vis titrations were carried out using a Perkin Elmer Lambda 18 spectrophotometer. ^1H and ^{13}C NMR spectra were registered on Bruker AC 200/300 instruments. Mass spectra were obtained using a Micromass Q-TOF instrument.

General procedure for the synthesis of compounds 9b-d.

Working under a slight flow of inert gas, a two-necked round bottomed flask equipped with a refrigerator is charged with X-substituted phenylboronic acid (**8b-d)** and $Pd(PPh_3)_4$ (5% mol). The system is evacuated for 30 minutes, then 3-bromo-2-hydroxybenzaldehyde **7** and degassed toluene are added. After dissolution of the solids, 2M Na_2CO_3 (or 2M K_2CO_3) is syringed into the flask and the mixture is stirred at reflux overnight. The crude product is extracted with DCM and purified by column chromatography to give the desired product.

2-hydroxy-4'-methoxy-[1,1'-biphenyl]-3-carbaldehyde (9b)

Synthetized starting from **7** (0.209 g, 1.04 mmol), **8b** (0.184 g, 1.21 mmol), $Pd(PPh_3)_4$ (0.061 g, 0.053 mmol) and 2M K_2CO_3 (3.4 mL) in 12 mL of toluene. Column chromatography of the crude product (SiO_2, eluent toluene) afforded pure **9b** (0.185 g, 0.81 mmol), Y = 78%.

^1H NMR (300 MHz, $CDCl_3$) δ (ppm): 11.51 (s, 1H); 9.92 (s, 1H); 7.59-6.95 (m, 7H); 3.83 (s, 3H) **^{13}C NMR (75 MHz, $CDCl_3$)** δ (ppm): 196.79; 159.12; 158.8; 137.42; 132.63; 130.31; 128.7; 120.9; 119.82; 113.69; 55.23 **Elemental analysis**: calculated for $C_8H_{12}O_3$: C 73.67 H 5.3; found C 73.23 H 5.74.

3'-formyl-2'-hydroxy-[1,1'-biphenyl]-4-carbonitrile (9c)

Synthetized using **7** (0.103 g, 0.51 mmol), **8c** (0.1 g, 0.68 mmol), $Pd(PPh_3)_4$ (0.037 g, 0.032 mmol) and 2M Na_2CO_3 (0.5 mL) in a 1:1 mixture toluene/methanol. Column chromatography of the crude product (SiO_2, eluent toluene) afforded pure **9c** (0.045 g, 0.2 mmol), Y = 39%.

^{1}H NMR (200 MHz, $CDCl_3$) δ (ppm): 11.17 (s, 1H); 9.51 (s, 1H); 7.19-7.16 (m, 4H); 6.79 (s, 2H); 6.68 (t, 1H, J = 7.6 Hz) **^{13}C NMR (75 MHz, $CDCl_3$)** δ, ppm: 196.7; 137.41; 134.26; 131.98; 128.89; 120.12.

2-hydroxy-4'-nitro-[1,1'-biphenyl]-3-carbaldehyde (9d)

Synthetized using **7** (0.264 g, 1.31 mmol), **8d** (0.289 g, 1.73 mmol), $Pd(PPh_3)_4$ (0.099 g, 0.086 mmol) and 2M Na_2CO_3 (1.8 mL) in a 1:1 mixture toluene/methanol (6 mL). Chromatographic purification of the crude product (SiO_2, eluent DCM) gave pure **9d** (0.189 g, 0.78 mmol), Y = 59%.

^{1}H NMR (200 MHz, CD_3CN) δ (ppm): 11.67 (s, 1H); 9.56 (s, 1H); 8.27-8.23 (m, 2H); 7.82-7.68 (m, 4H); 7.18 (t, 1H, J = 7.7 Hz) **^{13}C NMR (75 MHz, $CDCl_3$)** δ (ppm): 196.71; 158.84; 147.28; 143.25; 137.45; 134.48; 130.06; 128.57; 124.53; 123.43; 120.96; 120.15 **Elemental analysis**: calculated for $C_{13}H_9NO_4$: C 64.2 H 3.73 N 5.76 found C 63.87 H 3.69 N 5.72

General procedure for the synthesis of complexes 11a-d

Monoimine **10**, uranyl acetate dihydrate and the appropriate X-substituted aldehyde **9a-d** are mixed in methanol (or in a 1:1 mixture DCM/methanol when necessary), and the reaction is stirred at room temperature overnight. The crude product is extracted with DCM and purified by column chromatography to give pure complexes **11a-d**.

Complex 11a (X = H)

Obtained in 53% yield starting from monoimine **10** and aldehyde **9a**.

^{1}H NMR (300 MHz, DMSO-d$_6$) δ (ppm): 9.67 (s, 1H); 9.59 (s, 1H); 7.98 (d, 2H, J = 7.5 Hz); 7.81-7.69 (m, 5H); 7.57-7.5 (m, 5H); 7.39 (t, 1H, J = 7.5 Hz); 6.97 (d, 1H, J = 8.4 Hz); 6.78 (t, 1H, J = 7.5 Hz); 6.68 (t, 1H, J = 7.5 Hz).

Complex 11b (X = OMe)

Obtained in 57% yield starting from monoimine **10** and aldehyde **11b**.

^{1}H NMR (300 MHz, DMSO-d$_6$) δ (ppm): 9.66 (s, 1H); 9.58 (s, 1H); 7.94 (d, 2H, J = 8.4 Hz); 7.76-7.49 (m, 8H); 7.12 (d, 2H, J = 7.5 Hz); 6.97 (d, 1H, 8.7 Hz); 6.75 (t, 1H, J = 7.5 Hz); 6.68 (t, 1H, J = 7.5 Hz); 3.84 (s, 3H) **^{13}C NMR (75 MHz, DMSO-d$_6$)** δ (ppm): 170.09; 167.48; 167.04; 158.58; 147.18; 147.07; 136.4; 136.32; 136.32; 136.23; 135.56; 131.65; 131.25; 129.13; 125.33; 125.16; 124.64; 120.97; 120.71; 120.63; 117.39; 117.08; 113.79; 55.55 **ESI-MS**: 713.3 [M+Na$^+$], 729.3 [M+K$^+$] **HRMS** (ESI-TOF): calculated for $C_{27}H_{20}N_2O_5NaU^+$ 713.1778, found 713.1763 **Elemental analysis**: calculated for $C_{27}H_{20}N_2O_5U + CH_3OH$: C 46.54 H 3.35 N 3.88 found C 46.89 H 3.51 N 3.77

Complex 11c (X = CN)

Obtained in 22% yield starting from monoimine **10** and aldehyde **9c**.

^{1}H NMR (300 MHz, DMSO-d$_6$) δ (ppm): 9.68 (s, 1H); 9.61 (s, 1H); 8.12 (dd, 4H); 7.99-7.75 (m, 5H); 7.59-7.51 (m, 3H); 6.98 (d, 1H, J = 7.8 Hz); 6.82 (t, 1H, J = 7.5 Hz); 6.69 (t, 1H, J = 7.5 Hz) **^{13}C NMR (75 MHz, DMSO-d$_6$)** δ (ppm): 169.91; 167.44; 167.35; 167.16; 147.02; 144.27; 137.45; 136.78; 136.52; 136.36; 132.24; 130.95; 129.89; 129.36; 129.24; 125.52; 124.6; 120.92; 120.75; 120.68; 119.68; 117.56; 117.32; 109.33. **ESI-MS**: 707.8 [M+Na$^+$], 748.8 [M+CH$_3$CN] **HRMS** (ESI-TOF): calculated for $C_{27}H_{17}N_3O_4KU^+$ 724.1364, found 724.1348 **Elemental analysis**: calculated for $C_{27}H_{17}N_3O_4U + CH_3OH$: C 46.87 H 2.95 N 5.86 found C 46.58 H 2.55 N 5.52

Complex 11d (X = NO$_2$)

Obtained in 37% yield starting from monoimine **10** and aldehyde **9d**.

^{1}H NMR (300 MHz, DMSO-d$_6$) δ (ppm): 9.7 (s, 1H); 9.62 (s, 1H); 8.36 (dd, 4H); 7.92-7.75 (m, 5H); 7.62-7.51 (m, 3H); 6.99 (d, 1H, J = 8.1 Hz); 6.84 (t, 1H, J = 7.5 Hz); 6.69 (t, 1H, J = 7.2 Hz) **^{13}C NMR (75 MHz, DMSO-d$_6$)** δ (ppm): 167.52; 167.36; 167.18; 147.02; 146.44; 137.79; 136.84; 136.52; 136.36; 131.16; 129.51; 129.39; 129.25; 125.62; 124.6;

123.5; 120.9; 120.77; 117.57; 117.34. **ESI-MS**: 727.9 [M+Na^+], 768.9 [M+CH_3CN] 1441.4 [2M+CH_3CN] **HRMS** (ESI-TOF): calculated for $C_{26}H_{17}N_3O_6KU^+$ 744.1262, found 744.1225 **Elemental analysis**: calculated for $C_{26}H_{17}N_3O_6U$ + $2CH_3OH$: C 43.7 H 3.27 N 5.46 found C 43.24 H 3.12 N 5.09.

5. Bibliography

[1] (a) Bianchi, A.; Bowman-James, K.; García España, E. *Supramolecular chemistry of Anions,* Wiley, New York, **1997**. (b) Beer, P.D. and Gale, P.A. *Angew. Chem. Int. Ed.* **2001**, *40*, 486. (c) Llinares, J.H.; Powell, D; Bowman-James, K. *Coord. Chem. Rev.* **2003**, *57*, 240.

[2] (a) Oosting, P.H. *Rep. Prog. Phys.* **1979**, *42*, 1479. (b) Tuszynski, J.A. and Dixon, J.M. *Biomedical Applications of Introductory Physics*, Wiley, **2002**.

[3] For an overview of the most recent literature about anion recognition, see: (a) Caltagirone, C. and Gale, P.A. *Chem. Soc. Rev.* **2009**, *38*, 520. (b) Gale, P.A. *Chem. Soc. Rev.* **2010**, *39*, 3746-3771. (c) Wenzel, M.; Hiscock, J.R. and Gale, P.A. *Chem. Soc. Rev.* **2012**, *41*, 480-520 and references cited therein.

[4] Gokel, G.W. "Molecular Recognition Receptors for Cationic Guests" in *Comprehensive Supramolecular Chemistry*, eds J.M. Lehn, J.L. Atwood, J.E.D. Davies et al., Pergamon, Oxford, **1996**, vol.1.

[5] P.A. Gale "Simultaneous cation and anion receptors" in *Core Concepts in Supramolecular Chemistry and Nanochemistry*, eds. J.W. Steed, D.R. Turner and K.J. Wallace, John Wiley & Sons Inc., UK, **2007**, 73.

[6] (a) Smith, B.D. "Ion Pair Recognition by Ditopic Receptors" in *Macrocyclic Chemistry: Current Trends and Future Perspectives*, eds. K. Gloe and B. Antonioli, Kluwer, London, **2005**, 137 (b) Dalla Cort, A. "Ion-pair receptors" in *Supramolecular Chemistry: From Molecules to Nanomaterials*, eds. P.A. Gale and J.W. Steed, Wiley, **2012**, 1281. (c) Kim, S.K. and Sessler, J.L. *Chem. Soc. Rev.* **2010**, *39*, 3784 and references cited therein.

[7] Gokel, G.W.; Leevy, W.M. and Weber, M.E. *Chem. Rev.* **2004**, *104*, 2723-2750.

[8] (a) Ikeda, A., Shinkai, S. *Chem. Rev.* **1997**, *97*, 1713-1774. (b) Kim, J.S.; Quang, D.T. *Chem. Rev.* **2007**, *107*, 3780-3799.

[9] Selected references: (a) Ballistreri, F.P., Pappalardo, A.; Tomaselli, G.A.; Toscano, R.M. Trusso Sfrazzetto, G. *Eur. J. Org. Chem.* **2010**, 3806. (b) Amato, M.E.; Ballistreri, F.P.; Gentile, S.; Pappalardo, A.; Tomaselli, G.A.; Toscano, R.M. *J. Org. Chem.* **2010**, *75*, 1437. (c) Bartocci, S.; Bruschini, M.; Dalla Cort, A.; De Bernardin, P.; Forte, G.; Giannicchi, I. and Yafteh Mihan F., *Australian J. Chem*. **2012**, DOI: 10.1071/CH12353.

[10] Rudkevich, D.M.; Brzozka, Z.; Palys, M.; Visser, H.C.; Verboom, W. and Reinhoudt, D.N. *Angew. Chem. Int. Ed. Engl.* **1994**, *33*, 467-468.

[11] Rudkevich, D.M.; Verboom, W. and Reinhoudt, D.N. *J. Org. Chem.* **1994**, *59*, 3683-3686.

[12] Cametti, M.; Nissinen, M.; Dalla Cort, A.; Mandolini, L. and Rissanen, K. *Chem. Comm.* **2003**, 2420-2421.

[13] Cametti, M.; Nissinen, M.; Dalla Cort, A.; Mandolini, L. and Rissanen, K. *J. Am. Chem. Soc.* **2005**, *127*, 3831-3837.

[14] Cametti, M.; Nissinen, M.; Dalla Cort, A.; Mandolini, L. and Rissanen, K. *J. Am. Chem. Soc.* **2007**, *129*, 3641.

[15] Cametti, M.; Dalla Cort, A. and Mandolini, L. *Chem. Sci.* **2012**, *3*, 2119-2122.

[16] Dalla Cort, A.; Mandolini, L.; Schiaffino, L. *Chem. Comm.* **2005**, 3867-3869.

[17] (a) van Axel Castelli, V.; Dalla Cort, A.; Mandolini, L. and Reinhoudt, D.N. *J. Am. Chem. Soc.* **1998**, 1*20*, 12688-12689. (b) van Axel Castelli, V.; Dalla Cort, A.; Mandolini, L.; Reinhoudt, D.N. and Schiaffino, L. *Chem. Eur. J.* **2000**, *6*, 1193-1198. (c) van Axel Castelli, V.; Dalla Cort, A.; Mandolini, L.; Pinto, V.; Reinhoudt, D.N. and Schiaffino, L. *J. Org. Chem.* **2007**, 7*2*, 5383-5386.

[18] Suzuki, A. *Pure Appl. Chem.* **1991**, *63*, 419-422.

[19] Miyaura, N.; Suzuki, A. *Chem. Rev.* **1995**, *95*, 2457–2483.

[20] Suzuki, A. *J. Organometallic Chem.* **1999**, *576*, 147-168.

[21] Verner, E.; Katz, B. A.; Spencer, J. R.; Allen, D.; Hataye, J.; Hruzewicz, W.; Hui, H. C.; Kolesnikov, A.; Li, Y.; Luong, C.; Martelli, A. et al. *J. Med. Chem.* **2001**, *44*, 2753-2771.

[22] Li, J.Z.; Wang, Y.; Zeng, W.; Quin, S.Y. *Supramolecular Chemistry* **2008**, *20*, 249-254.

[23] Connors, K.A. *Binding Constants: The Measurement of Molecular Complex Stability*, Wiley-InterScience, New York, **1987**.

[24] Hirose, K. *J. Incl. Phenom. Macrocycl. Chem.* **2001**, *39*, 193-209.

[25] Wilcox, C.S. in *Frontiers in Supramolecular Organic Chemistry and Photochemistry*, eds. H.J. Schneider and H. Dürr, VCH, Weinheim, **1991**, 123-144.

[26] Weber, G. in *Molecular Biophysics*, eds. B. Pullman and M. Weissbluth, Academic Press, New York, **1965**, 369-397.

[27] Thordarson, P. *Chem. Soc. Rev.* **2011**, 4*0*, 1305-1323.

CHAPTER 3

Novel fluorescent benzimidazole-based receptors for sensing of carboxylate anions in a competitive medium.

Anion recognition is one of the research fields at the frontier of modern Supramolecular Chemistry. The important and often crucial role played by anions in biochemical and industrial processes has certainly prompted many researchers towards the development of molecules designed to perform anion recognition both in organic and aqueous solution. A second and not least important factor responsible for the great appeal of this research field is the wide availability of anion binding motifs, whose clever combination into an organic framework is responsible for the affinity and the selectivity of the binding process.

The research reported in this chapter moves within this research area, and was performed during a four month stage in the group of Prof. P.A. Gale at the School of Chemistry of the University of Southampton. After a brief introduction regarding the most important features of anionic species and the challenge of anion recognition in organic and aqueous media, the second part of this chapter focuses on the use of benzimidazole-based receptors for the detection of anions, with an overview on the most recent literature examples. In the third part of the chapter the synthesis of novel benzimidazole-based receptors is illustrated, and the preliminary results obtained using these molecules for the fluorescent sensing of carboxylate anions are discussed.

1. Introduction.

The first steps towards the Supramolecular recognition of ionic species were moved during the 60's, with the pioneristic work of Pedersen on the recognition of alkali metal ions performed by crown ethers.[1] Other receptors able to bind metal ions belonging to groups I and II, as well as ammonium ions, were also synthesised taking inspiration from naturally occurring molecules, as the antibiotics nonactin[2] and valinomycine[3] (**Fig. 3.1**).

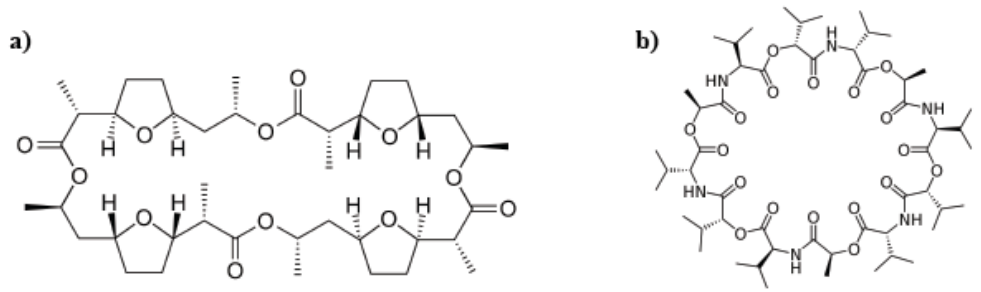

Figure 3.1 Structure of the antibiotics a) nonactin and b) valinomycine.

The interest in recognition of anionic species, on the other hand, is quite recent and, with the exception of few noteworthy examples, developed during the last decades. The important role exerted by anions in biochemical and industrial processes encouraged many research teams to devote their efforts towards the supramolecular recognition of anionic species, as witnessed by the large number of reviews[4] and some monographs[5] appeared over the last years on this topic.

The reasons for the late development of this research field have to be found in some intrinsic properties of the anions. In **Table 3.1** are reported the ionic radii and the experimental enthalpy hydration values for some selected ions.[6] Through the analysis of these data, it is evident that anions have bigger ionic radii than the corresponding isoelectronic cations and also higher free enthalpies of hydration in comparison with cations of similar size. This means that a suitable anion receptor should be of considerably greater size than a cation receptor and also able to compete more effectively with the surrounding solvating medium.

Ion	r (Å)	ΔH_{hydr} (KJ/mol)
Na^+	1.16	-416
K^+	1.52	-334
Cs^+	1.81	-283
F^-	1.19	-510
Cl^-	1.67	-367
Br^-	1.82	-336
I^-	2.06	-291

Table 3.1 Ionic radii, r and hydration enthalpies ΔH_{hydr} for selected ionic species in octahedral environments.

Moreover, anions may exist only in narrow pH range due their involvement in acid-base equilibria, and compared with the simple spherical shape of cations come with different geometries such as sphere, linear, trigonal, tetrahedral and octahedral. In particular cases, such as the DNA double helix, the shape is even more complex (**Fig. 3.2**). Further considerations deserve to be made on the role of hydrophobicity in anion binding since, according to Hofmeister series, lipophilic anions tend to bind more strongly to hydrophobic binding sites.[7]

All the previously mentioned aspects must be taken into account for the correct design of molecules capable to selectively bind anionic species. While in the case of a simple spherical-shaped cation the selectivity of the recognition process depends mainly on the size of the receptor's cavity, the selective binding of anionic species requires a higher degree of structural design and particular topological features of the binding cavity, in order to meet precise geometrical requirements. Design of cyclic and polycyclic receptors has revealed to be the most successful approach for the synthesis of anion receptors. These structures are not only able to provide a close environment and a tuneable stiffness that affects the binding affinity, but also a pre-organization of the anchor sites in the cavity which plays a crucial part in determining the selectivity of the binding event.[8]

The latter point is particularly important when the interactions involved in the binding process are highly directional; amongst these, the most exploited in anion receptor designing is undoubtedly represented by hydrogen bonding, which combines its high directionality with a remarkable strength.[9]

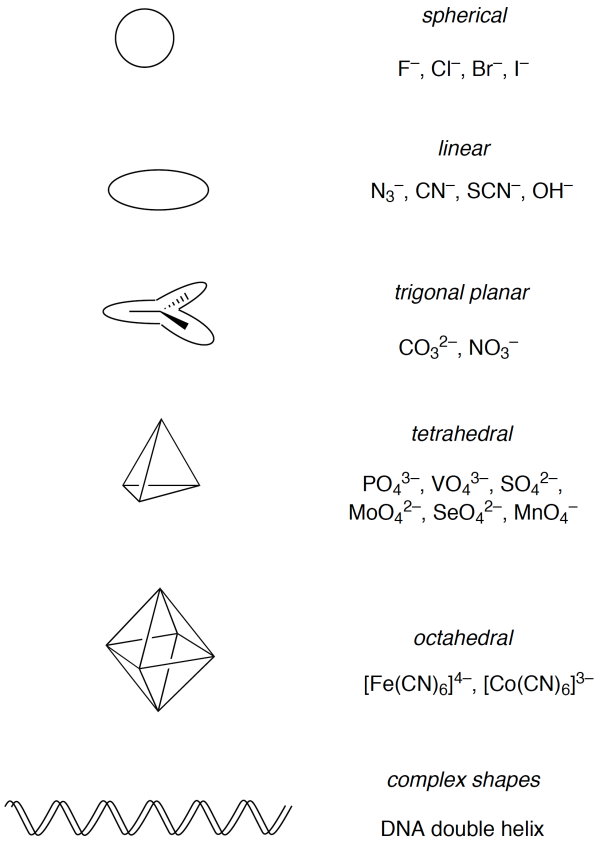

Figure 3.2 Structural geometries of anions.

The most obvious strategy used to achieve anion binding is to design a molecular host containing an electrostatic charge, whose interaction with the anion is usually modulated by directional interactions with hydrogen bonding donors or acceptors. In this framework we can consider the serendipitous discovery of *katapinands* reported by C.H. Park and H.E. Simmons in 1968, the first known example of receptors for anions.[10] X-ray and ^{1}H NMR studies showed that these macrocycles, containing two bridgehead ammonium ions, are able to bind halides in a process named *katapinosis*[11] by the authors. In particular, katapinand **1a** (n = 9, **Fig. 3.3**) shows selectivity for chloride over bromide and iodide. The authors suggested that chloride anion is more likely included into the cavity through formation of two hydrogen bonds with the bridgehead ammonium ions [N^{+}-H•••Cl^{-}•••H-N^{+}] rather than interacting separately with the two ammonium ions outside the cavity [N^{+}-H•••Cl^{-} N^{+}-H•••Cl^{-}]. The simultaneous binding of the anion to the ammonium ions inside the cavity is the major driving force for the inclusion process, while the selectivity is controlled by the cage size, in its turn arising from the chain length joining the bridgehead nitrogen atoms. Indeed, while receptor **1a** (n = 9, **Fig. 3.3**) includes chloride more favourably than bromide and iodide, the bigger receptor **1b** (n = 10, **Fig. 3.3**) does not discriminate between the three halides and readily forms *katapinandi* with all the three anions.

1a, n = 9
1b, n = 10

1a-Cl

Figure 3.3 Schematic representations of katapinands **1a** (n = 9) and **1b** (n = 10) and the complex between **1a** and Cl^-.

Due to the directionality and to the strength of hydrogen bonding, a plethora of anion receptors containing hydrogen bond donors as binding motifs have been synthesised. These motifs can be both neutral (indole, pyrrole, hydroxyl group, urea, and thiourea) or positively charged groups (guanidinium, imidazolium and ammonium moieties).[4-5] In the next paragraph, our attention will be mainly focused on the use of (thio)urea moieties for the design of fluorescent anion receptors, of which some significant literature examples will be reported and commented.

2. Urea and thiourea-based receptors for anions.

2.1 Introduction.

Amongst the neutral hydrogen bonding donors mentioned above, urea and thiourea have been extensively used as binding motifs for the construction of anion receptors.[12] These compounds are known since 1828 when the German chemist Friederich Wöhler, father of modern Organic Chemistry, reported the synthesis of urea starting from ammonium cyanate.[13] This finding had a revolutionary impact on the chemical community, because for the first time it was demonstrated that an organic compound could be synthesised starting from an inorganic material, infringing the vitalistic theory dominating until then.[14]

Since the serendipitous discovery of urea, a number of synthetic procedures for the synthesis of N,N'-substituted (thio)ureas have been developed.[15] The most commonly used for the synthesis of symmetrical derivatives rely on the nucleofilic addition of a substituted amine to a (thio)carbonyl-X-disubstituted compound derived from phosgene ($COCl_2$). Among these derivatives, the most versatile for the synthesis of ureas revealed to be bis(trichloromethyl)(thio)carbonate (BTC)[16] **2a**, while triphosgene **2b** is commonly used for the synthesis of thioureas. Both these compounds have been widely used in the synthesis of

symmetrical (thio)urea derivatives (**Fig. 3.4**, a).[17] On the other hand, non-symmetrical (thio)ureas can be synthesised using the approach described previously for the synthesis of the symmetrical ones (but using two different amines) or, more conveniently, by the nucleophilic substitution reaction between an iso(thio)cyanate and a substituted amine (**Fig. 3.4**, b). The wide commercial availability of differently substituted isocyanates and isothiocyanates (where the oxygen atom on the carbonyl group is replaced by sulphur) offers countless possibility for the synthesis of (thio)urea derivatives decorated in different fashions.

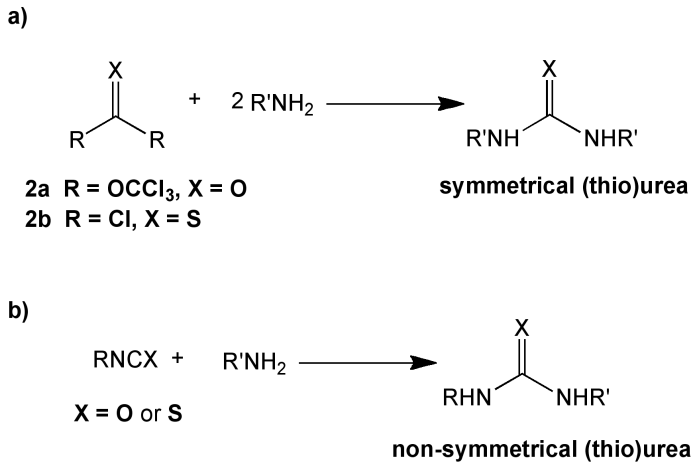

Figure 3.4 Synthesis of a) symmetrical and b) non-symmetrical ureas and thioureas.

In general, thioureas N-H protons are more acidic than the ureido NHs, as indicated by the pKa values of 21.1 and 26.9, measured in DMSO for thiourea and urea respectively.[18] The higher acidity of the thioureidic protons is essentially due to the sulphur atom, which can delocalize a negative charge better than the oxygen atom due to its higher nuclear charge, and is responsible for a stronger binding to anions in comparison to ureas.

Taking into account all the previously mentioned issues that make anion recognition more challenging than that of cation, several aspects must be considered in design of (thio)ureas as receptors for anions. First of all, the strength of the hydrogen bonding interactions between the (thio)urea moiety and the anion, as well the relative position of the two donor sites with respect to the C=X (X = O, S) need to be accurately controlled. Different strategies have been used hitherto to achieve this goal, which are:

- Increase the acidity of the N-H bonds by substitution of the nitrogen atoms with aromatic groups bearing electron-withdrawing substituents.
- Incorporate the (thio)urea moiety into a pre-organized binding cleft using rigid or flexible structures, which offer size and shape complementarity to the anion.

- Decorate the nitrogen atoms of the (thio)urea with additional hydrogen bond donors, either charged or neutral.

Other considerations deserve to be made regarding the experimental techniques (optical or electrochemical) used to sense the binding event with these receptors. Amongst the optical techniques, UV-Vis and fluorescence are the most commonly used for their operative simplicity. UV-Vis is particularly convenient when the anion binding process is accompanied by a color change of the solution, often due to the additional deprotonation equilibrium of the receptor. Also fluorescence spectroscopy, due to its high sensitivity, has been used for detecting the binding event in solution with use of receptors decorated with fluorophore groups. However, these techniques do not allow gaining insights into the structural features of the binding event. Detailed information in this regard can be obtained in solution using ^{1}H NMR spectroscopy and, in the solid state, X-ray crystallography.

Coming back to the quest for highly sensitive and selective anion recognition using (thio)urea-based receptors, the insertion of aromatic or heteroaromatic moieties within the receptor's backbone revealed to be, from a structural viewpoint, the most effective approach to achieve this goal. Aromatic groups can indeed modulate the acidity of the (thio)ureidic protons through substitution of the benzenic ring with different substituents. Furthermore, aryl frameworks can be decorated with additional hydrogen bond donors (using for example heteroaromatic rings such as indole, imidazole or benzimidazole) and can also be employed to achieve a better pre-organization in receptors containing multiple hydrogen-bonding donor sites.[19] Besides their important role in modulating the selectivity and the affinity in the anion recognition process, some aromatic moieties have been also exploited for the synthesis of fluorescent (thio)urea-based receptors, as will be described in next paragraph.

2.2 Anion sensing with use of fluorescent (thio)urea-based receptors.

Anion sensing has been gaining an increasing attention during the past years, and this is mostly related to the important role played by anions in biology and in environmental processes. The presence of anions inside the human body is related to health, and variations in the blood concentration values of anionic species are usually related to pathological conditions.[20] Moreover, anions are the most common anthropogenic pollutants of waste and groundwater.[21] Therefore the design and the synthesis of simple molecules able to qualitatively and quantitatively sense anionic species is a valuable task.

Amongst the techniques employable for sensing the binding event, fluorescence in undoubtedly the most appealing, due to its high sensitivity and its operational simplicity. In this paragraph, our attention will be addressed to the use of (thio)urea moiety for the synthesis of receptors able to sense anions by fluorescence spectroscopy.

Many examples of fluorescent (thio)-urea based receptors decorated with different fluorophores have been published in recent years. Amongst these examples, Gunnlaugsson et al. reported in 2003 the synthesis of receptor **3** (**Fig. 3.5**), which incorporates in its backbone a naphthalimide fluorophore.[22]

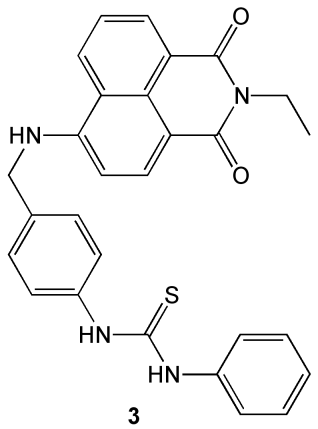

Figure 3.5 Structure of receptor **3**.

Receptor **3**, in which a N-arylthiourea moiety is connected through a CH_2 spacer to the naphthalimide fluorophore at its 4-amino position, showed fluorescence quenching upon addition of several anions, like F^-, $H_2PO_4^-$ and CH_3COO^-. The quenching process follows a PET (Photoinduced Electron Transfer) mechanism, which takes place between the thiourea moiety and the fluorophore in the presence of the anion. To explain the fluorescence quenching, the authors suggested that the formation of the anion-receptor hydrogen bonded complex causes a decrease of the reduction potential of the thiourea, making the electron transfer from the thiourea to the fluorofore more feasible. The fluorescence quenching observed in the presence of an excess of fluoride was stronger compared to that observed in the presence of acetate and dihydrogen phosphate, and led the authors to consider this receptor as an "on-off" fluorescent switch for the selective detection of fluoride anion.

The same research group reported in 2005 the synthesis of receptor **4** (**Fig. 3.6**), in which the anthracene core is decorated with two arylthiourea moieties.[23] Fluorescence quenching measurements performed on this receptor with different mono-anions showed that the emission is selectively switched off in the presence of acetate and fluoride, while amongst the dianions investigated only biologically relevant pyrophosphate, malonate and fumarate

switched off selectively the emission process. Also in this case, as previously seen for receptor **3** a PET mechanism is likely involved in the deactivation of the excited state after the binding of the anion.

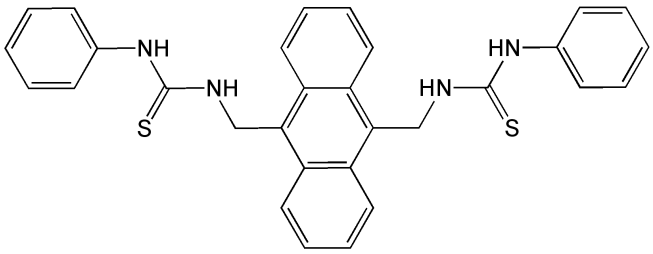

4

Figure 3.6 Structure of receptor **4**.

During the last years, other receptors for the fluorescent sensing of anionic species were synthesised by decorating the (thio)urea core with heteroaromatic rings, such as carbazoles[24] and benzimidazoles.[25] These groups have not only good emitting properties, but can also be employed for the construction of highly pre-organized multiple hydrogen bond donor arrays.

In 2009 Gale and coworkers reported the synthesis of the dicarbazolylurea **5** (**Fig. 3.7**), which in addition to form strong complexes with oxoanions such as acetate, benzoate and bicarbonate, can also be used as fluorescent sensors for anions. Remarkably, fluorescence titrations performed in DMSO/0.5% H_2O using several anions (benzoate, acetate, chloride, fluoride, benzoate and dihydrogen phosphate) revealed a selective quenching of the fluorescent emission in the presence on benzoate anion, with a residual fluorescence intensity I_{res} = 10%.[26]

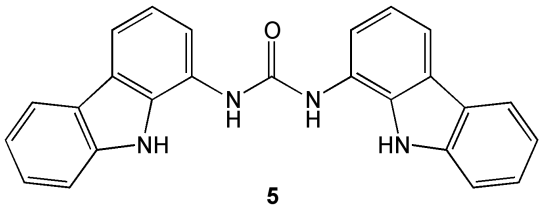

5

Figure 3.7 Structure of receptor **5**, used by Gale et al. for the selective fluorescent sensing of benzoate anion.

Lee, Singh and Jang reported in 2008 the synthesis of the hybrid receptor **6** (**Fig. 3.8**), in which two benzimidazole pendants are covalently linked to an aromatic core through two thiourea groups.[27] The finding that **6** undergoes a near complete quenching of the fluorescence emission (I_{res} = 20%) upon addition of only 5 equivalents of phosphate anion in

a DMSO/H_2O 8:2 mixture led the authors to suppose that the benzimidalole pendants play an important role in organizing the pseudocavity of the receptor for the selective inclusion of a tetrahedral guest, namely the phosphate anion. To prove this idea, the authors synthesised the control receptor **7**, where the N-H protons on the benzimidazole ring were substituted with sulphur atoms. Fluorescence titrations carried out with this receptor showed that, upon addition of phosphate, the relative changes in the fluorescence emission were smaller than those observed using receptor **6**. Furthermore, the loss of selectivity for phosphate anion with the new receptor **7** reinforced the initial hypothesis of the authors, according to which the hydrogen bond donors from the benzimidazole moieties play a crucial role in determining the selectivity of the binding event.

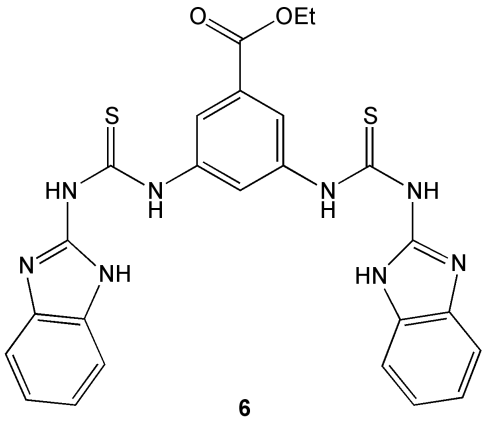

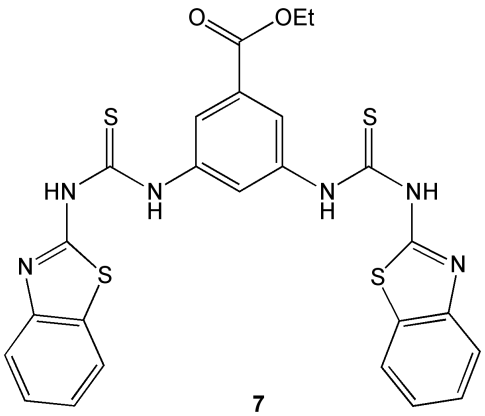

Figure 3.8 Structure of receptor **6** and **7**.

The great interest towards the synthesis of simple molecules able to qualitatively and quantitatively sense anionic species by means of fluorescence spectroscopy motivated us to proceed further on this research field. As witnessed by the literature examples cited above, the insertion of suitable fluorophores into a receptor endowed with a well-defined arrangement of hydrogen bonding donors has been the simplest approach followed hitherto. Taking advantage of the indole-(thio)urea array, extensively used in our laboratory for the synthesis of receptors that selectively bind to carboxylate anions, we decided to incorporate this array into a series of novel (thio)ureas functionalized with naphthalene and benzimidazole rings. The reasons that have led us to do this choice will be discussed, after a short introduction, in the next paragraph.

3. Benzimidazole-based ureas and thioureas for the fluorescent sensing of anions.

The research group of Prof. Gale, in which the work reported in this chapter has been done, began to develop during the past few years some simple ureas decorated with benzimidazole units, as compounds **8**, **9** and **10** depicted in **Fig. 3.9**.[28]

The reason for using this heteroaromatic ring was that, as noted by Causey and Allen in 2002 studying the anion complexation properties of fluorescent diamides, tautomerism processes may affect the nature of the hydrogen bonding array offered to an anionic guest, thus influencing the selectivity of the binding process.[29]

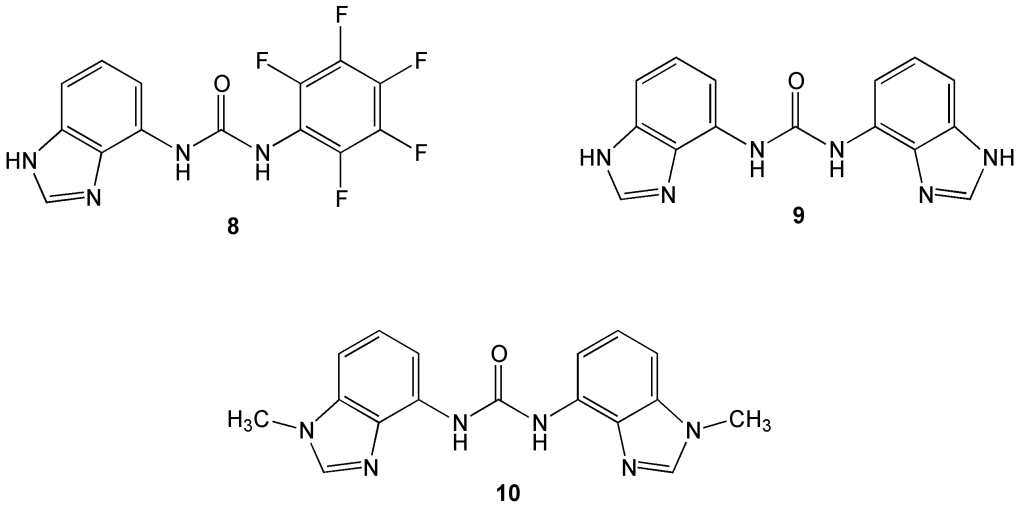

Figure 3.9 Structure of receptors **8**, **9** and **10**.

Analysis of the ^{1}H NMR titration profiles obtained with receptor **8** in the presence of different anions, as well as X-ray crystallography, showed that basic anions such as acetate and benzoate are able to promote the tautomeric switch of the benzimidazole ring, which on the contrary was not observed with less basic anions such as hydrogen sulphate, nitrate and chloride.

Also receptors **9** and **10** were used to point out the role of tautomeric switching in the anion binding process. Remarkably receptor **10**, in which the methylation of the benzimidazole ring prevents tautomerization to occur, revealed to selectively bind dihydrogen phosphate over other anions. The authors related this observation to the donation of two hydrogen bonds from the anion to the nitrogen atoms of the benzimidazole moieties (**Fig. 3.10**).

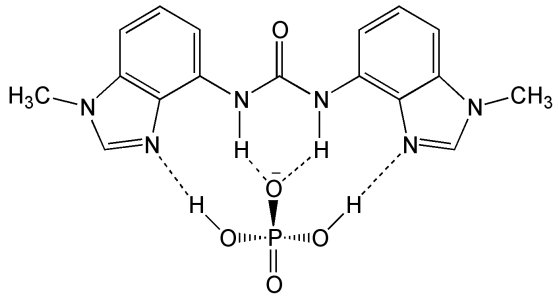

Figure 3.10 Structure of the complex between receptor **10** and dihydrogen phosphate.

More recently, the same research group developed receptors **11** and **12**, in which differently N-substituted benzimidazole cores were appended to diindolylurea framework (**Fig. 3.11**).[30]

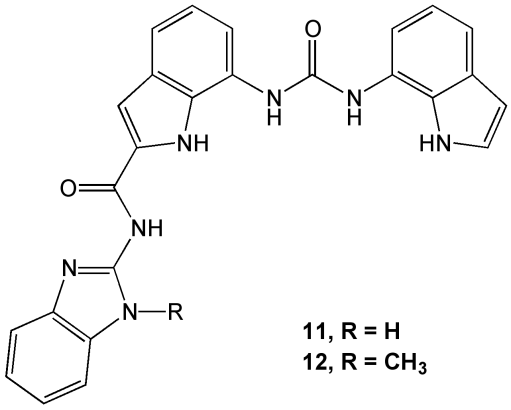

Figure 3.11 Structure of receptors **11** and **12**.

^{13}C NMR analysis gave the evidence that receptor **12** is predominantly in the tautomeric form **B**, in which the carbonylic oxygen is involved into a intramolecular hydrogen bond with the N-H group, while **11** is present as a mixture of tautomers **A** and **B** (**Fig. 3.12**).

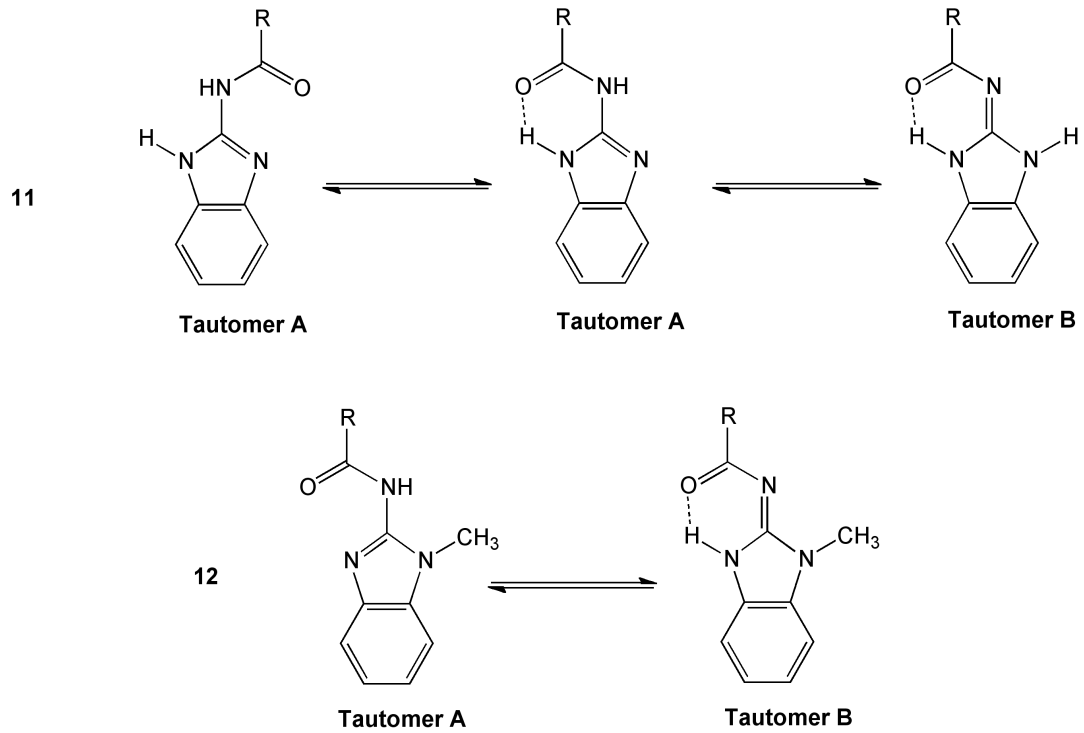

Figure 3.12 Potential tautomerisms and hydrogen bond stabilization in receptors **11** and **12**.

^{1}H NMR titrations performed with different anions in a DMSO/0.5% H_2O mixture revealed a strong binding affinity of these receptors towards carboxylate anions. Remarkably, both receptors showed selectivity for the L-lactate anion over the structurally similar pyruvate, and the observed selectivity was higher for compound **11** than for **12**. According to the authors, this was likely due to the fact that both anions trigger a tautomeric switching of the benzimidazole moiety in **11** from structure **A** to **B**. In this form, the intramolecular hydrogen bond between the carbonyl oxygen and the N-H group is maintained, and the receptor offers two further binding sites for the anion, namely a hydrogen bond acceptor (the iminic nitrogen) and a donor (the N-H group), as depicted in **Fig. 3.13**. The absence of a hydrogen bond donor in pyruvate able to interact with the iminic nitrogen of the receptor is probably responsible for the lower affinity of receptor **11** towards this anion.

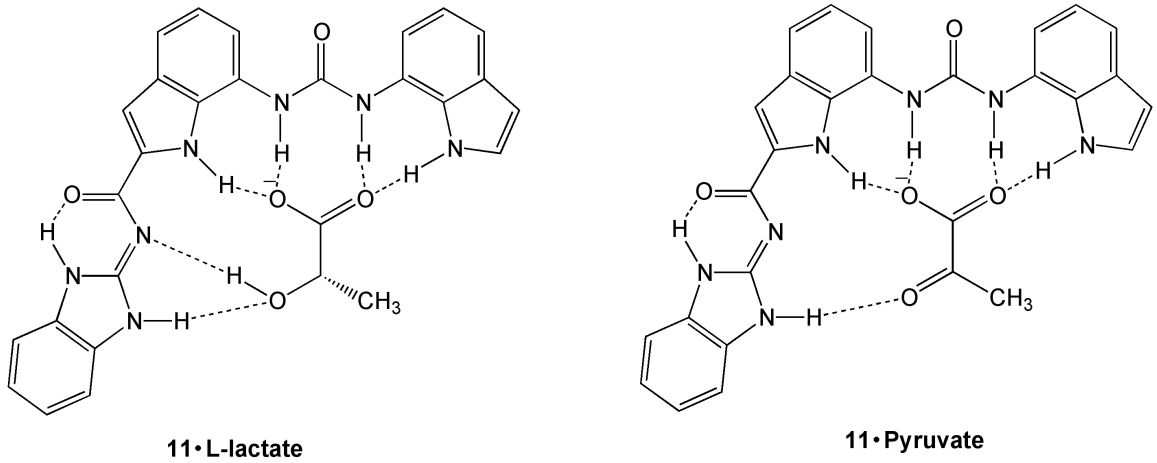

Figure 3.13 Structures of the complexes between receptor **11** and L-lactate (left) and pyruvate (right).

Moving from these premises, we thought that the tautomeric switching of the benzimidazole unit triggered by L-lactate could be usefully exploited for the selective sensing of this anion over similar pyruvate and other carboxylate anions (acetate, propionate and isobutyrate) using fluorescent receptors **19-20**.

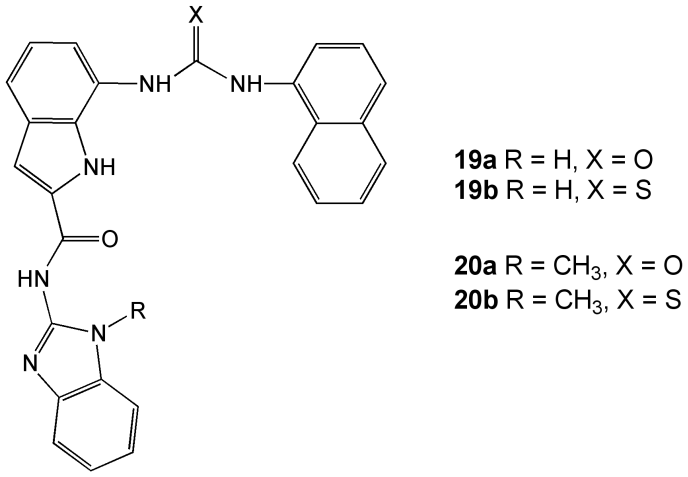

Scheme 3.1 Structures of receptors **19a-b/20a-b**.

These receptors are structurally similar to receptors **11** and **12** described previously, with the only difference that the undecorated indole moiety is replaced in **19a-b/20a-b** with a fluorophore, which is the naphthalene ring. This structural modification opens the way to the use of these molecules as potential fluorescent receptors for the above mentioned carboxylate anions (acetate, isobutyrate, propionate, L-lactate and pyruvate). Fluorescent sensing of these anions using synthetic receptor would be a valuable tool in different applications, ranging from medicinal chemistry to material sciences.

For example, L-lactate and pyruvate are important metabolites that occur naturally in the human body. L-lactate is produced by the anaerobic metabolism of pyruvate, which in its turn is the final product of Glycolysis.[31] On the industrial scale, L-lactate is widely produced as food preservative[32] and as starting material for the synthesis of biomaterials.[33] Moreover, L-lactate has also an important medicinal relevance: an alteration of the blood level of this anion, indeed, can be indicative of several life-threatening conditions.[34] Another important biological role is played by acetate anion, which is used by organisms in the form of acetyl coenzyme A.[31] It was recently found that injection of sodium acetate is able to induce headache in sensitized rats, and it was proposed that the oxidation of ethanol to acetate is the main factor causing hangovers.[35] As regards the propionate anion, inorganic derivatives such as the sodium and calcium salts have been used as food preservatives in bakery products, especially as mold inhibitor,[36] while inorganic isobutyrates have found technological applications for the production of yttrium aluminate ceramic fibers.[37]

4. Aim of the Work

4.1 Synthesis of receptors 19a-b/20a-b.

The synthetic pathway followed for the synthesis of these compounds is shown in Scheme **3**.**2**. Amides **15a** and **15b** were prepared from 7-nitroindole-2-carboxylic acid **13** and the appropriate benzimidazole-2-amine **14a-b**, using benzotriazol-1-yl-oxy-tris-pyrrolidinophosphonium hexafluorophosphate (PyBOP) as coupling agent together with a catalytic amount of hydroxybenzotriazole (HOBt). PyBOP was developed by Castro et al. in 1990 as a non-toxic substituted of benzotriazol-1-yl-oxy-tris-(dimethylamino)phosphonium hexafluorophosphate (BOP) in peptide coupling processes.[38] Indeed, peptide coupling performed with BOP leads to the formation of high toxic and carcinogenic hexamethylphosphoramide (HMPA). In **Fig. 3.14** are reported the structures of PyBOP, BOP and HOBt.

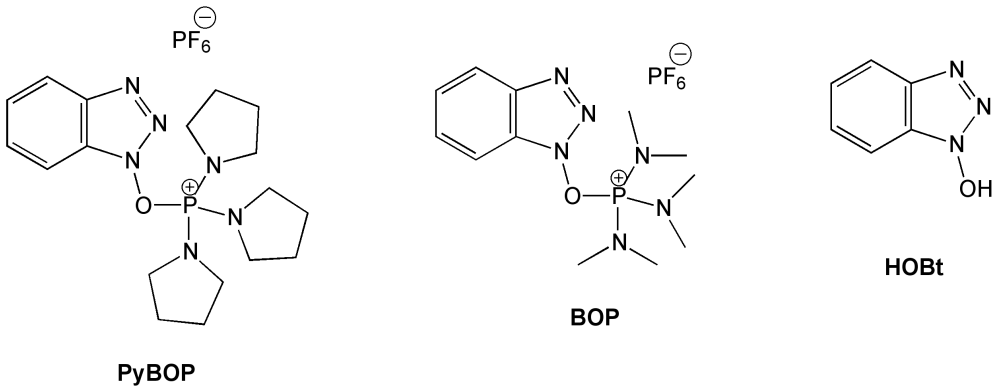

Figure 3.14 Structures of PyBOP (left), BOP (centre) and HOBt (right). Abbreviations used: PyBOP = benzotriazol-1-yl-oxy-tris-pyrrolidinophosphonium hexafluorophosphate; BOP = benzotriazol-1-yl-oxy-tris-(dimethylamino)phosphonium hexafluorophosphate; HOBt = hydroxybenzotriazole.

The mechanism of the amidic coupling is described in **Fig. 3.15**. The role of PyBOP in this reaction is to activate the carboxylic group of **13** through the formation of an acyl-phosphonium species and HOBt. The latter readily reacts with the activated acid to produce a reactive benzotriazol-ester, which finally reacts with the amine (**14a-b**) to give the amidic product (**15a-b**). A catalytic amount of HOBt was added to the reaction mixture in order to promote the formation of the benzotriazole-ester and therefore a more efficient coupling.[39-40]

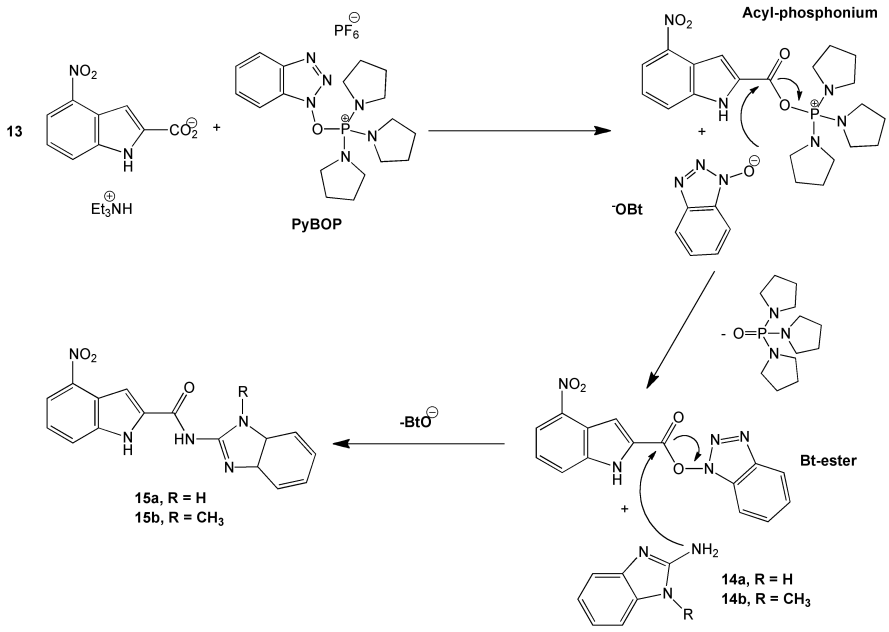

Figure 3.15 Proposed mechanism for peptide coupling in the presence of PyBOP and HOBt.

Reduction of the nitro derivatives **15a-b** using Pd/C 10 % under a hydrogen atmosphere in DMF afforded amines **16a-b**, which were directly put to react with the corresponding isothio/isocyanate (**17** or **18**) to give the receptors **19a-b/20a-b**.

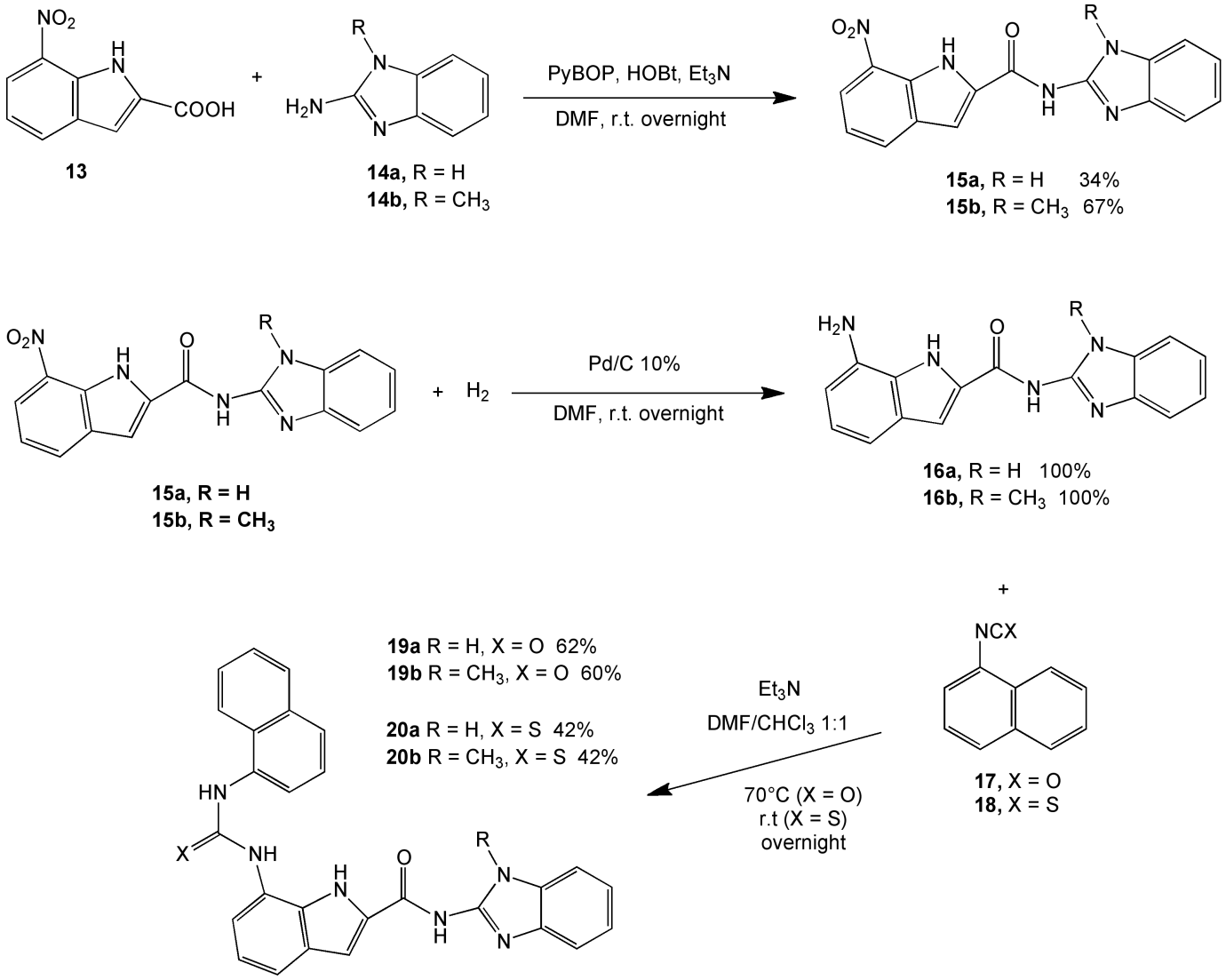

Scheme 3.2 Synthesis of receptors **19a-b** and **20a-b**

The anions used to perform UV-Vis and fluorescence studies were all used as their tetrabutylammonium (TBA) salts, and their chemical structures are reported in **Fig. 3.16**. With the only exception of TBA acetate, which is commercially available, they were prepared mixing one equivalent of tetrabutylammonium hydroxide (1M in methanol) with the appropriate acid at room temperature for two hours.

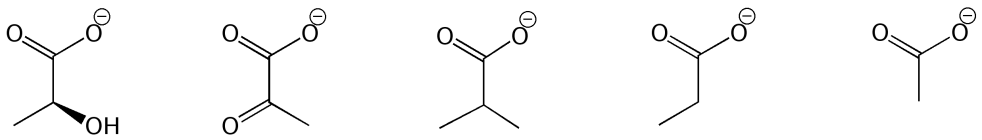

L-lactate 21 | pyruvate 22 | isobutyrate 23 | propionate 24 | acetate 25

Figure 3.16 Chemical structures of the five anions studied in the UV-Vis and fluorescence studies, all used as their TBA salt (TBA is omitted for clarity).

4.2 UV-Vis and fluorescence measurements

In order to set up suitable concentration values to carry on the fluorescence experiments, preliminary UV-Vis studies were performed in DMSO/0.5% H_2O mixtures at 25°C. The spectral changes upon addition of a stock solution of the anionic guest were monitored for each receptor between 270 and 450 nm, being careful to keep A < 0.1 at the excitation wavelength (λ_{exc} = 365 nm). This condition is mandatory for a proper execution of a fluorescence experiment, because only in very diluted solutions there is a direct relationship between the concentration of the emitting species and the intensity of the emitted light, according to Equation 1.

$$I_f = 2.3 \cdot I_0 \cdot \Phi \cdot \left(1 - 10^{-\varepsilon \cdot c \cdot l}\right) \quad (1)$$

In this equation, I_f is the fluorescence intensity emission, I_0 is the intensity of the incident light, ε is the molar absorptivity of the fluorescent species measured at the excitation wavelength, l the optical path (usually l = 1 cm) and Φ is the quantum yield of fluorescence, defined as the ratio between the emitted and the absorbed photons, which usually varies between 0 and 1.

Keeping absorption as low as possible at the excitation wavelength is important for two reasons. The first is mathematically implicit in equation 1, in which the emission intensity and the intensity of the absorbed light are related through an exponential factor ($1\text{-}10^{ecl}$). If the concentration of the fluorescent analyte is sufficiently low, the exponential term can be neglected and thus I_f is linearly related to I_0. The second is a physical reason, and is related to auto-absorption phenomena. In a concentrated solution of the fluorophore, indeed, the molecules near the cuvette surface absorb most of the incident light, while those in the bulk only a little amount of it. This issue can be easily prevented using a dilute solution, because in

these conditions the concentration of the excited states along the optical path of the excitation light can be considered constant.[41]

In **Fig. 3.17** are reported for example the UV-Vis spectra of receptor **20b** upon addition of increasing amounts of a stock solution of TBA L-lactate. In general, the spectral variations observed with the four receptors in the presence of all the five anions investigated were too small to allow a reliable calculation of the binding constant values.

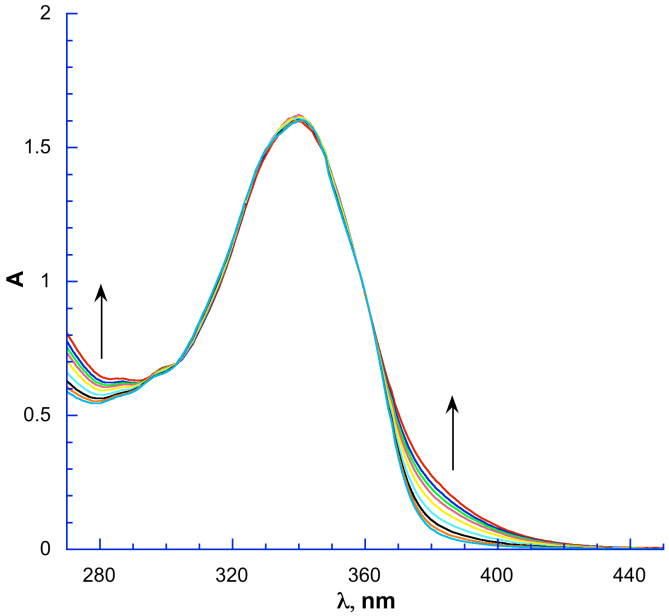

Figure 3.17 UV-Vis titration of receptor **20b** (1.18×10^{-5} M) with TBA L-lactate (3.72×10^{-2} M) in DMSO/0.5% H_2O at 25°C.

On the other hand, fluorescence studies were performed in DMSO/0.5% H_2O mixtures at 25°C by irradiating the receptor solution at λ_{exc} = 365 nm and following the emission intensities between 380 and 600 nm. The emission spectra of the four receptors show all a maximum at 440 nm, and two shoulders at 415 nm and 468 nm respectively.

Upon addition of increasing amounts of a stock solution of each anionic guest, an increase of the fluorescence emission was observed for all the four receptors. An example is reported in **Fig. 3.18**, in which are shown fluorescence changes upon addition of different aliquots of TBA L-lactate to a solution of receptor **20b**.

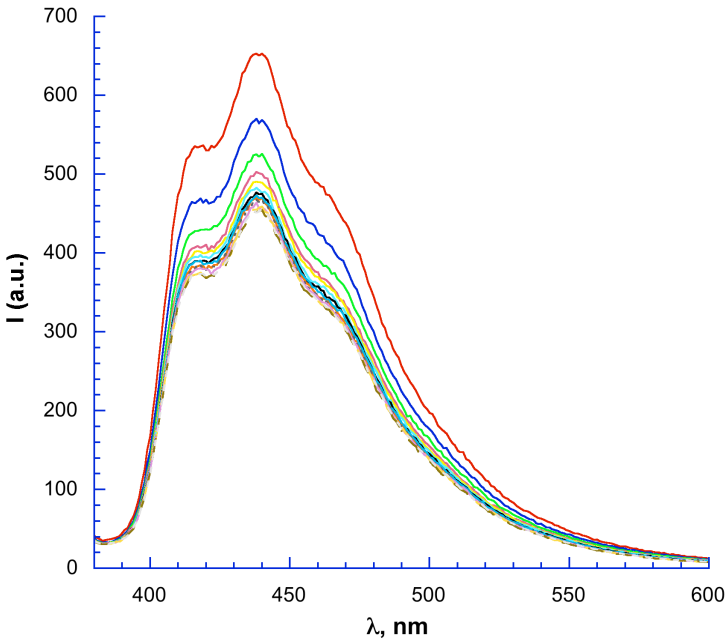

Figure 3.18 Emission changes upon addition of increasing aliquots of TBA L-lactate (stock solution 0.101 mM) to receptor **20b** (1.16 μM) in DMSO/0.5% H_2O at 25°C.

As shown in **Fig. 3.18**, a continuous increase of the fluorescent emission was observed upon addition of increasing amounts of TBA L-lactate (up to 40 equivalents of salt). The same observation were made also with the other receptors **20a** and **19a-b**, in the presence of each of the five anionic guests considered in this study.

The titration plots for the four receptors **19a-b** and **20a-b** were obtained plotting the relative emission intensity I/I_0 at λ_{em}= 440 nm vs. the number of equivalents of the different anions added.

In **Fig. 3.19** are shown as example the titration profiles obtained for the thioureidic receptor **20b** with the five anion studied. In the presence of an excess of the anionic guest (about 40 equivalents), an increase of the 56% in the fluorescence emission is observed in the presence of TBA acetate, of about 50% in the cases of TBA pyruvate, isobutyrate and propionate, and of the 43% for the L-lactate. A similar trend was observed also in the cases of receptors **20a** and **19a-b**. In all cases, however, no tendency to saturation is observed neither in the presence of an excess of the anionic guest. According to our hypotheses, this behaviour could be due to the presence of multiple equilibria in solution between the receptors **19a-b** and **20a-b** and the guests, one of which could reasonably be the equilibrium between the different tautomers of the receptors. To prove the validity of these suppositions, further studies must be carried on using ^{1}H NMR spectroscopy. This technique can be helpful not only for elucidating the mechanisms involved in the binding processes but also to gain quantitative information about

these phenomena; unfortunately, due to time constrains, it was not possible to proceed further on doing these studies.

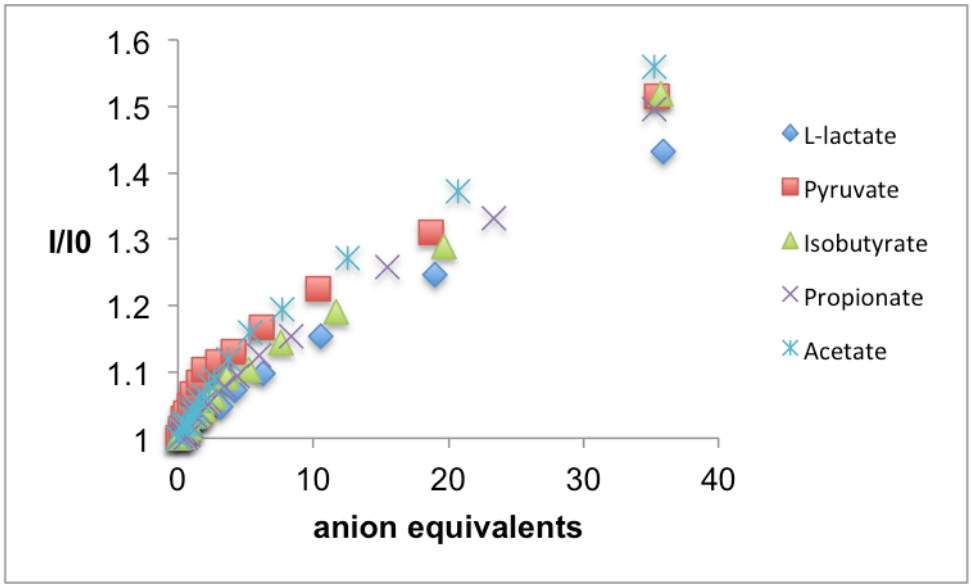

Figure 3.19 Titration plots of receptor **20b** obtained with the five anionic guests studied.

In **Table 3.1** are reported the observed fluorescence increases with the four receptors **19a-b** and **20a-b** in the presence of an excess of the five anions studied (L-lactate, pyruvate, isobutyrate, propionate and acetate). The maximum fluorescence increases were observed for receptor **20b** upon addition of L-lactate, pyruvate, acetate and isobutyrate, while receptors **19a** showed a maximum fluorescence increase with propionate. The value of the observed increases do not allow saying that the fluorescence intensity is selectively "switched on" in the presence of a certain anion, due to the similarity of the values obtained.

Table 3.1 Observed fluorescence increases (percentage, %) after the addition of ca. 40 equivalents of the five anionic guests (used as their TBA salts) in DMSO/0.5% H_2O at 25°C

Receptor	L-lactate	Pyruvate	Isobutyrate	Propionate	Acetate
19a	33	36	41	55	55
19b	30	40	40	30	30
20a	30	30	30	30	30
20b	43	50	50	50	56

5. Conclusions

In conclusion, four novel benzimidazole-based ureas and thioureas receptors **19a-b** and **20a-b** (**Fig. 3.20**) were synthesised, and their fluorescence properties upon complexation with different anions, used as their tetrabutylammonium (TBA) salts (L-lactate, pyruvate, propionate, isobutyrate and acetate) were evaluated in DMSO/0.5% H_2O mixtures at 25°C. The titration plots obtained for each of the four receptors showed an increase of the fluorescent emission in the presence of increasing amount of the anionic guests, but no tendency to saturation even in the presence of a strong excess of a 40-fold excess of the anion. These observations, as well as the lack of selectivity observed in all cases, could be likely due to the coexistence of multiple equilibria in solution, among which an important part could be played by the tautomeric switching of the benzimidazole unit. In order to gain more insights on these phenomena, detailed ^{1}H NMR titrations need to be carried with the aim of quantifying the association. Anyway, on the basis of the data available at the moment, we can think about possible applications of receptors **19a-b** and **20a-b** to the qualitative and quantitative detection of anions in aqueous mixtures, and in their use as potential anion transporters and phase-transferring agents.

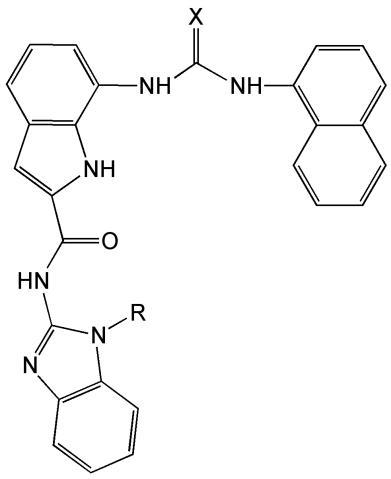

19a R = H, X = O
19b R = H, X = S

20a R = CH_3, X = O
20b R = CH_3, X = S

Figure 3.20 Structures of receptors **19-20**

6. Experimental section

General remarks: All reactions were performed under slight positive pressure of nitrogen using oven-dried glassware. All solvents and starting materials were purchased from chemical stores where available. ^{1}H-^{13}C NMR spectra were collected using a Bruker AV300 and AV400 spectrometer respectively; UV-Vis spectra were recorded using a Cary Varian spectrophotometer and fluorescence spectra were recorded on a Cary Varian Eclipse spectrofluorometer. All the TBA salts used for the Uv-Vis and fluorescence measurements were carefully dried under high vacuum overnight prior to their use.

N-(1H-benzo[d]imidazol-2(3H)-ylidene)-7-nitro-1H-indole-2-carboxamide (15a).

7-nitroindole-2-carboxylic acid **13** (1.0 g, 4.84 mmol), 1H-benzo[d]imidazol-2-amine **14a** (0.598 g, 4.49 mmol), PyBOP (2.899 g, 5.57 mmol), triethylamine (0.7 mL) and a catalytic amount of HOBt were dissolved in dry DMF (20 mL). The solution was stirred overnight at room temperature. The crude product was then removed by filtration, washed with DCM (100 mL) and triturated in water (100 mL) overnight. The yellow solid was then removed from the aqueous solution by filtration and dried under reduced pressure. Yield 44 % (0.63 g, 1.96 mmol)

^{1}H NMR (400 MHz, DMSO-*d*$_6$) δ (ppm): 12.57 (s, 2H, benzimidazole NH); 11.25 (s, 1H, indole NH); 8.27-8.22 (m, 2H); 7.53-7.45 (m, 3H); 7.34 (t, J = 8.1 Hz, 1H); 7.2-7.16 (m, 2H) **^{13}C NMR (100 MHz, DMSO-*d*$_6$)** δ (ppm): 149.8; 136.2, 133.0, 131.2, 130.8, 128.9, 122.1, 121.3, 120.0, 112.8, 107.6.

N-(1-methyl-1H-benzo[d]imidazol-2(3H)-ylidene)-7-nitro-1H-indole-2-carboxamide (15b).

7-nitroindole-2-carboxylic acid **13** (0.359 g, 1.74 mmol), 1-methyl-1H-benzoimidazol-2-amine **14b** (0.229 g, 1.56 mmol), PyBOP (1.024 g, 1.97 mmol), triethylamine (0.2 mL) and a catalytic amount of HOBt were dissolved in dry DMF (10 mL). The solution was stirred overnight at room temperature. The crude product was then removed by filtration, washed with DCM (100 mL) and triturated in water (100 mL) overnight. The yellow solid was then removed from the aqueous solution by filtration and dried under reduced pressure. Yield 67 % (0.353 g, 1.05 mmol).

^{1}H NMR (400 MHz, DMSO-d_6) δ (ppm): 12.74 (s, 2H, benzimidazole NH); 10.65 (s, 1H, indole NH); 8.24-8.20 (m, 2H); 7.58-7.51 (m, 2H); 7.40 (s, 1H); 7.36-7.26 (m, 3H); 3.78 (s, 3H) **^{13}C NMR (100 MHz, DMSO-d_6)** δ (ppm): 151.7, 132.7, 131.7, 130.4, 129.8, 128.7, 128.4, 122.7, 120.4, 119.6, 112.0; 109.5; 105.8; 28.2

7-amino-*N*-(1*H*-benzo[*d*]imidazol-2(3H)-ylidene)-1*H*-indole-2-carboxamide (16a).

Compound **15a** (0.2 g, 0.62 mmol) and Pd/C 10% (catalytic amount) were suspended in DMF (5 mL). The flask was then evacuated, the suspension placed under a hydrogen atmosphere and stirred vigorously overnight. The palladium was then removed by filtration, and the filtrate taken directly on to the next step of the reaction. Assumed yield 100 %.

7-amino-*N*-(1-methyl-1*H*-benzo[*d*]imidazol-2-ylidene)-1*H*-indole-2-carboxamide (16b).

Compound **15b** (0.2 g, 0.6 mmol) and Pd/C 10% (catalytic amount) were suspended in DMF (5 mL). The flask was then evacuated and the suspension stirred under a hydrogen atmosphere overnight. The palladium was then removed by filtration, and the filtrate taken directly on to the next step of the reaction due to the high instability of the product. Assumed yield 100 %.

***N*-(1*H*-benzo[*d*]imidazol-2-ylidene)-7-(3-(naphthalen-1-ylidene)ureido)-1*H*-indole-2-carboxamide (19a).**

The DMF solution containing compound **16a** (0.62 mmol) was added to a stirring solution of 1-naphthylisocyanate **17** (0.09 mL, 0.63 mmol) and triethylamine (0.5 mL) in DMF (5 mL) and chloroform (10 mL). The reaction mixture was heated at 70°C overnight under nitrogen atmosphere. After cooling, 30 mL of chloroform and 50 mL of water were poured into the flask and the mixture was stirred for two hours at room temperature. A precipitate appeared, which was filtered and washed with diethyl ether. The crude material was finally purified via flash column chromatography (basic SiO_2, eluent 7M ammonia in methanol), to afford 0.182 g (0.4 mmol) of product, yield 65%.

^{1}H NMR (400 MHz, DMSO-d_6) δ (ppm): 12.26 (s, 2H, benzimidazole NH); 11.28 (s, 1H, indole NH); 9.26 (s, 1H); 8.84 (s, 1H); 8.27 (d, 1H, J = 8 Hz); 8.03 (d, 1H, J = 8 Hz); 8.00 (d, 1H, J = 8 Hz); 7.74-7.42 (m, 9H); 7.17-7.06 (m, 3H) **^{13}C NMR (100 MHz, DMSO-d_6)** δ

(ppm): 188.4, 179.89, 153.42, 134.29, 133.7, 128.5, 128.39, 126.42, 125.94, 125.85, 125.76, 124.86, 123.43, 121.6, 120.43, 118.25, 116.71, 114.28, 106.17.

***N*-(1-methyl-1*H*-benzo[*d*]imidazol-2-yliden)-7-(3-(naphthalen-1-yliden)ureido)-1*H*-indole-2-carboxamide (19b).**

Under nitrogen atmosphere, the DMF solution containing compound **16b** (0.6 mmol) was added to a stirring solution of 1-naphthylisocyanate **17** (0.09 mL, 0.63 mmol) and triethylamine (0.5 mL) in DMF (5 mL) and chloroform (10 mL). The reaction mixture was heated at 70°C overnight, during which time a precipitate appeared. After cooling, the crude product was filtered off, washed with diethyl ether and triturated with methanol for two hours at room temperature. 0.173 g (0.36 mmol) of pure product were obtained, yield 60 %.

^{1}H NMR (300 MHz, DMSO-d_6) δ (ppm): 12.6 (s, 1H, benzimidazole NH); 11.07 (s, 1H, indole NH); 9.3 (s, 1H); 8.84 (s, 1H); 8.21 (d, 1H, J = 8 Hz); 8.02 (d, 1H, J = 8 Hz); 7.97 (d, 1H, J = 8 Hz); 7.7-7.18 (m, 11H); 7.03 (t, 1H, J = 12 Hz); 3.77 (s, 3H) **^{13}C NMR (75 MHz, DMSO-d_6)** δ (ppm): 210.94, 208.58, 181.12, 168.42, 153.4, 151.98, 136.5, 134.33, 133.74, 129.98, 129.57, 128.91, 128.39, 128.25, 126.67, 125.93, 125.84, 125.0, 123.29, 122.61, 121.57, 120.0, 118.06, 116.28, 113.0, 111.84, 109.51, 105.32, 28.16.

***N*-(1*H*-benzo[*d*]imidazol-2-ylidene)-7-(3-(naphthalen-1-ylidene)thioureido)-1*H*-indole-2-carboxamide (20a).**

Compound **16a** (0.97 mmol) in DMF was added to a stirring solution of 1-naphthylisothiocyanate **18** (0.288 g, 1.55 mmol) and triethylamine (1 mL) in DMF (5 mL) and chloroform (10 mL). The reaction mixture was stirred overnight at room temperature under a nitrogen atmosphere. Finally, 30 mL of chloroform and 50 mL of water were poured into the flask and the mixture was stirred for two hours at room temperature. A precipitate appeared, which was filtered and washed with diethyl ether. The crude product was finally purified via flash column chromatography (basic SiO_2, eluent 7M ammonia in methanol), to afford 0.194 g (0.41 mmol) of product, yield 42%.

^{1}H NMR (400 MHz, DMSO-d_6) δ (ppm): 12.2 (s, 2H, benzimidazole NH); 11.39 (s, 1H, indole NH); 9.98 (s, 1H); 9.78 (s, 1H); 8.09 (d, 1H, J = 8 Hz); 7.97 (d, 1H, J = 8 Hz); 7.88 (d, 1H, J = 8 Hz); 7.66-7.48 (m, 9H); 7.18-7.04 (m, 3H) **^{13}C NMR (100 MHz, DMSO-d_6)** δ

(ppm): 181.75, 172.43, 135.46, 133.86, 132.0, 129.88, 129.71, 128.0, 126.56, 126.04, 125.57, 125.21, 124.68, 123.35, 121.51, 120.0, 119.37.

***N*-(1-methyl-1*H*-benzo[*d*]imidazol-2-yl)-7-(3-(naphthalen-1-yl)thioureido)-1*H*-indole-2-carboxamide (20b).**

Compound **16b** (0.6 mmol) in DMF was added to a stirring solution of 1-naphthylisothiocyanate **18** (0.116 g, 0.63 mmol) and triethylamine (0.5 mL) in DMF (5 mL) and chloroform (10 mL). The reaction mixture was stirred overnight at room temperature under a nitrogen atmosphere, then 30 mL of chloroform and 50 mL of water were poured into the flask and the mixture stirred for two hours at room temperature. A precipitate appeared, which was filtered and washed with diethyl ether. 0.123 g (0.25 mmol) of product were obtained, yield 42%.

^{1}H NMR (300 MHz, DMSO-d_6) δ (ppm): 12.6 (s, 1H, benzimidazole NH); 10.91 (s, 1H, indole NH); 10.0 (s, 1H); 9.85 (s, 1H); 8.13 (d, 1H, J = 8 Hz); 7.98 (d, 1H, J = 8 Hz); 7.87 (d, 1H, J = 8 Hz); 7.66-7.48 (m, 8H); 7.29-7.22 (m, 3H); 7.06 (t, 1H, J = 9 Hz); 3.77 (s, 3H) **^{13}C NMR (75 MHz, DMSO-d_6)** δ (ppm): 212.55, 181.58, 168.39, 151.98, 136.93, 135.5, 133.87, 129.98, 129.5, 128.75, 128.06, 126.5, 126.03, 125.58, 125.24, 124.5, 123.31, 122.62, 119.63, 118.66, 111.87, 109.51, 105.65, 28.25.

NMR characterizations of TBA L-lactate, pyruvate, isobutyrate and propionate)

TBA L-lactate (21)

^{1}H NMR (300 MHz, $CDCl_3$) δ (ppm): 3.93 (quartet, 1H, J = 6 Hz); 3.34-3.29 (m, 8H); 1.7-1.57 (m, 8H); 1.5-1.34 (m, 11H); 1.0 (t, 12H, J = 6 Hz).

TBA pyruvate (22)

^{1}H NMR (300 MHz, $CDCl_3$) δ (ppm): 3.27-3.21 (m, 8H); 2.28 (s, 3H); 1.63-1.53 (m, 8H); 1.43-1.3 (m, 8H); 0.93 (t, 12H, J = 6 Hz).

TBA isobutyrate (23)

^{1}H NMR (400 MHz, $CDCl_3$) δ (ppm): 3.29-3.25 (m, 8H); 2.28 (eptuplet, 1H, J = 8 Hz); 1.59 (quintet, 8H, J = 8 Hz); 1.37 (sextet, 8H, J = 8 Hz); 1.04 (d, 6H, J = 8 Hz); 0.93 (t, 12H, J = 8 Hz).

TBA propionate (24)

^{1}H NMR (400 MHz, $CDCl_3$) δ (ppm): 3.34-3.28 (m, 8H); 2.11 (quartet, 2H, J = 8 Hz); 1.59 (quintet, 8H, J = 8 Hz); 1.37 (sextet, 8H, J = 8 Hz); 1.04 (d, 6H, J = 8 Hz); 0.93 (t, 12H, J = 8 Hz).

7. Bibliography

[1] Pedersen, C.J. *J. Am. Chem, Soc.* **1967**, *89*, 7017-7036

[2] Kilbourn, B.T.; Dunits, J.D.; Pioda, L.A.R., Simon, W. *J. Mol. Biol.* **1967**, *30*, 559-563.

[3] Pinkerton, M.; Steinrauf, L.K.; Dawkins, P. *Biochem. Bioph. Res. Co.,* **1969**, *35*, 512-518.

[4] For recent reviews, see: (a) Schmidtchen, F.P.; Berger, M. *Chem. Rev*., **1997**, *97*, 1609-1646. (b) Gale, P.A. *Coord. Chem. Rev*., **2000**, *199*, 181-233. (c) Beer, P.D.; Gale, P.A. *Angew. Chem. Int. Ed*. **2001**, *40*, 486-516. (d) Gale, P.A. *Coord. Chem. Rev*., **2001**, *213*, 79-128. (e) Special issues on anion coordination chemistry in *Coord. Chem. Rev*. **2003**, 240 and **2006**, 250. (f) Kubik, S.; Reyheller, C.; Stüwe, S. *J. Inclusion Phenom. Macrocyclic Chem.,* **2005**, *52*, 137-187. (g) Gale, P.A.; Garcia-Garrdo, S.E.; Garric, J. *Chem. Soc. Rev.* **2008**, *37*, 151-90 (h) Caltagirone, C.; Gale, P.A. *Chem. Soc. Rev*., **2009**, *38*, 520-563. (h) Themed issue: *Chem. Soc. Rev*. **2010**, *39,* 3581-4008. (i) Wenzel, M.; Hiscock, J.R.; Gale, P.A. *Chem. Soc. Rev.* **2012**, *41*, 480-520.

[5] For monographs, see (a) Supramolecular Chemistry of Anions, eds. A. Bianchi, K. Bowman-James, E. Garcia-España, Wiley-VCH, New York, **1997.** (b) Anion Receptor Chemistry, J.L. Sessler, P.A. Gale and W.-S. Cho, RSC publishing, **2006.**)

[6] Marcus, Y. *J. Chem. Soc., Faraday Trans. 1* **1987**, *83*, 339 and **1986**, *82*, 233; *J. Chem. Soc., Faraday Trans.* **1991**, *87*, 2995. Shannon, R.D. *Acta Crystallogr. Sect. A*, **1976**, *32*, 751-767.

[7] Hofmeister, F. *Arch. Exp. Pathol. Pharmakol.* **1888**, *24*, 247-266.

[8] Cram, D.J. *Angew. Chem. Int. Ed.* **1988**, *27*, 1009-1020.

[9] Jeffrey, G. A. *An Introduction to Hydrogen bonding*, Oxford University Press, **1997.**

[10] Park, C.H.; Simmons, H.E. *J. Am. Chem. Soc.* **1968**, *90*, 2431-2432.

[11] The authors define *katapinosis* as " the diffusion of molecules into a larger molecule with a sensible cavity to give a discrete molecular species".

[12] (a) P. A. Gale, Amide- and Urea-Based Anion Receptors, in *Encyclopedia of Supramolecular Chemistry*, ed. J. L. Atwood and J. W. Steed, Marcel Dekker, New York, 2004, pp. 31–41; (b) J. L. Sessler, P. A. Gale and W.-S. Cho, *Anion Receptor Chemistry*, Royal Society of Chemistry, Cambridge, UK, 2006; (c) G. W. Bates and P. A. Gale, *Struct. Bonding*, **2008**, *129*, 1–44; (d) Z. Zhang and P. R. Schreiner, *Chem. Soc. Rev*., **2009**, *38*, 1187–1198.

[13] F. Wöhler, *Poggendorfs Ann. Phys. Chem.,* **1828**, *12*, 253–256.

[14] E. Mayr, *The Growth of Biological Thought*, Harvard University Press, Harvard, NY, 1982.)

[15] Bigi, F.; Maggi, R.; Sartori, G. *Green Chem.,* **2000**, *2*, 140–148.

[16] Wu, J.; He, Y.; Zeng, Z.; Wei, L.; Meng, L.; Yang, T. *Tetrahedron*, **2004**, *60*, 4309-4314.

[17] L. Cotarca and H. Eckert, Phosgenations-A Handbook, Wiley-VCH, Weinheim, 2004.

[18] Bordwell, F.G. *Acc. Chem. Res.* **1988**, *21*, 456-463.

[19] Li, A.-F.; Wang, J.-H.; Wang, F. and Jiang, Y.-B. *Chem. Soc. Rev.* **2010**, *39*, 3729-3745.

[20] J. L. Sessler, P. A. Gale and W.-S. Cho, *Anion Receptor Chemistry*, Royal Society of Chemistry, Cambridge, UK, 2006.

[21] Abdalla, O.A.E.; Suliman, F.O.; Al-Ajmi, H.; Al-Hosni, T.; Rollinson, H. *Environ. Earth Sci.* **2010**, *60*, 885-892.

[22] Gunnlaugsson, T.; Kruger, P.E.; Clive lee, T.; Parkesh, R.;Pfeffer, F.M. and Hussey, G.M. *Tetrahedron Lett.* **2003**, *44*, 6575-6578.

[23] Gunnlaugsson, T.; Davis, A.p.; O'Brien, J.E. and Glynn, M. *Org. Biomol. Chem.* **2005**, *3*, 48-56.

[24] (a) Curiel, D.; Cowley, A. and Beer, P.D. *Chem. Comm.* **2005**, 236-238. (b) Thangadurai, T.D.; Singh, J.N.; Hwang, I.-C.; Lee, J.W.; Chandran, R.P. and Kim, K.S. *J. Org. Chem.* **2007**, *72*, 5461-5464. (c) Qing, G.-Y-; He, Y.-B-; Wang, F.; Qin, H.J.; Hu, C.-G. and Yang, X. *Eur. J. Org. Chem*., **2007**, 1768–1778.

[25] (a) Singh, N.; Jang, D.O. *Org. Lett.* **2007**, *9*, 1991-1994. (b) Joo, T.Y.; Singh, N.; Lee, G.W.; Jang, D.O. *Tetrahedron Lett.* **2007**, *48*, 8846-8850. (c) Kar, C.; Basu, A.; Das, G. *Tetrahedron Lett.* **2012**, *53*, 4754-4757. (d) Gosh, K.; Kar, D.; Chowdhury, P.R. *Tetrahedron Lett.* **2011**, *52*, 5098-5103. 8846-8850. (e) Lee, D.Y.; Singh, N.; Kim, M.J. and Jang, D.O. *Org. Lett.* **2011**, *27*, 3024-3027. (f) Molina, P.; Tárraga, A. and Otón, F. *Org. Biomol. Chem.* **2012**, *10*, 1711-1724 and references cited therein.

[26] Hiscock, J.R.; Caltagirone, C.; Light, M.E.; Hursthouse, M.B. and Gale, P.A. *Org. Biomol. Chem.* **2009**, *7*, 1781-1783.

[27] Lee, G.W.; Singh, N. Jang, D.O. *Tetrahedron Lett.* **2008**, *49*, 1952-1956.

[28] Gale, P.A.; Hiscock, J.R.; Lalaoui, N.; Light, M.E.; Wells, N.J. and Wenzel, M. *Org. Biomol. Chem.* **2012**, *10*, 5909-5915.

[29] Causey, C.P. and Allen, W.E. *J. Org. Chem.* **2002**, *67*, 5693-5698.

[30] Gale, P.A.; Hiscock, J.R.; Lalaoui, N.; Light, M.E.; Wells, N.J. *Org. Biomol. Chem.* **2012**, Advance article.

[31] Voet, D and Voet, J., *Biochemistry*, 4th edition, Wiley, **2011**.

[32] (a) Shrestha, B.M.; Mundorff, S.A.; Bibby, B.G. *Caries Research* **1982**, *16*, 12-17 (b) http://www.foodditive.com/additive/calcium-lactate.

[33] (a) Middleton, J.C.; Tipton, A.J. *Biomaterials*, **2000**, *21*, 2335-2346 (b) Södergård, A.; Stolt, M. *Prog. Polym. Sci.* **2002**, *27*, 1123–1163.

[34] Bakker, J.; Pinto de Lima, A. *Critical Care* **2004**, *8*, 96-98.

[35] Maxwell, C.R.; Spangenberg, R.J.; Hoek, J.B.; Silberstein, S.D.; Oshinsky, M.L. *PLoS ONE*, **2010**, *5*, 1-9.

[36] UK Food Standards Agency: "Current EU approved additives and their E Numbers". Retrieved 2011-10-27.

[37] Liu, Y.; Zhang, Z.-F.; King, B.; Halloran, J. and Laine, R.M. *J. Am. Ceram. Soc.* **1996**, *79*, 385-394.

[38] Coste, J.; Le-Nguyen, D. and Castro, B. *Tetrahedron Lett.* **1990**, *31*, 205-208.

[39] Hudson, D. *J. Org. Chem.* **1988**, *53*, 617.

[40] Castro, B.; Dormoy, J.-R.; Dourtoglou, B.; Evin, G.; Selva, C.; Ziegler, J.-C. *Synthesis*, **1976**, 751.

[41] Moggi, L.; Juris, A. and Gandolfi, M.T. *Handbook of Photochemistry,* Bononia University Press.